SUPPLEMENTARY INFORMATION

Radical C–H ^{18}F-Difluoromethylation of Heteroarenes with [^{18}F]Difluoromethyl Heteroaryl-Sulfones by Visible Light Photoredox Catalysis

Agostinho Luís Pereira Lemos [1,#,*], Laura Trump [1,2,#], Bénédicte Lallemand [2], Patrick Pasau [2], Joël Mercier [2], Christian Lemaire [1], Jean-Christophe Monbaliu [3], Christophe Genicot [2,*], André Luxen [1,*]

[1] GIGA-Cyclotron Research Centre *In Vivo* Imaging, University of Liège, 8 Allée du Six Août, Building B30, Sart Tilman, 4000 Liège, Belgium; agostinholemos43@gmail.com (A.L.P.L.); laura.trump@ucb.com (L.T.); christian.lemaire@uliege.be (C.L.); aluxen@uliege.be (A.L.)

[2] Global Chemistry, UCB NewMedicines, UCB Biopharma SPRL, 1420 Braine-l'Alleud, Belgium; patrick.pasau@ucb.com (P.P.); benedicte.lallemand@ucb.com (B.L.); joel.mercier@ucb.com (J.M.); christophe.genicot@ucb.com (C.G.)

[3] Center for Integrated Technology and Organic Synthesis, Research Unit MolSys, University of Liège, (Sart Tilman), B-4000, Liège, Belgium; jc.monbaliu@uliege.be (J.C.M.)

* Correspondence: agostinholemos43@gmail.com (A.L.P.L.); christophe.genicot@ucb.com (C.G.); aluxen@uliege.be (A.L.); Tel: (+32)499509436

[#] The authors contributed equally to this work

Table of contents

1. NMR spectra of the compounds 4a-4f, 5a-5f, and 6a-6f

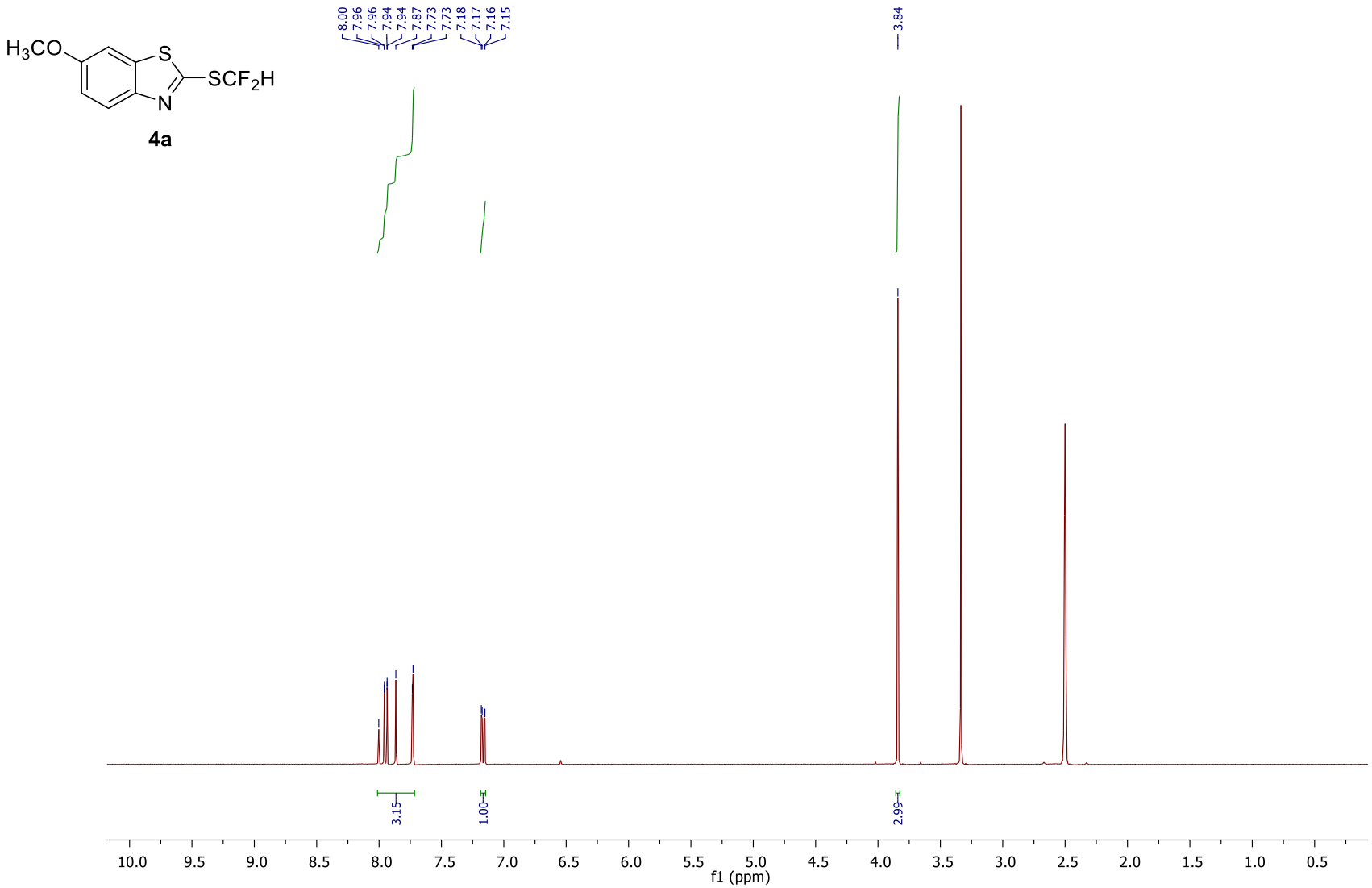

Figure S1. ^{1}H-NMR spectrum of 2-((difluoromethyl)thio)-6-methoxybenzo[*d*]thiazole (**4a**).

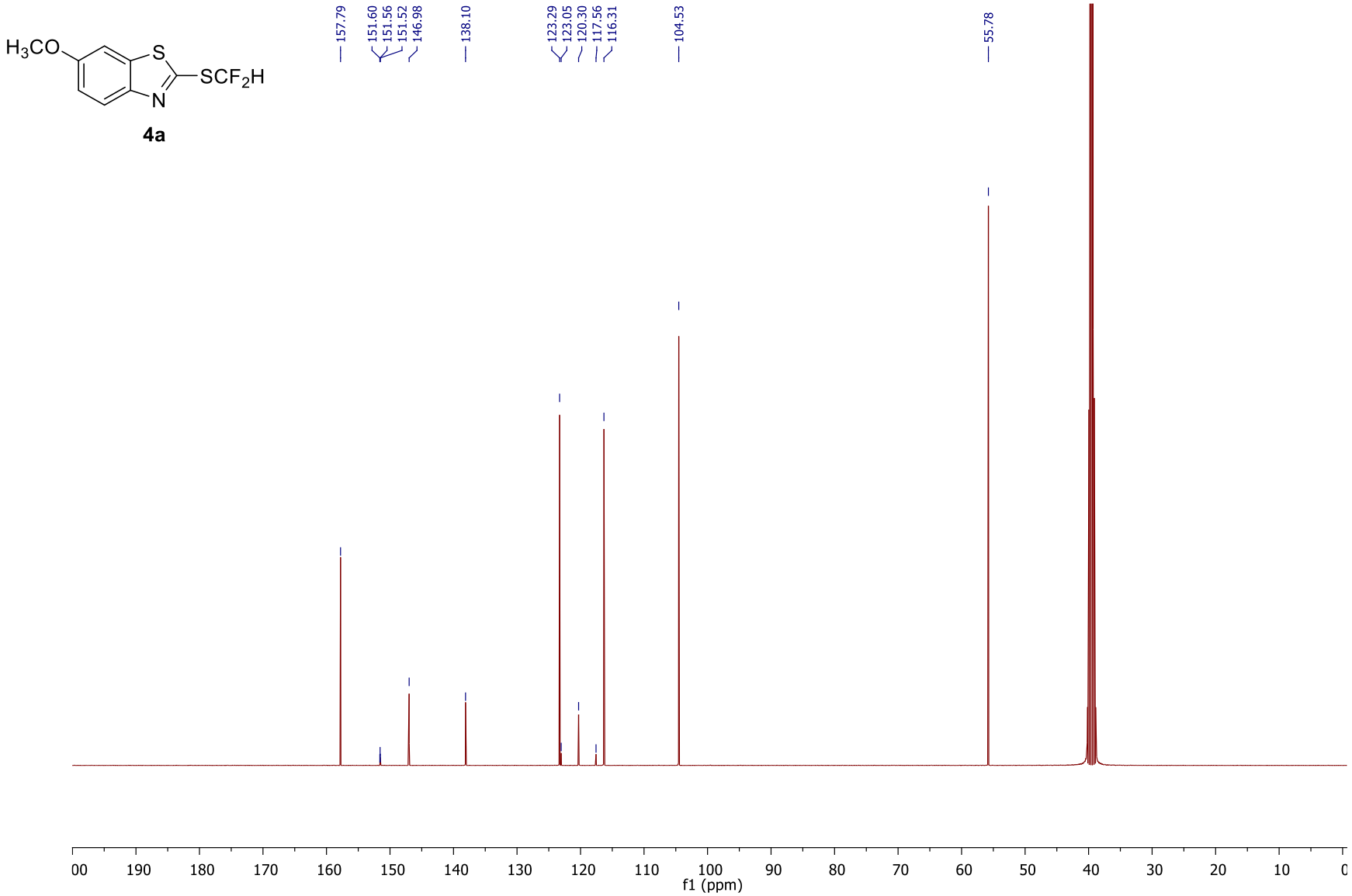

Figure S2. ^{13}C-NMR spectrum of 2-((difluoromethyl)thio)-6-methoxybenzo[*d*]thiazole (**4a**).

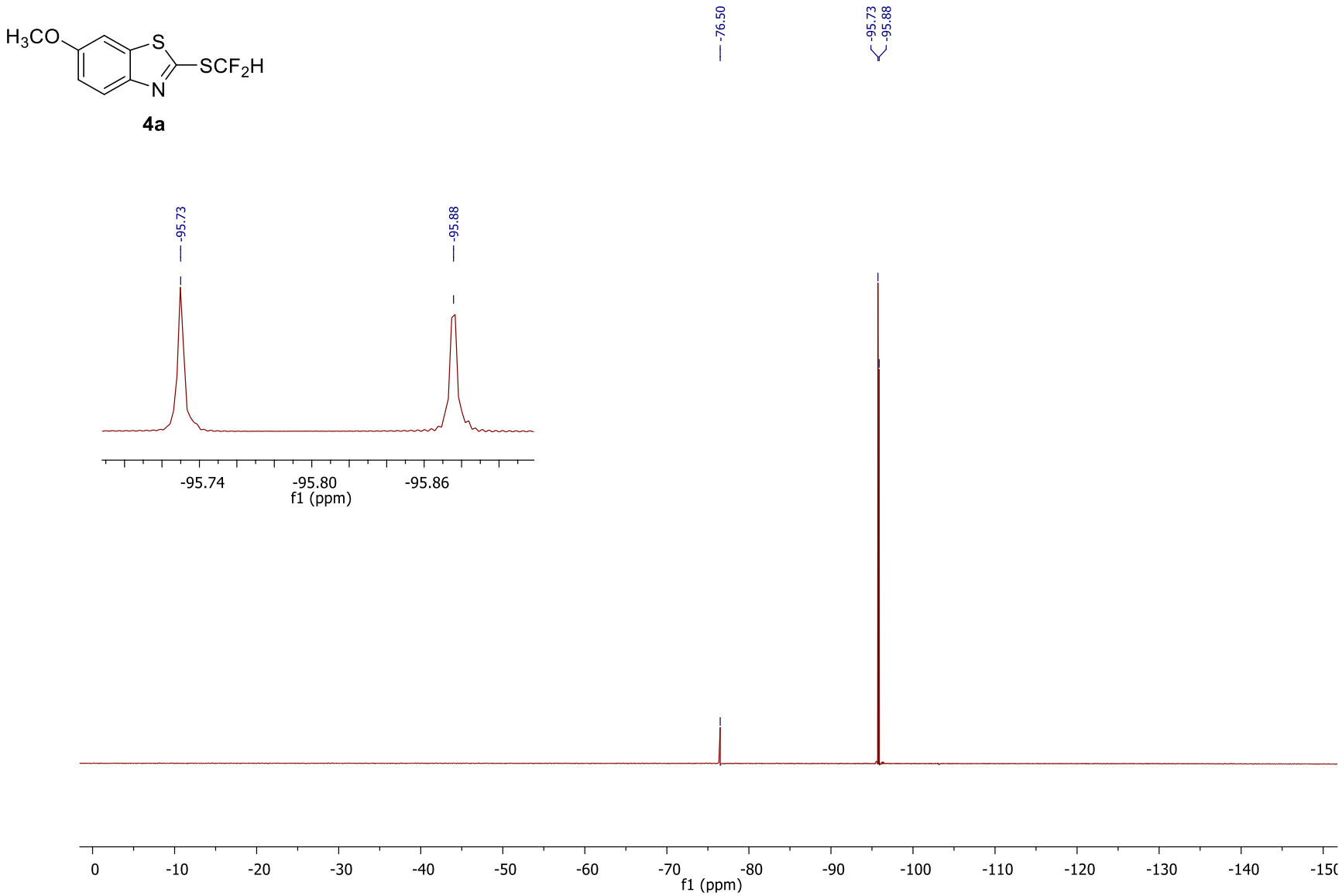

Figure S3. ^{19}F-NMR spectrum of 2-((difluoromethyl)thio)-6-methoxybenzo[*d*]thiazole (**4a**).

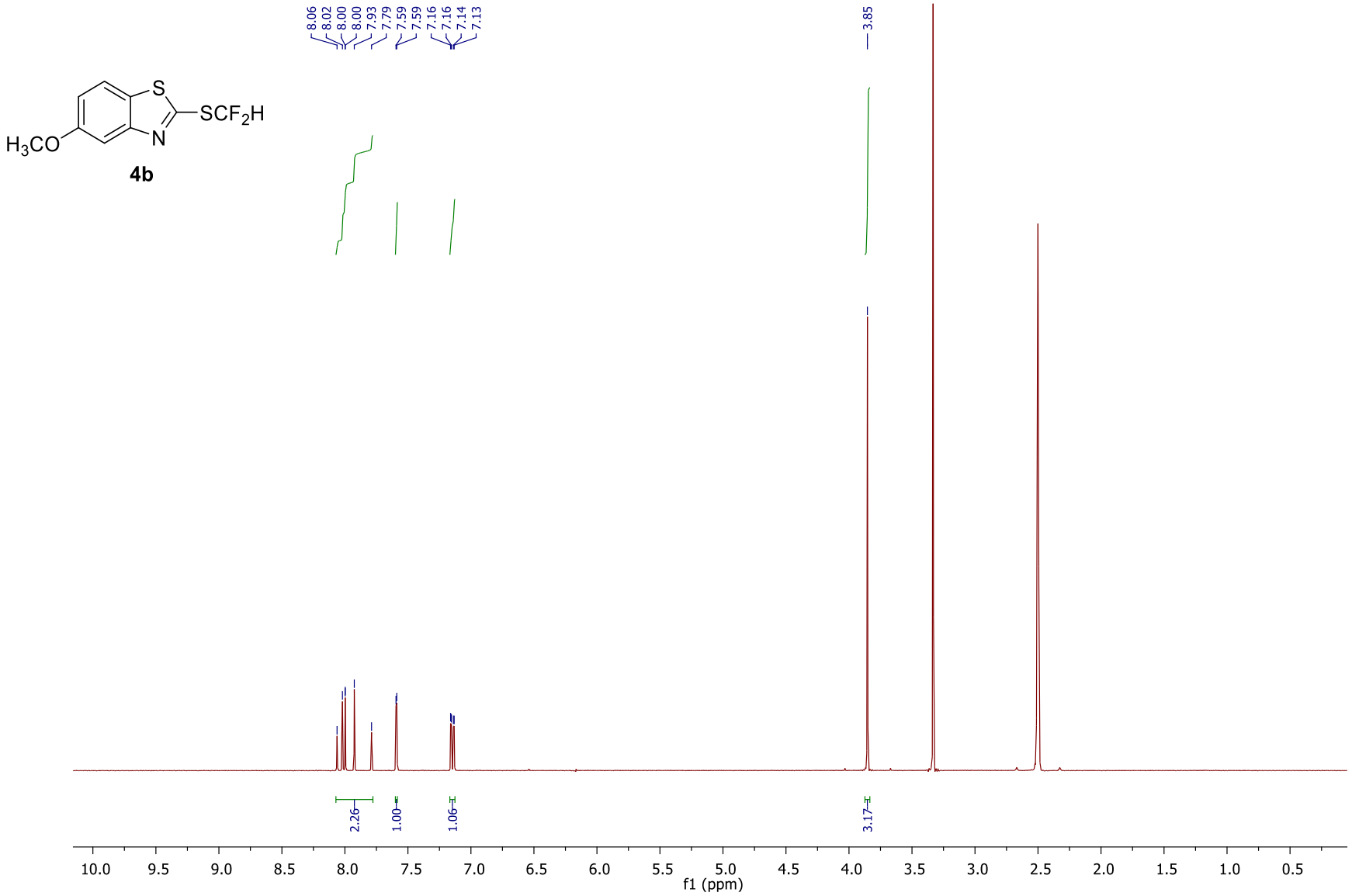

Figure S4. ^{1}H-NMR spectrum of 2-((difluoromethyl)thio)-5-methoxybenzo[*d*]thiazole (**4b**).

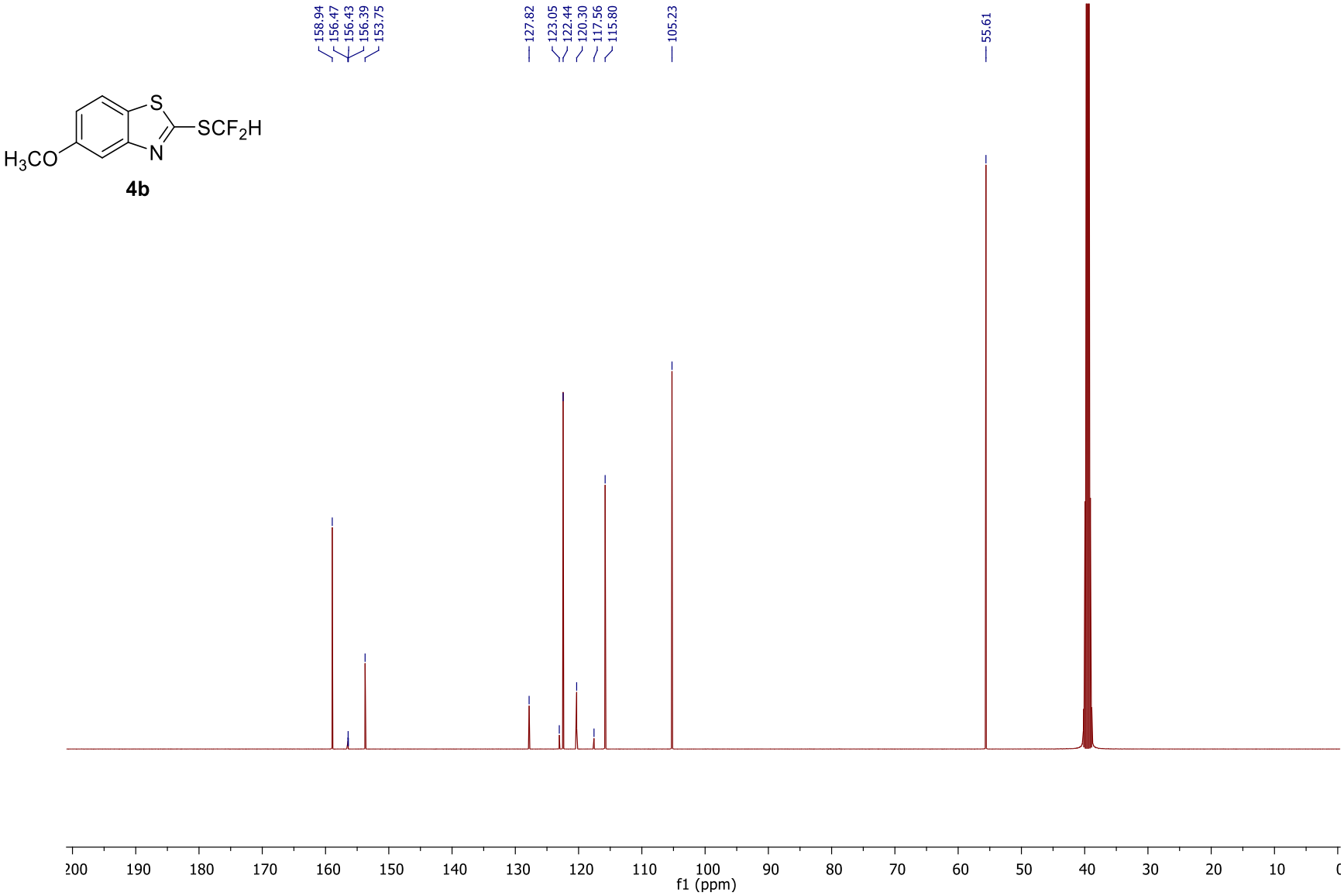

Figure S5. ^{13}C-NMR spectrum of 2-((difluoromethyl)thio)-5-methoxybenzo[*d*]thiazole (**4b**).

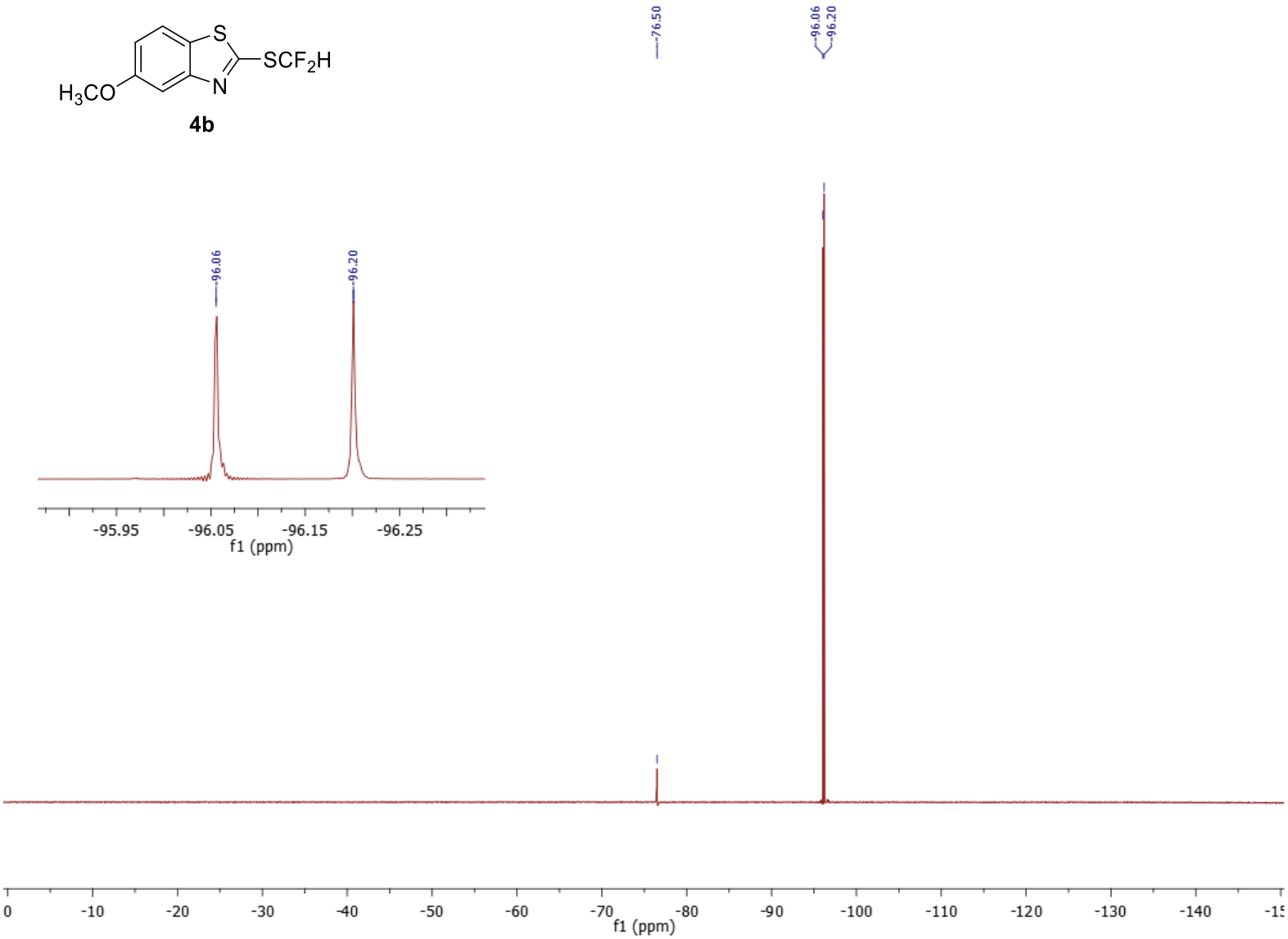

Figure S6. ^{19}F-NMR spectrum of 2-((difluoromethyl)thio)-5-methoxybenzo[*d*]thiazole (**4b**).

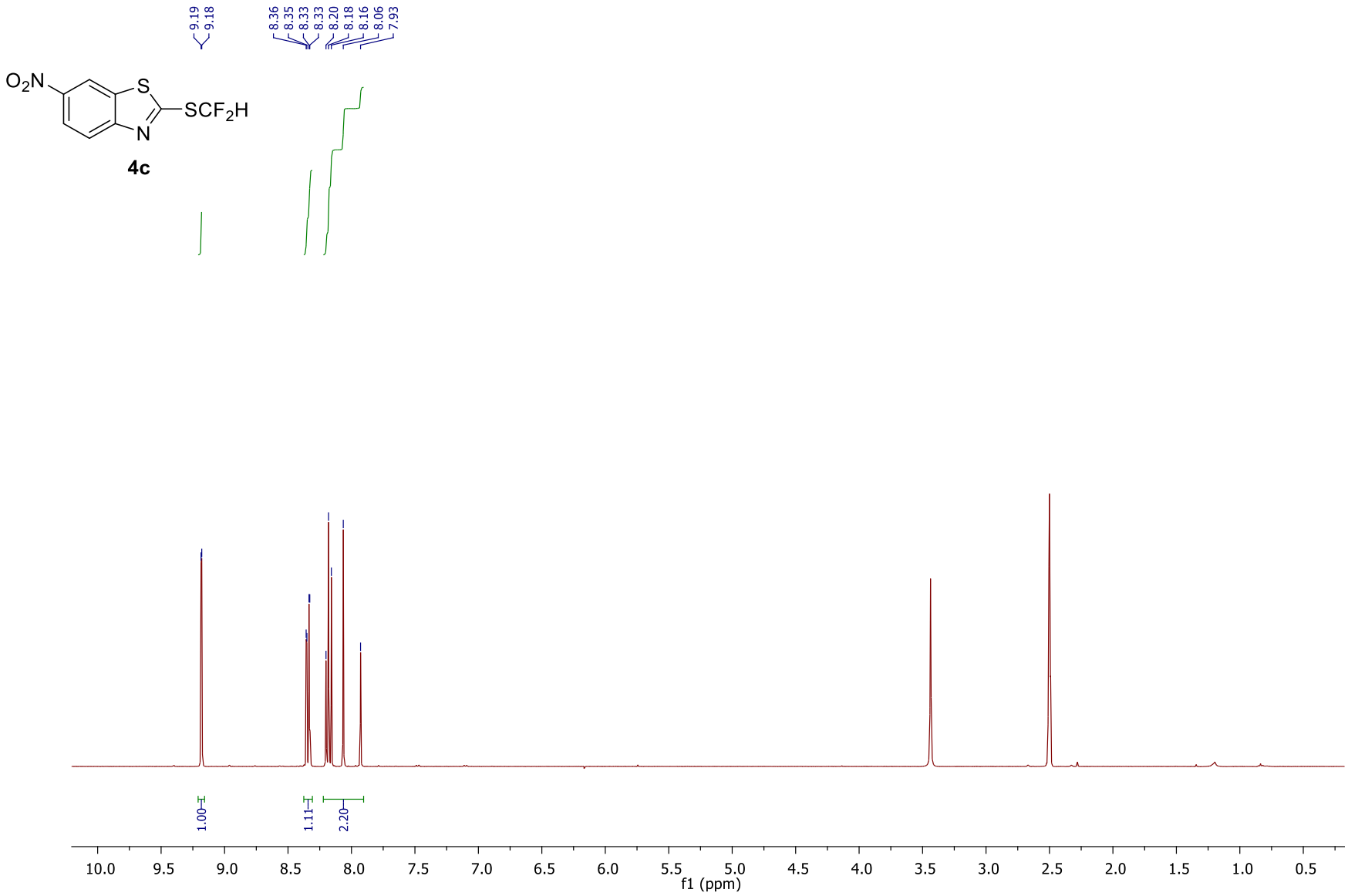

Figure S7. ^{1}H-NMR spectrum of 2-((difluoromethyl)thio)-6-nitrobenzo[*d*]thiazole (**4c**).

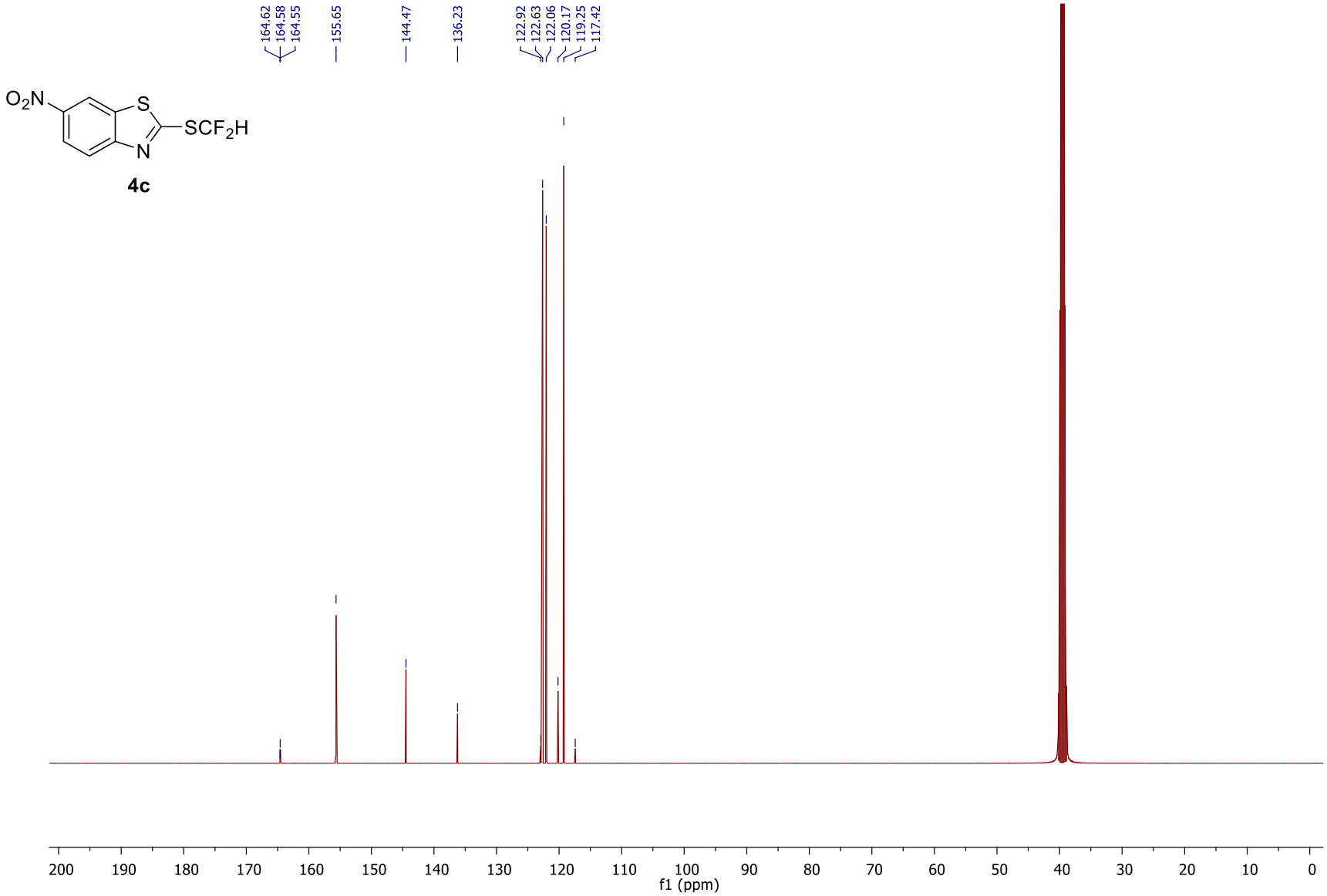

Figure S8. ^{13}C-NMR spectrum of 2-((difluoromethyl)thio)-6-nitrobenzo[*d*]thiazole (**4c**).

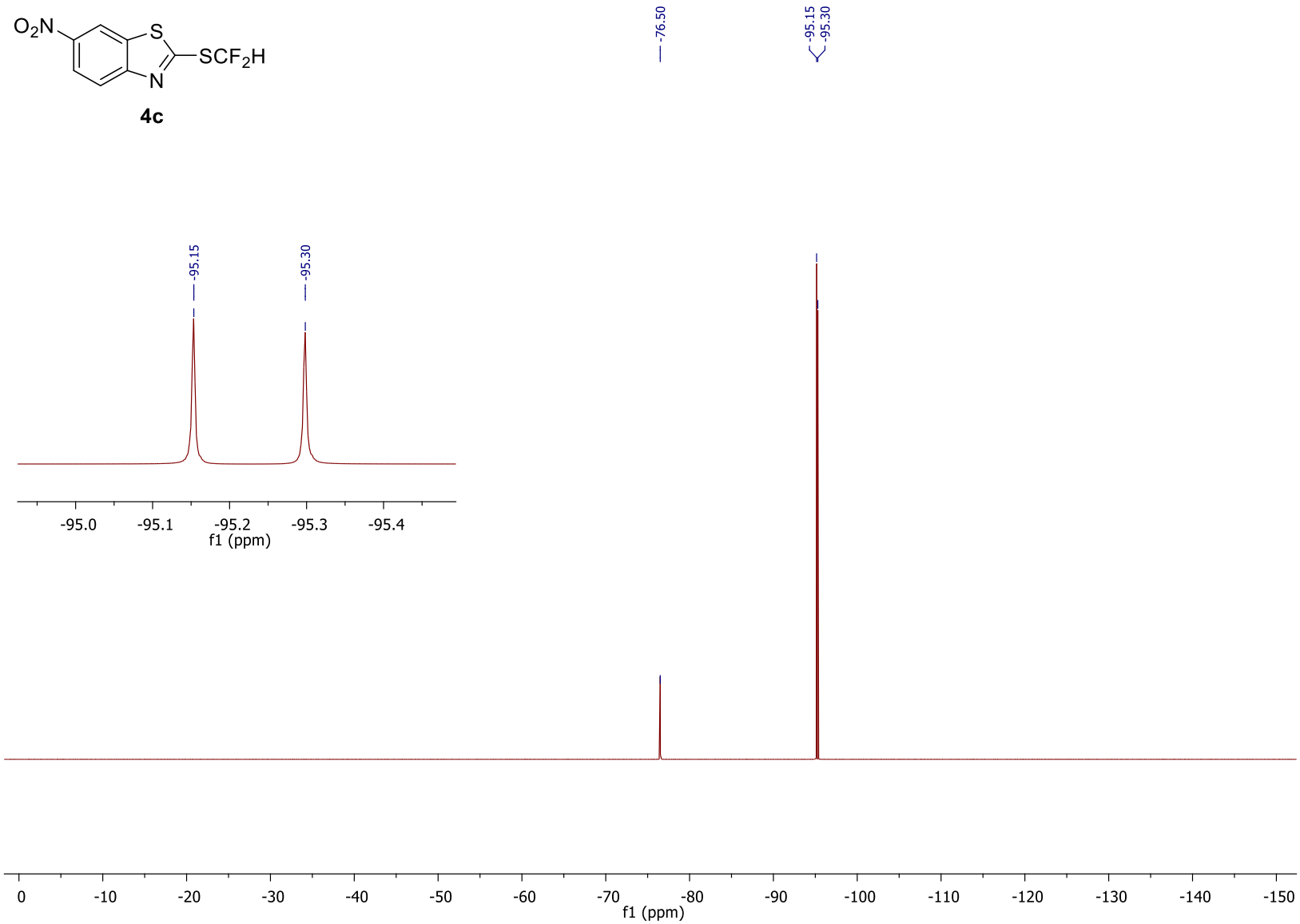

Figure S9. ^{19}F-NMR spectrum of 2-((difluoromethyl)thio)-6-nitrobenzo[*d*]thiazole (**4c**).

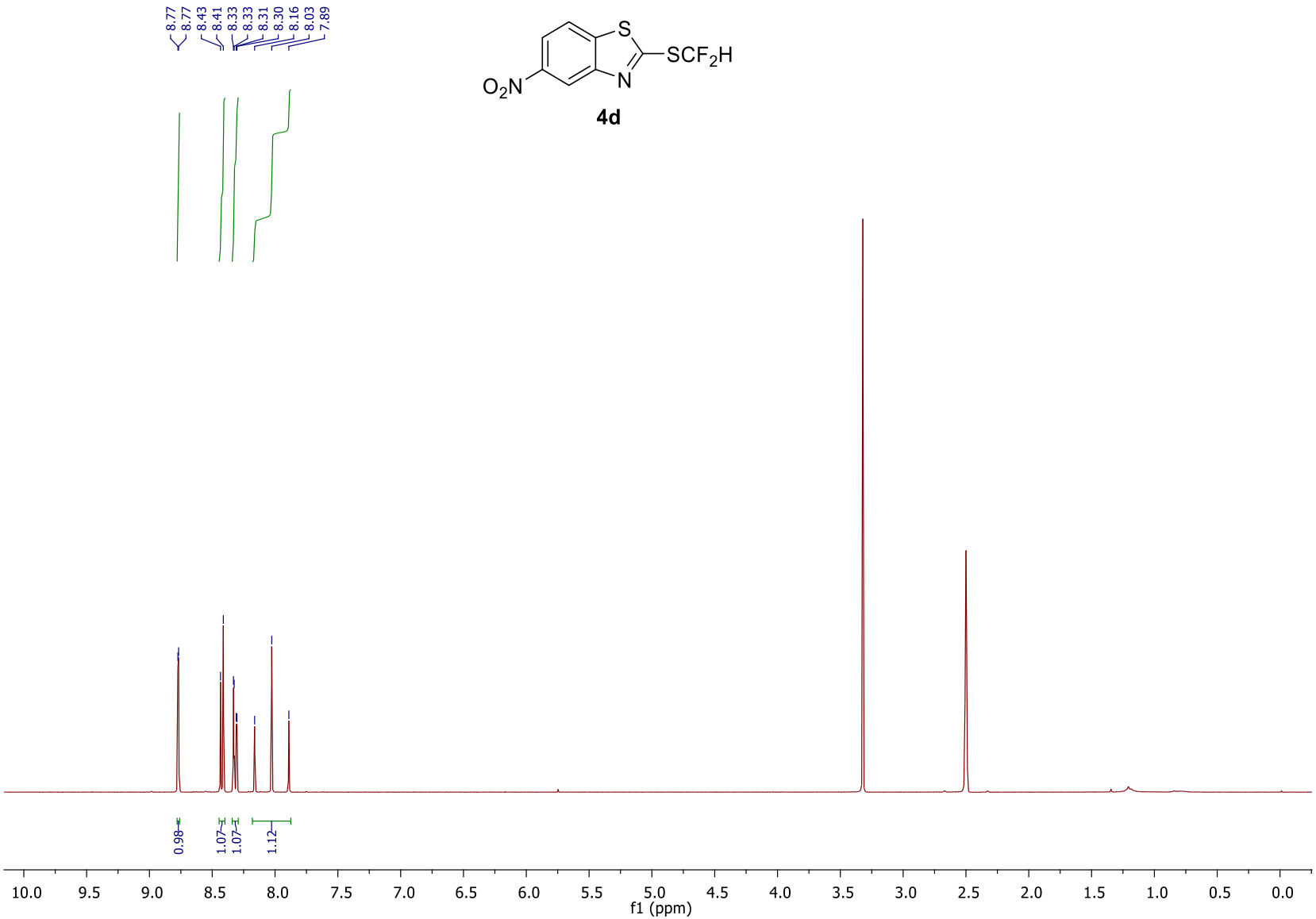

Figure S10. ^{1}H-NMR spectrum of 2-((difluoromethyl)thio)-5-nitrobenzo[*d*]thiazole (**4d**).

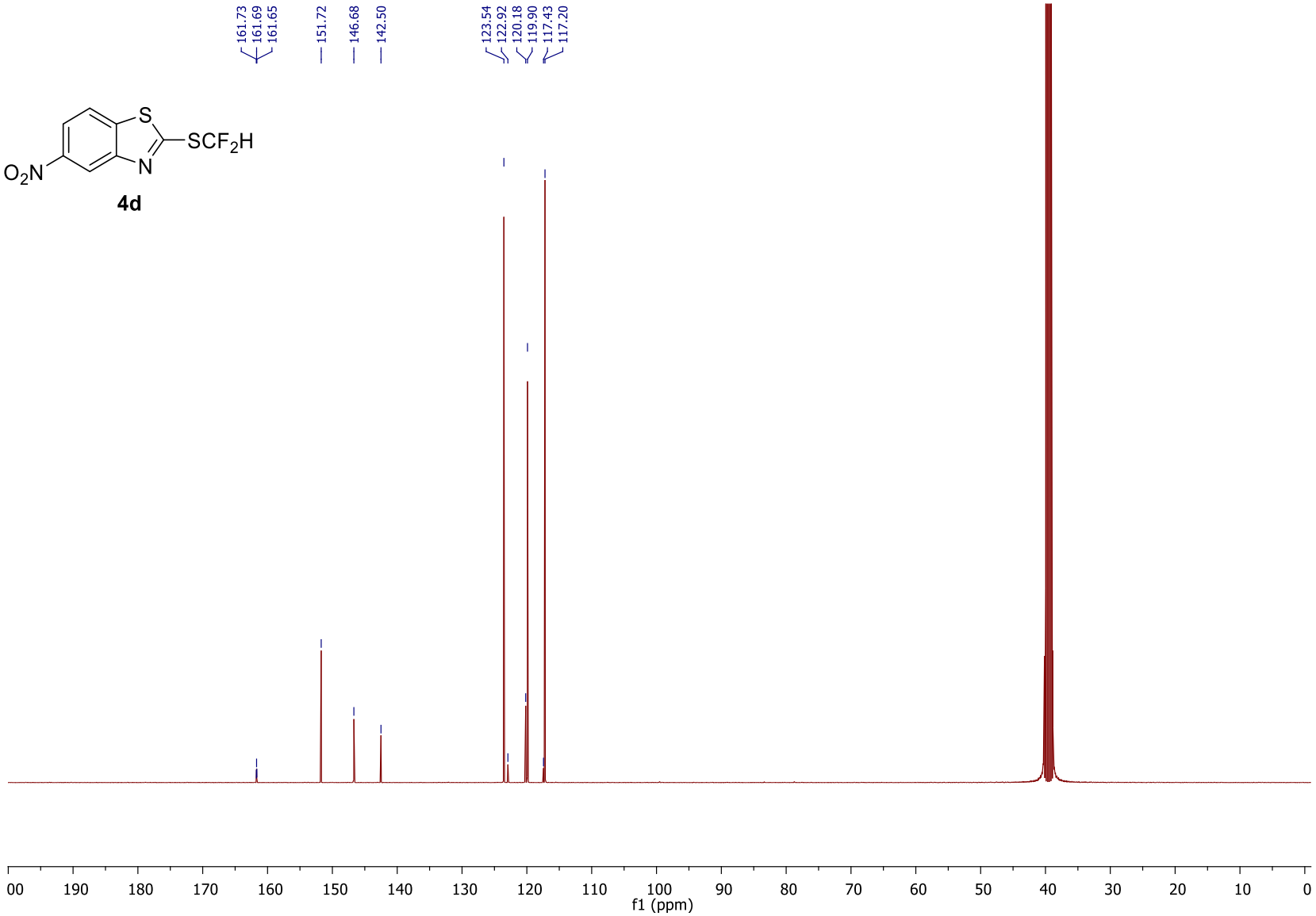

Figure S11. ^{13}C-NMR spectrum of 2-((difluoromethyl)thio)-5-nitrobenzo[*d*]thiazole (**4d**).

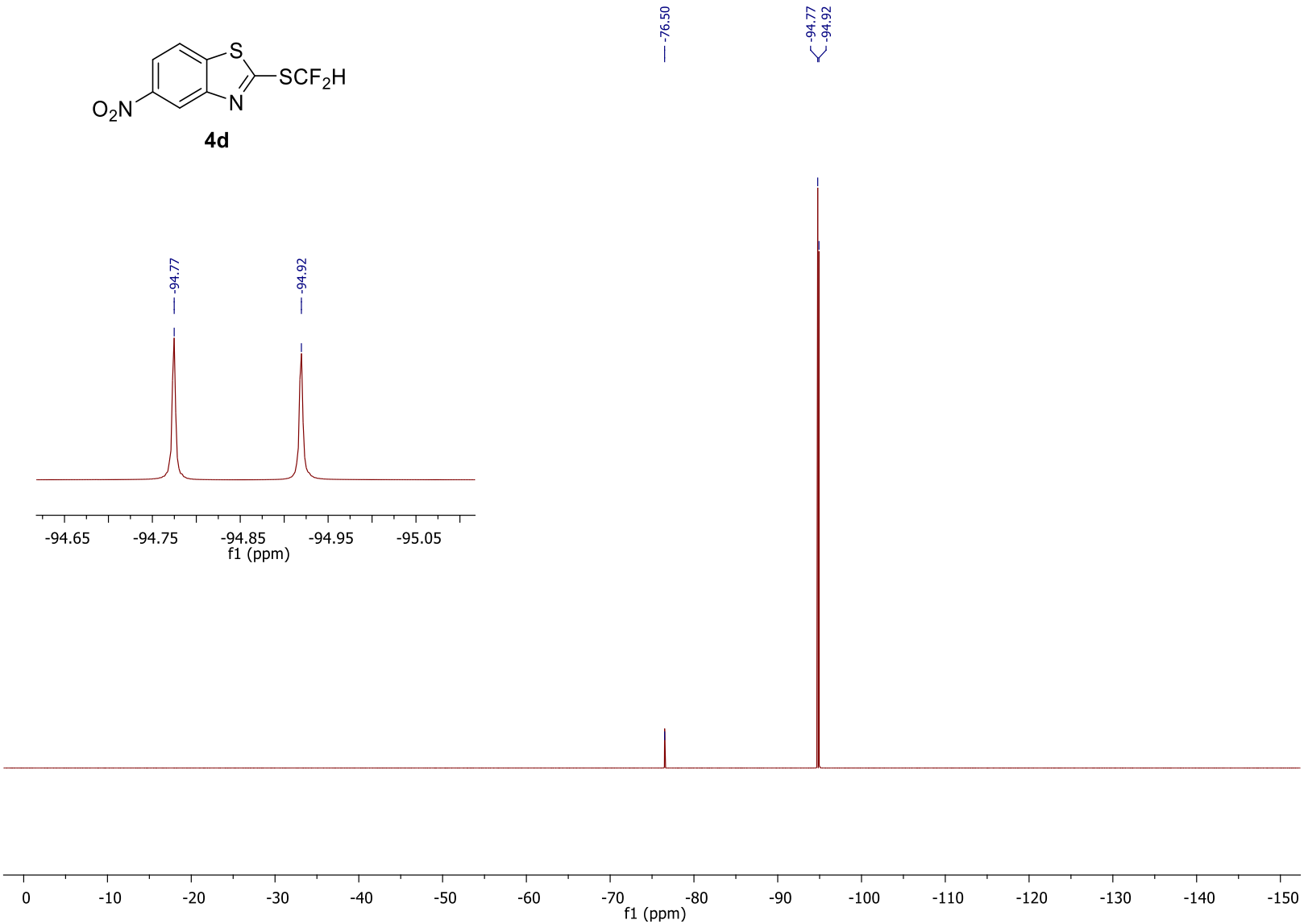

Figure S12. ^{19}F-NMR spectrum of 2-((difluoromethyl)thio)-5-nitrobenzo[*d*]thiazole (**4d**).

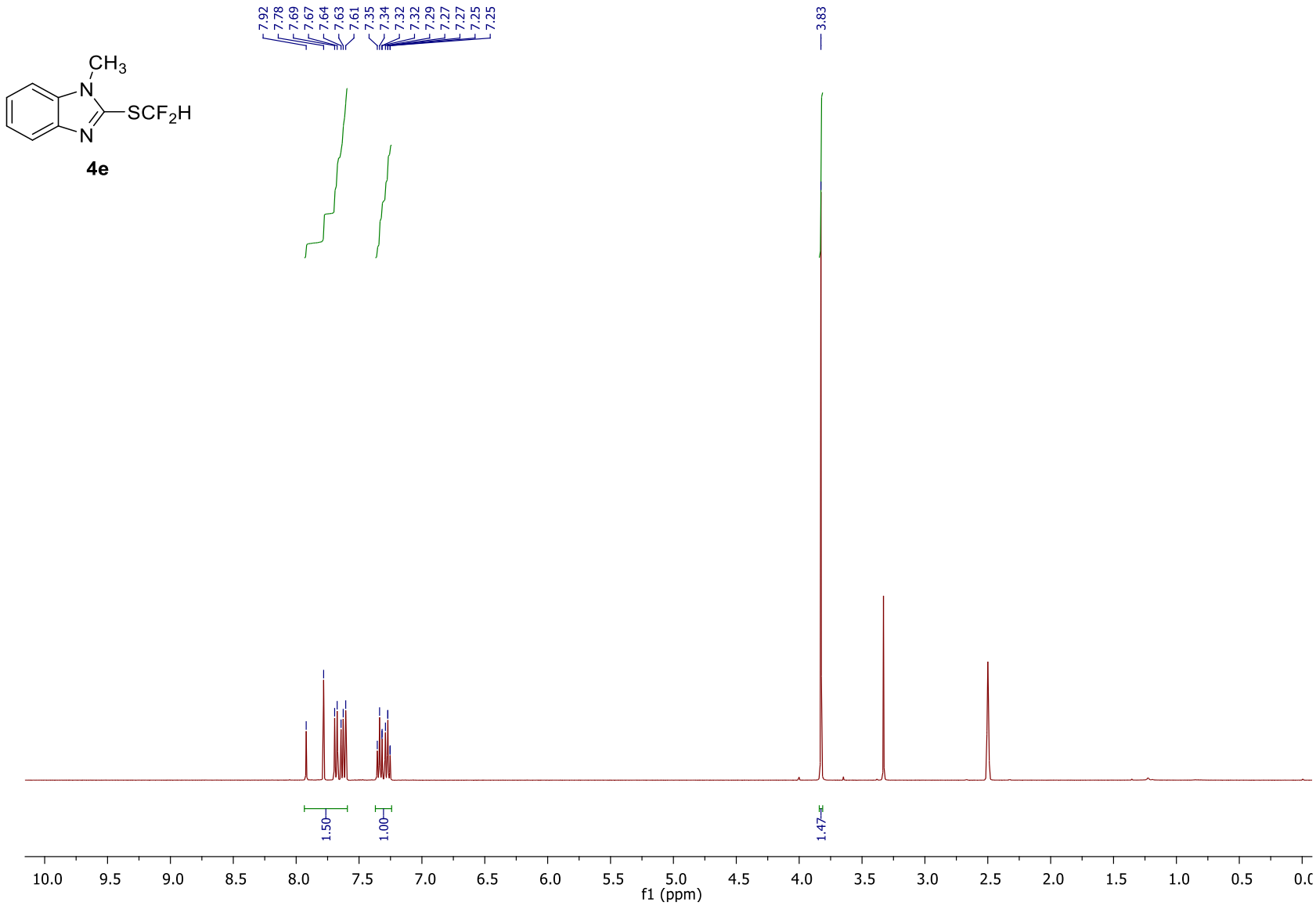

Figure S13. ^{1}H-NMR spectrum of 2-((difluoromethyl)thio)-1-methyl-1*H*-benzo[*d*]imidazole (**4e**).

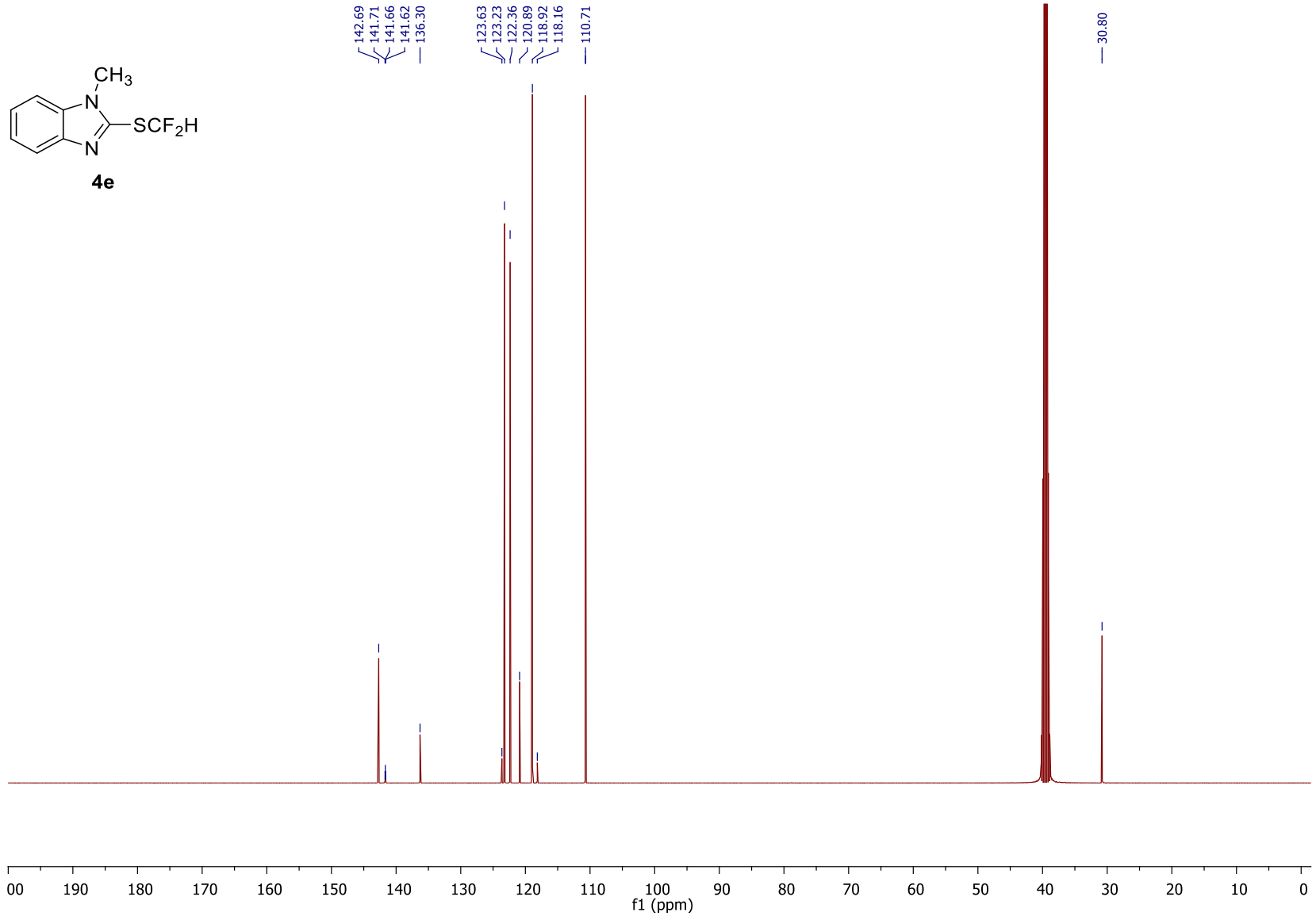

Figure S14. ^{13}C-NMR spectrum of 2-((difluoromethyl)thio)-1-methyl-1*H*-benzo[*d*]imidazole (**4e**).

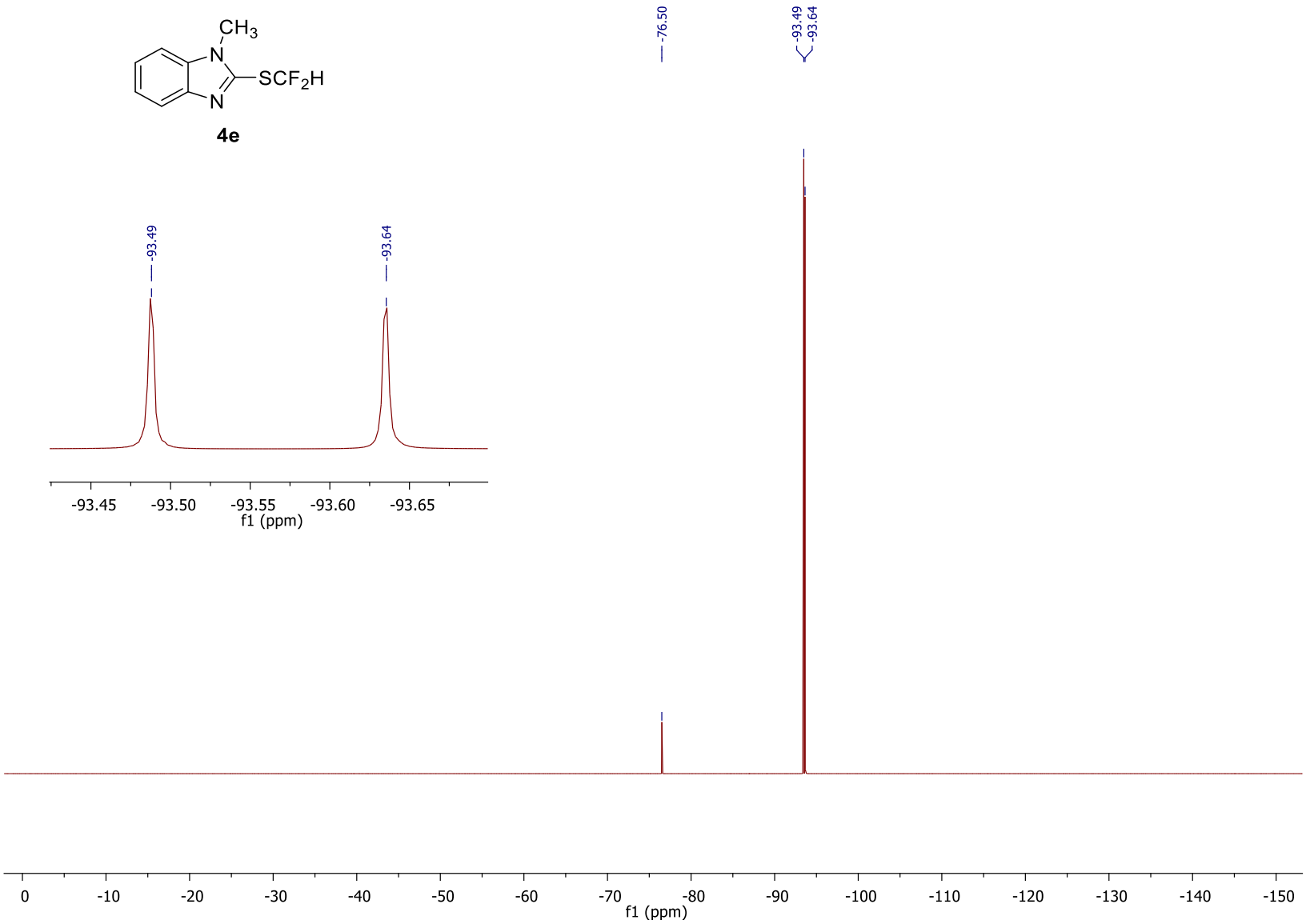

Figure S15. ^{19}F-NMR spectrum of 2-((difluoromethyl)thio)-1-methyl-1*H*-benzo[*d*]imidazole (**4e**).

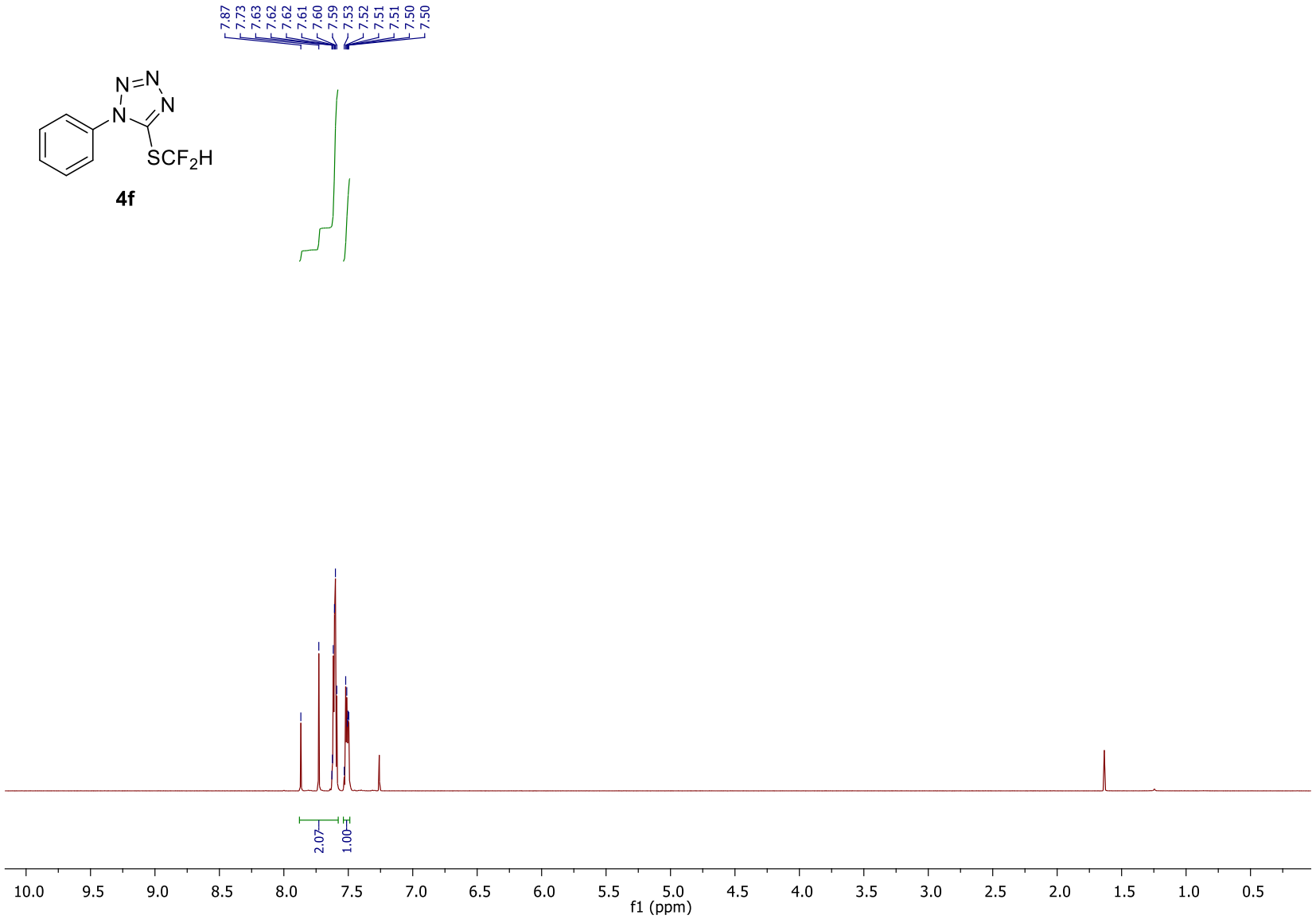

Figure S16. ^{1}H-NMR spectrum of 5-((difluoromethyl)thio)-1-phenyl-1*H*-tetrazole (**4f**).

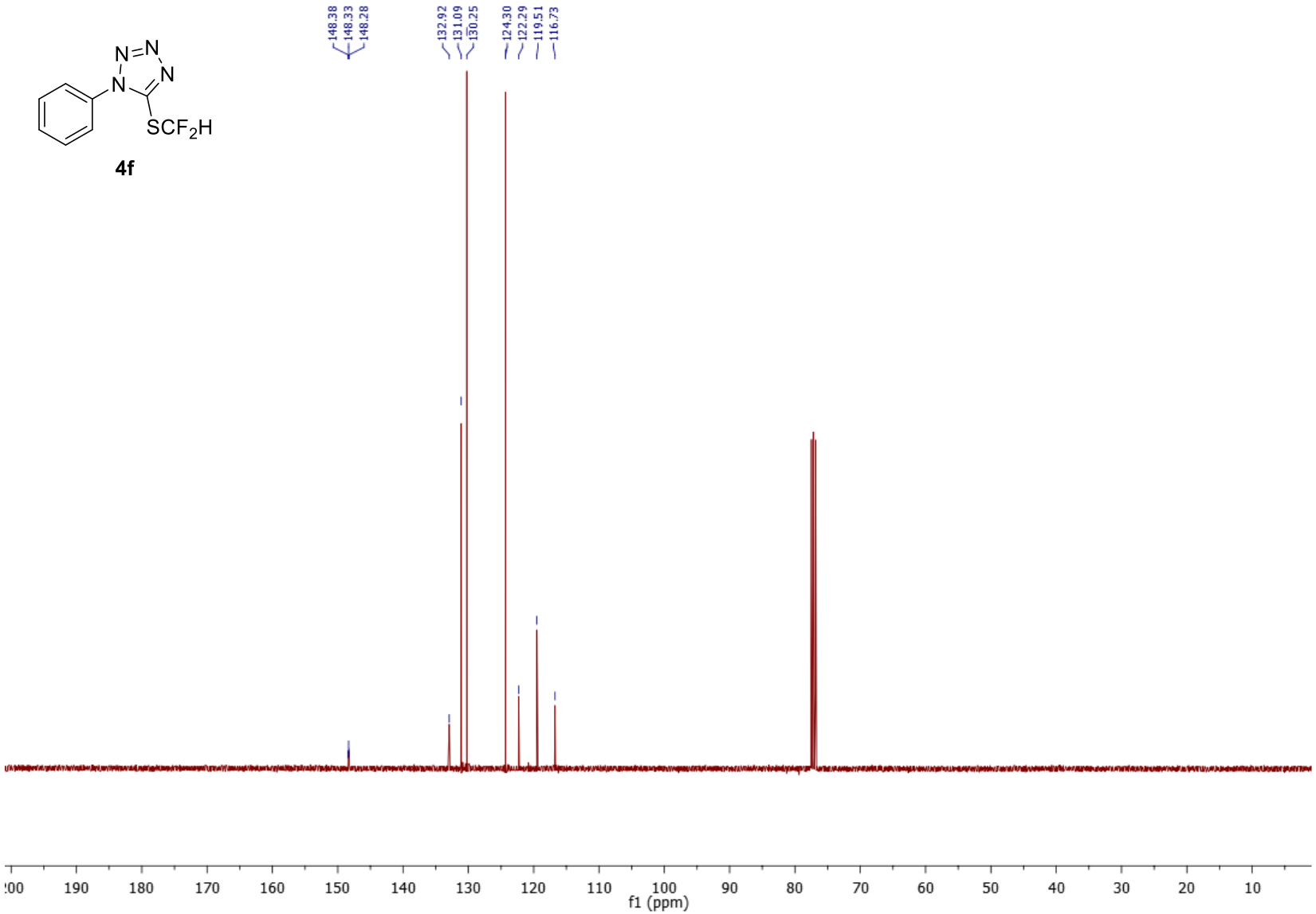

Figure S17. ^{13}C-NMR spectrum of 5-((difluoromethyl)thio)-1-phenyl-1*H*-tetrazole (**4f**).

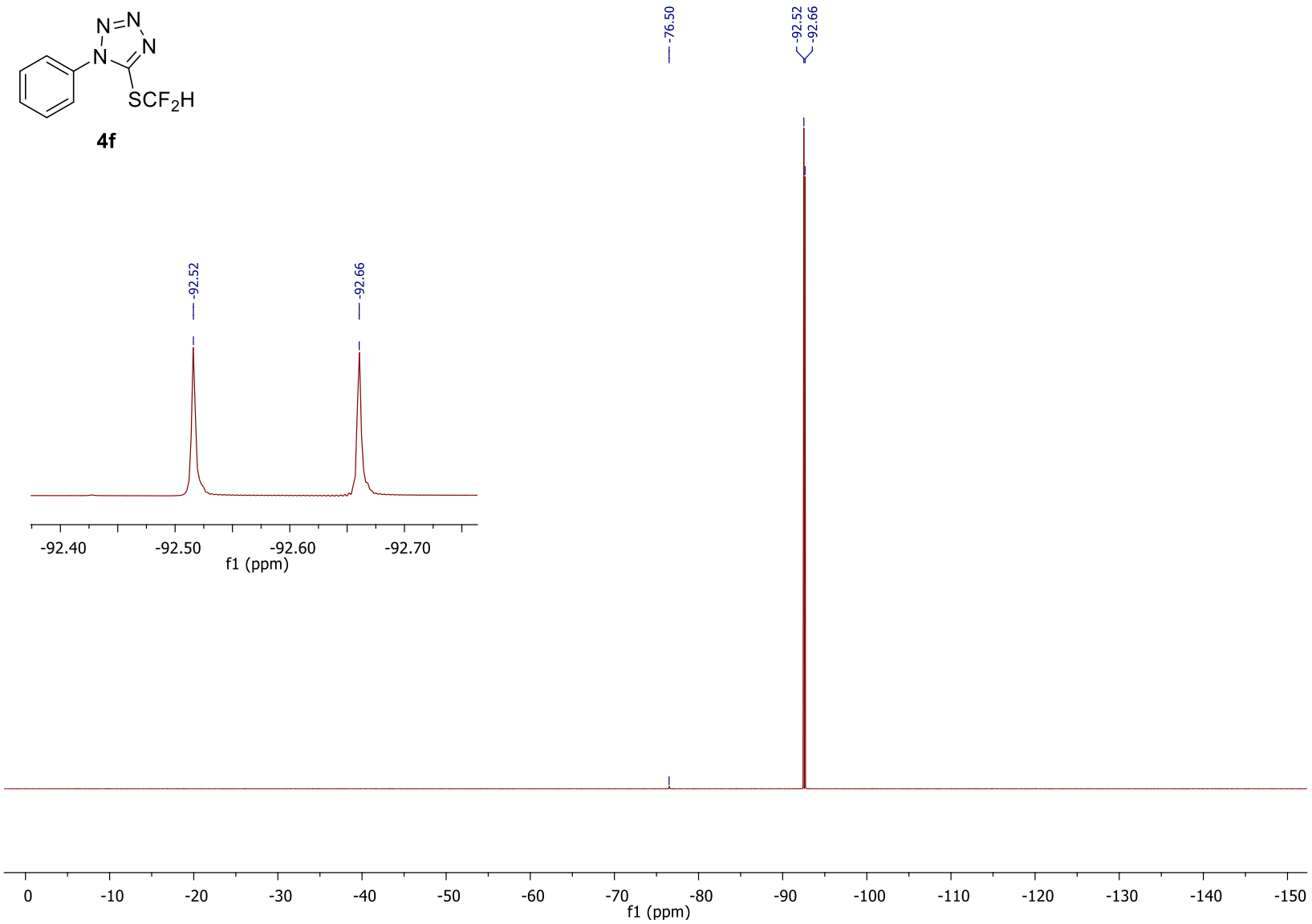

Figure S18. ^{19}F-NMR spectrum of 5-((difluoromethyl)thio)-1-phenyl-1*H*-tetrazole (**4f**).

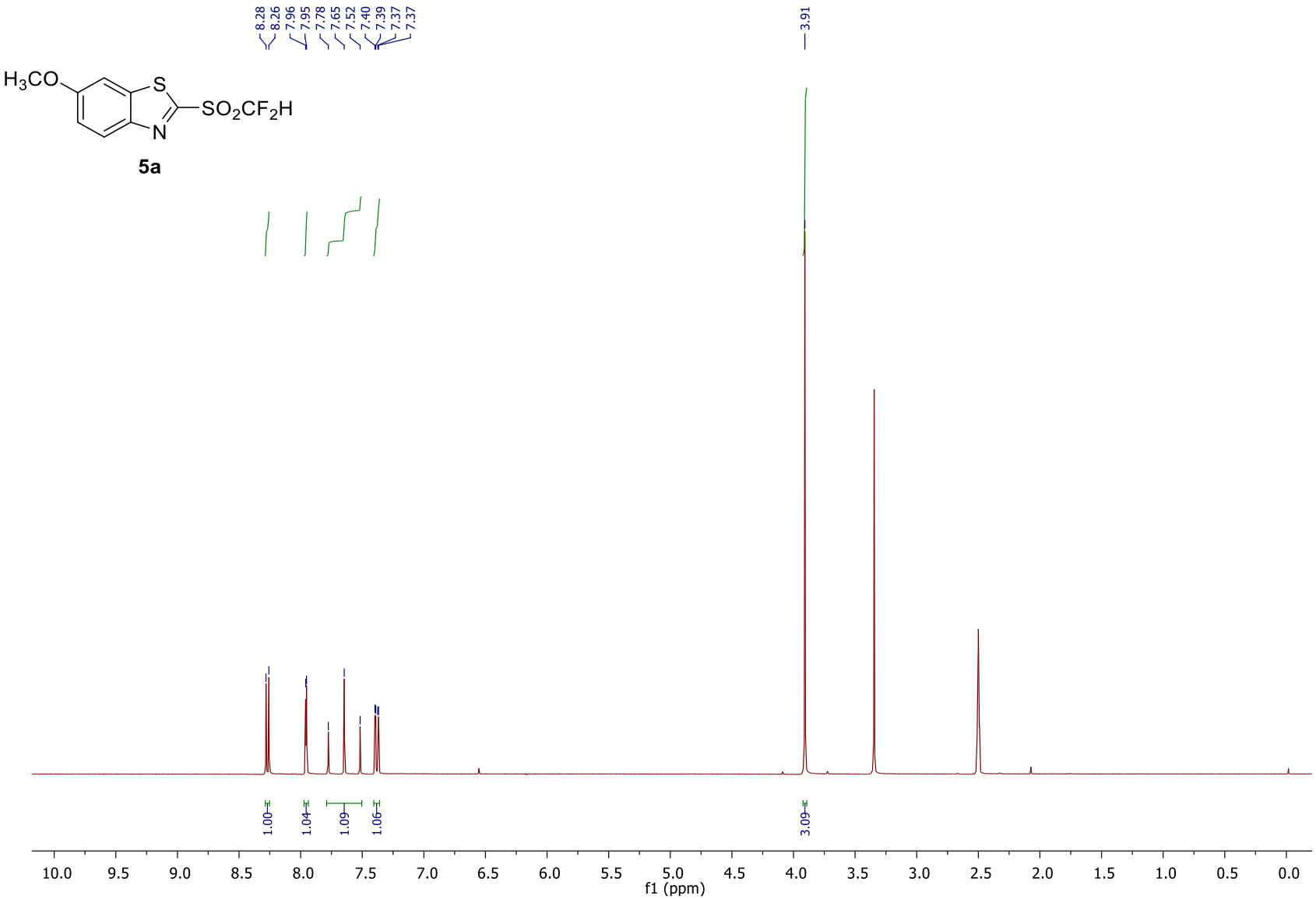

Figure S19. ^{1}H-NMR spectrum of 2-((difluoromethyl)sulfonyl)-6-methoxybenzo[*d*]thiazole (**5a**).

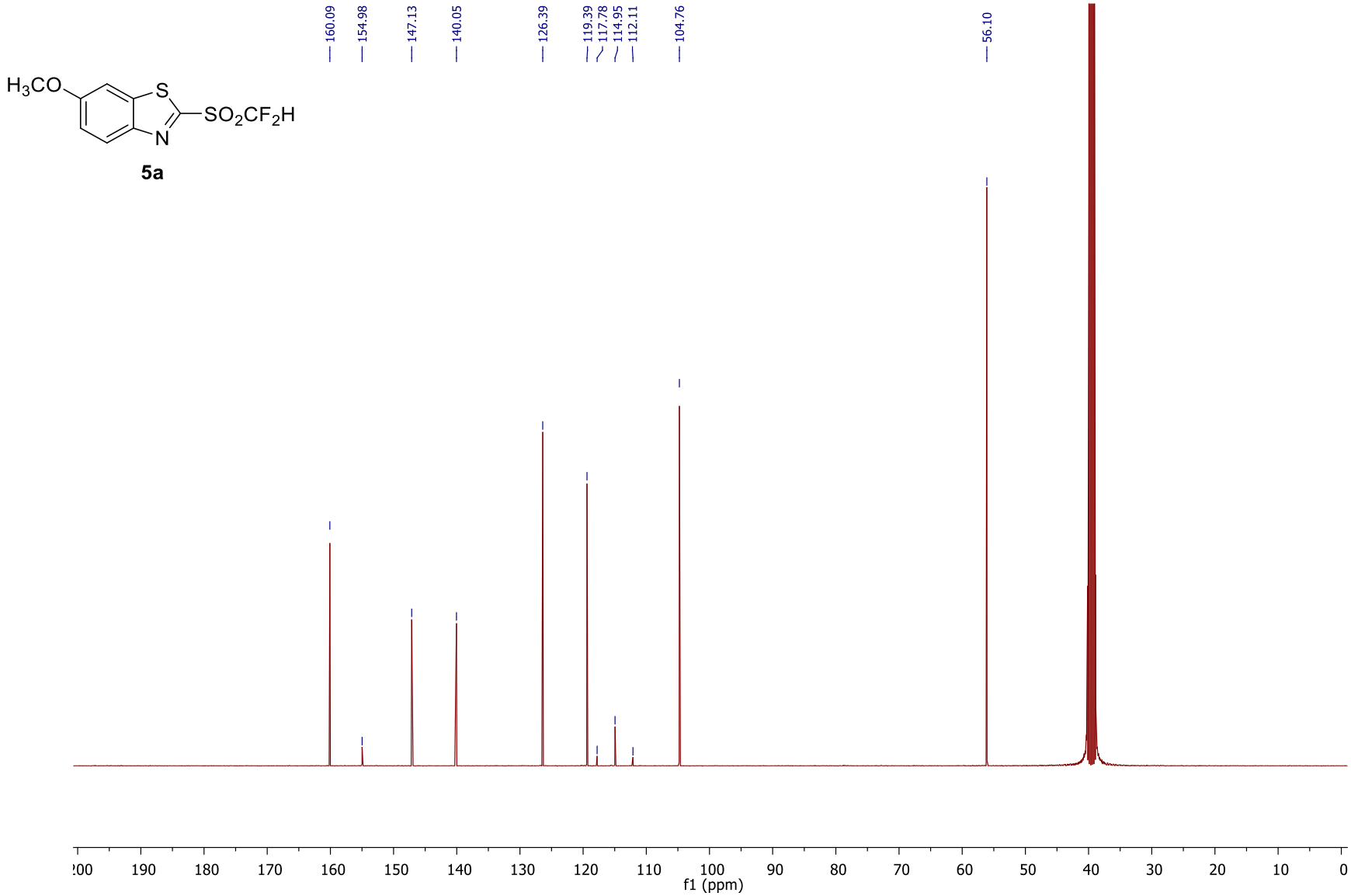

Figure S20. ^{13}C-NMR spectrum of 2-((difluoromethyl)sulfonyl)-6-methoxybenzo[*d*]thiazole (**5a**).

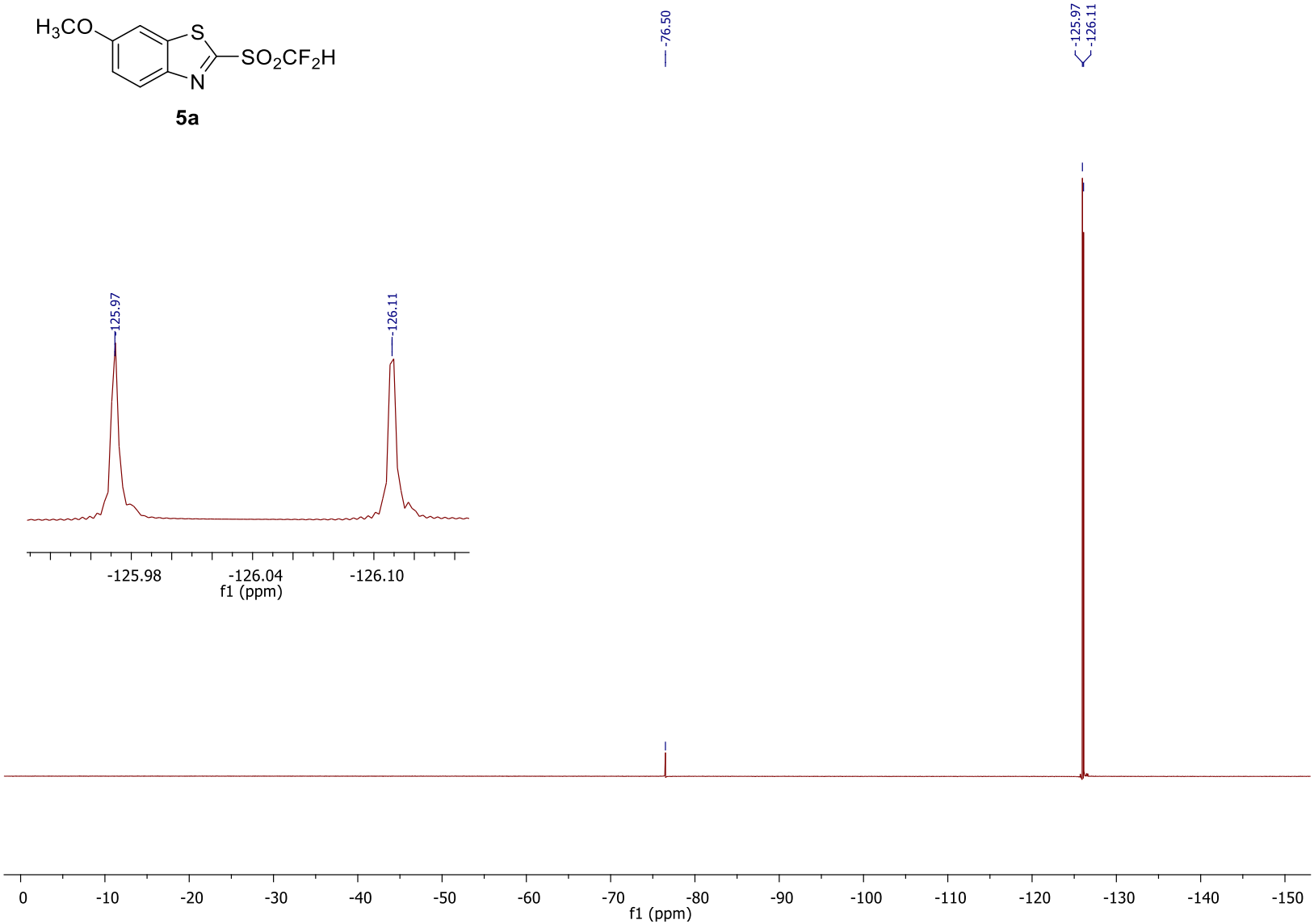

Figure S21. ^{19}F-NMR spectrum of 2-((difluoromethyl)sulfonyl)-6-methoxybenzo[*d*]thiazole (**5a**).

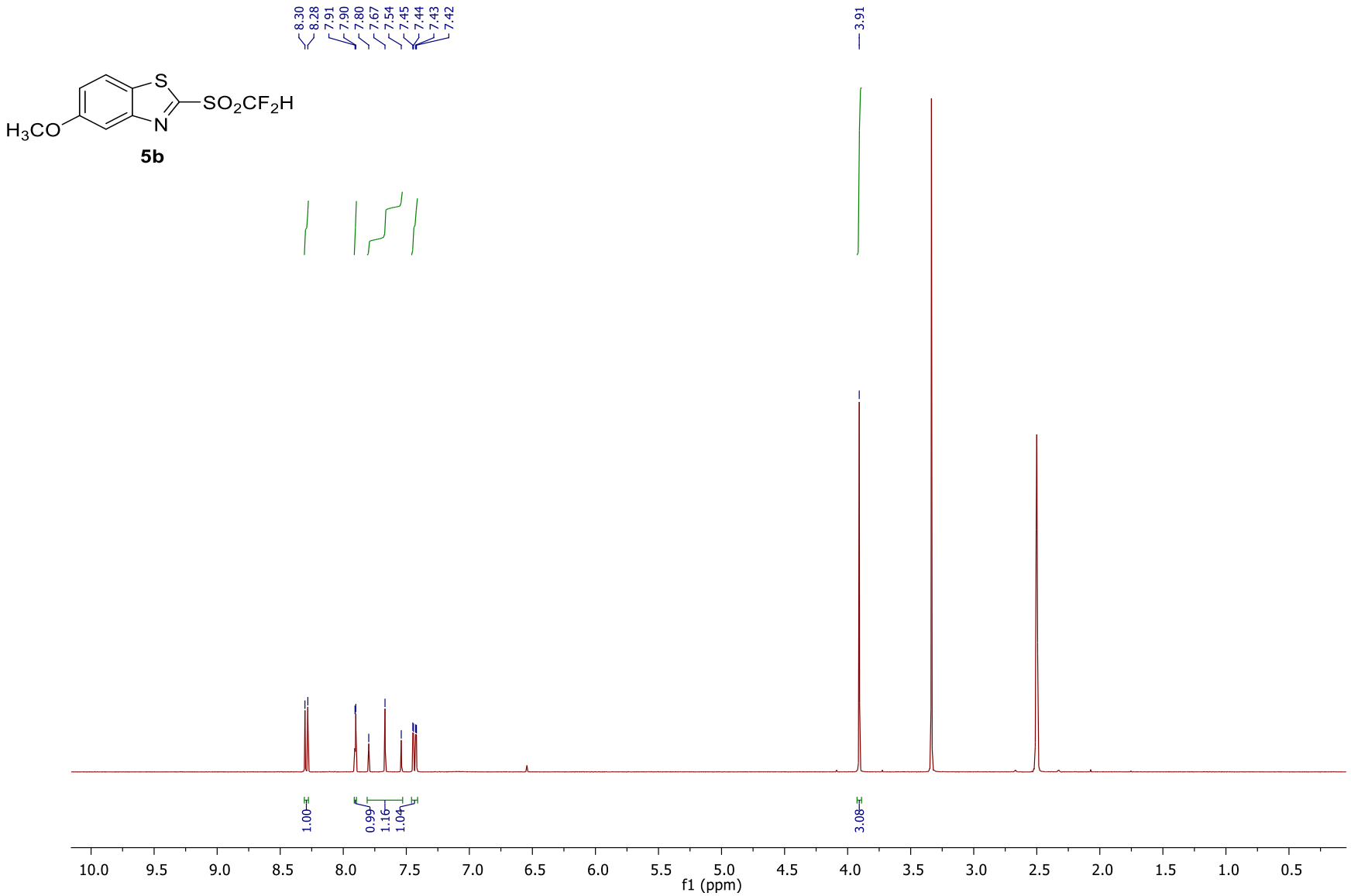

Figure S22. ^{1}H-NMR spectrum of 2-((difluoromethyl)sulfonyl)-5-methoxybenzo[*d*]thiazole (**5b**).

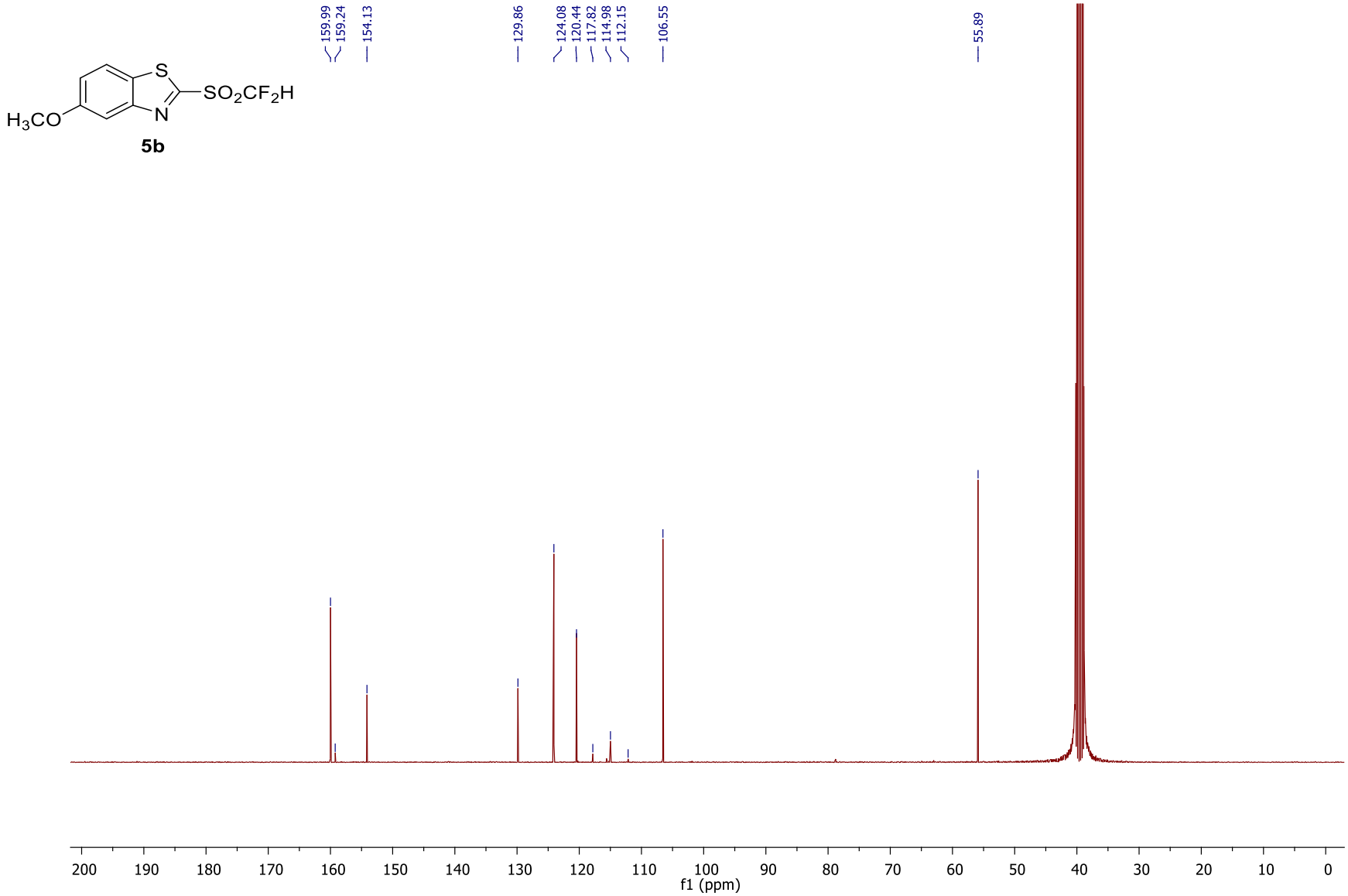

Figure S23. ^{13}C-NMR spectrum of 2-((difluoromethyl)sulfonyl)-5-methoxybenzo[*d*]thiazole (**5b**).

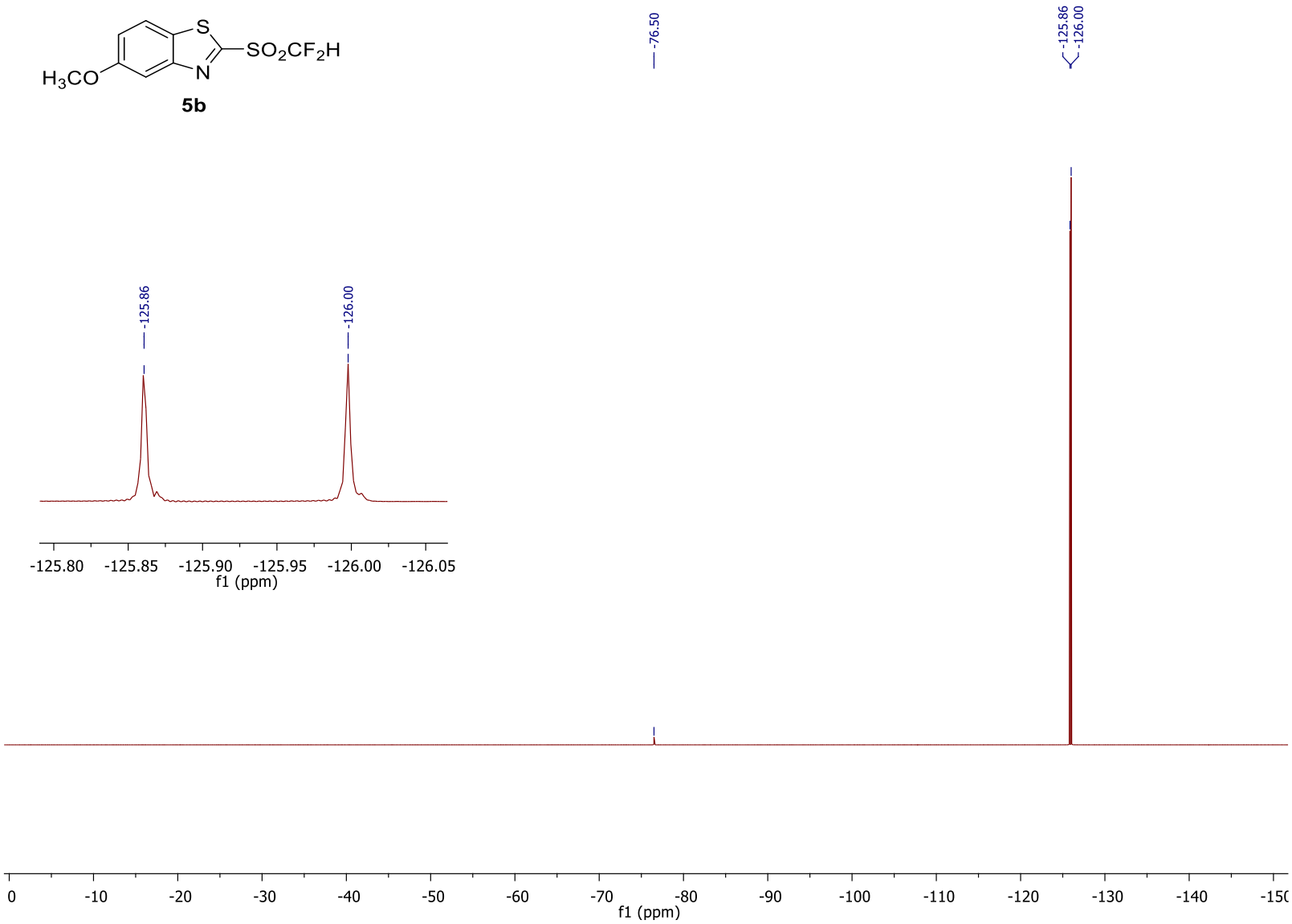

Figure S24. ^{19}F-NMR spectrum of 2-((difluoromethyl)sulfonyl)-5-methoxybenzo[*d*]thiazole (**5b**).

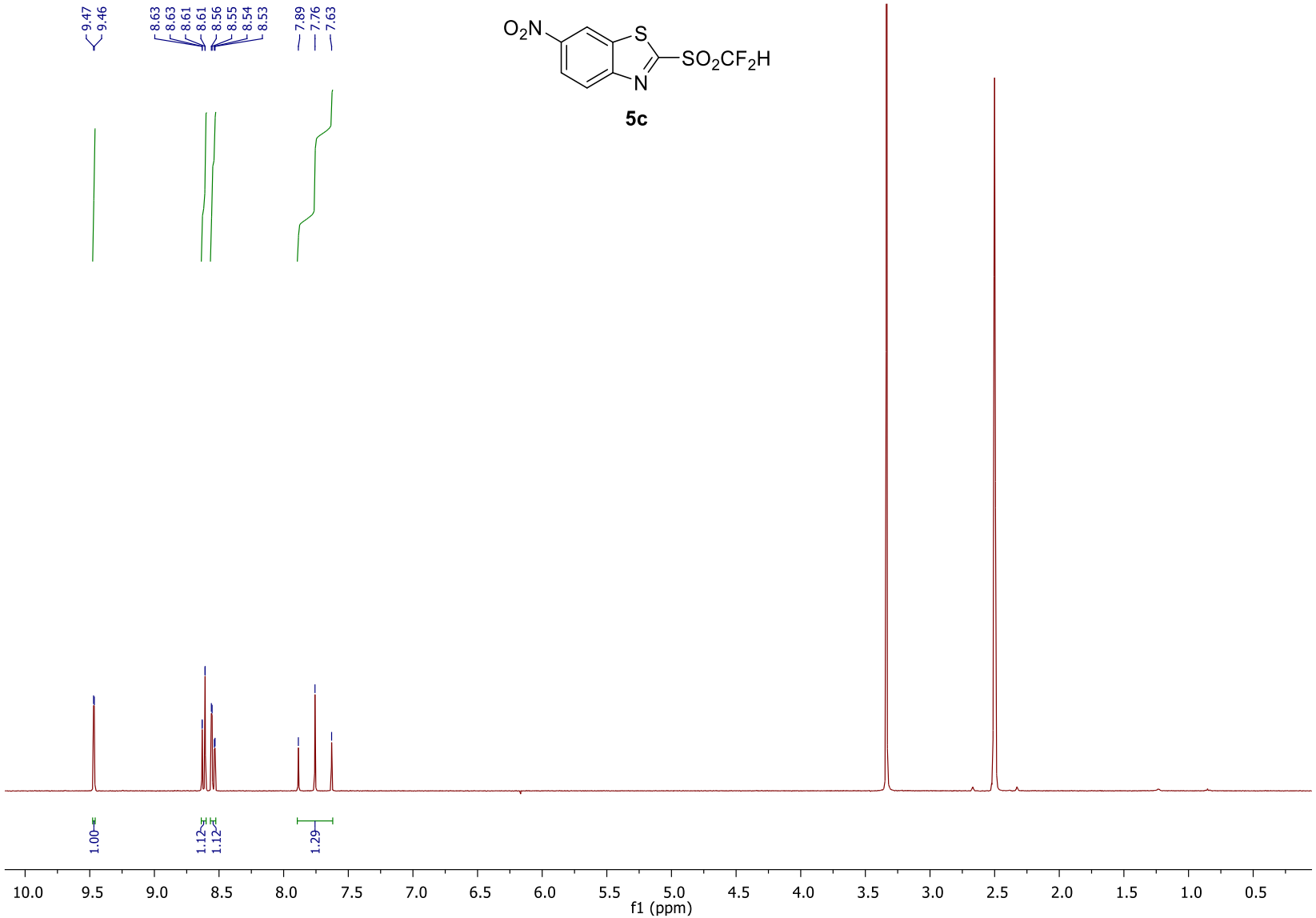

Figure S25. ^{1}H-NMR spectrum of 2-((difluoromethyl)sulfonyl)-6-nitrobenzo[*d*]thiazole (**5c**).

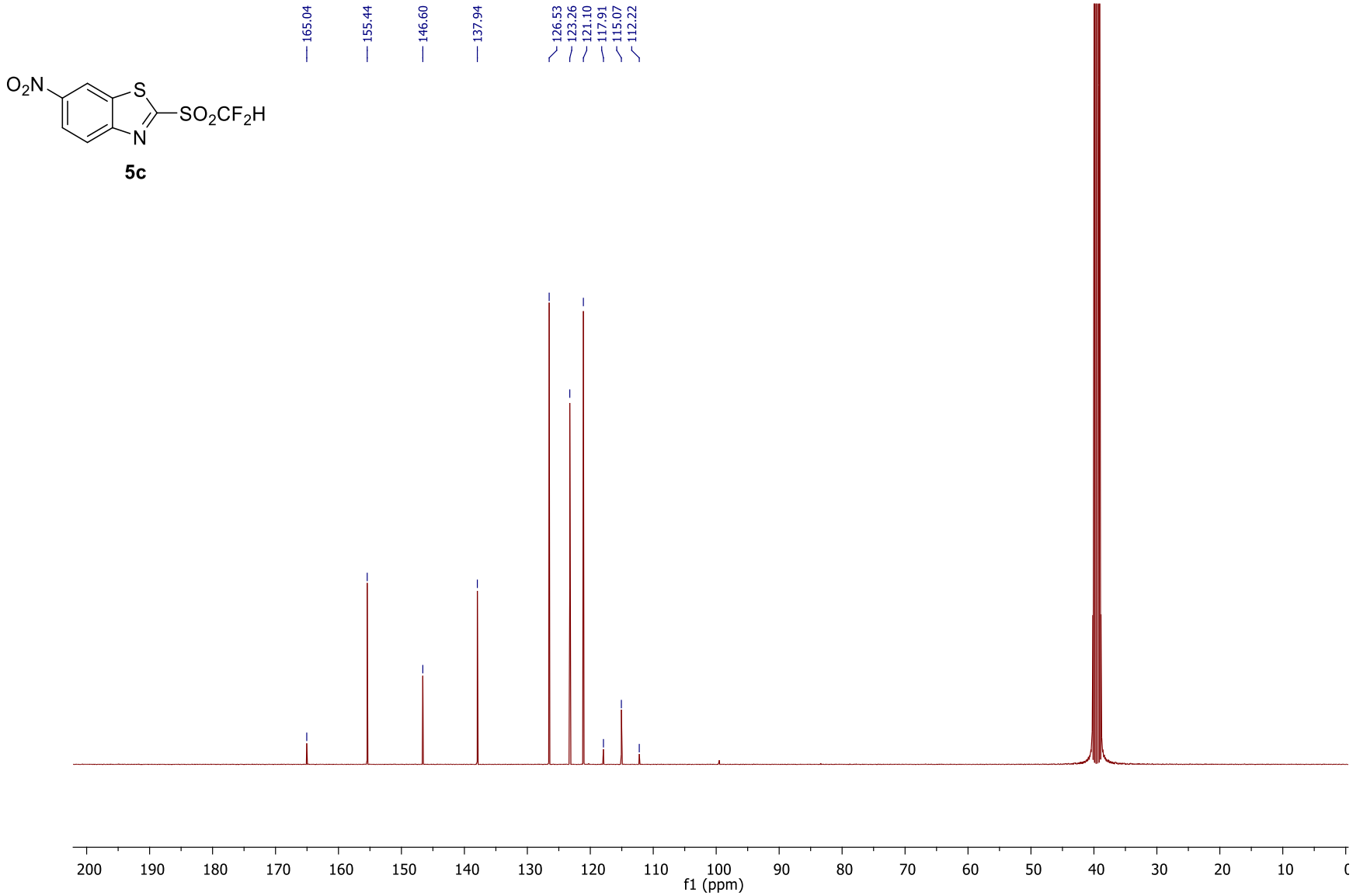

Figure S26. ^{13}C-NMR spectrum of 2-((difluoromethyl)sulfonyl)-6-nitrobenzo[*d*]thiazole (**5c**).

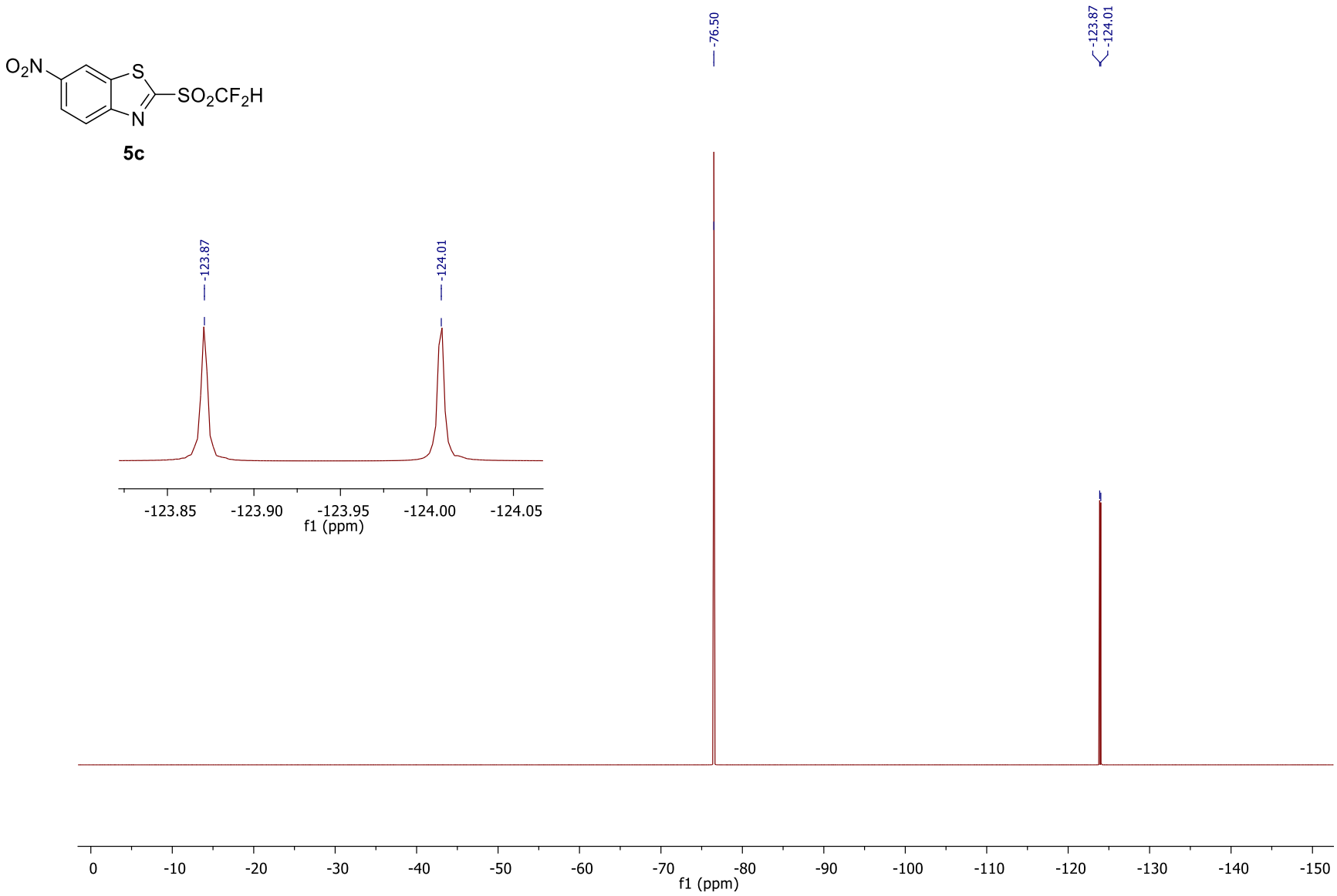

Figure S27. ^{19}F-NMR spectrum of 2-((difluoromethyl)sulfonyl)-6-nitrobenzo[*d*]thiazole (**5c**).

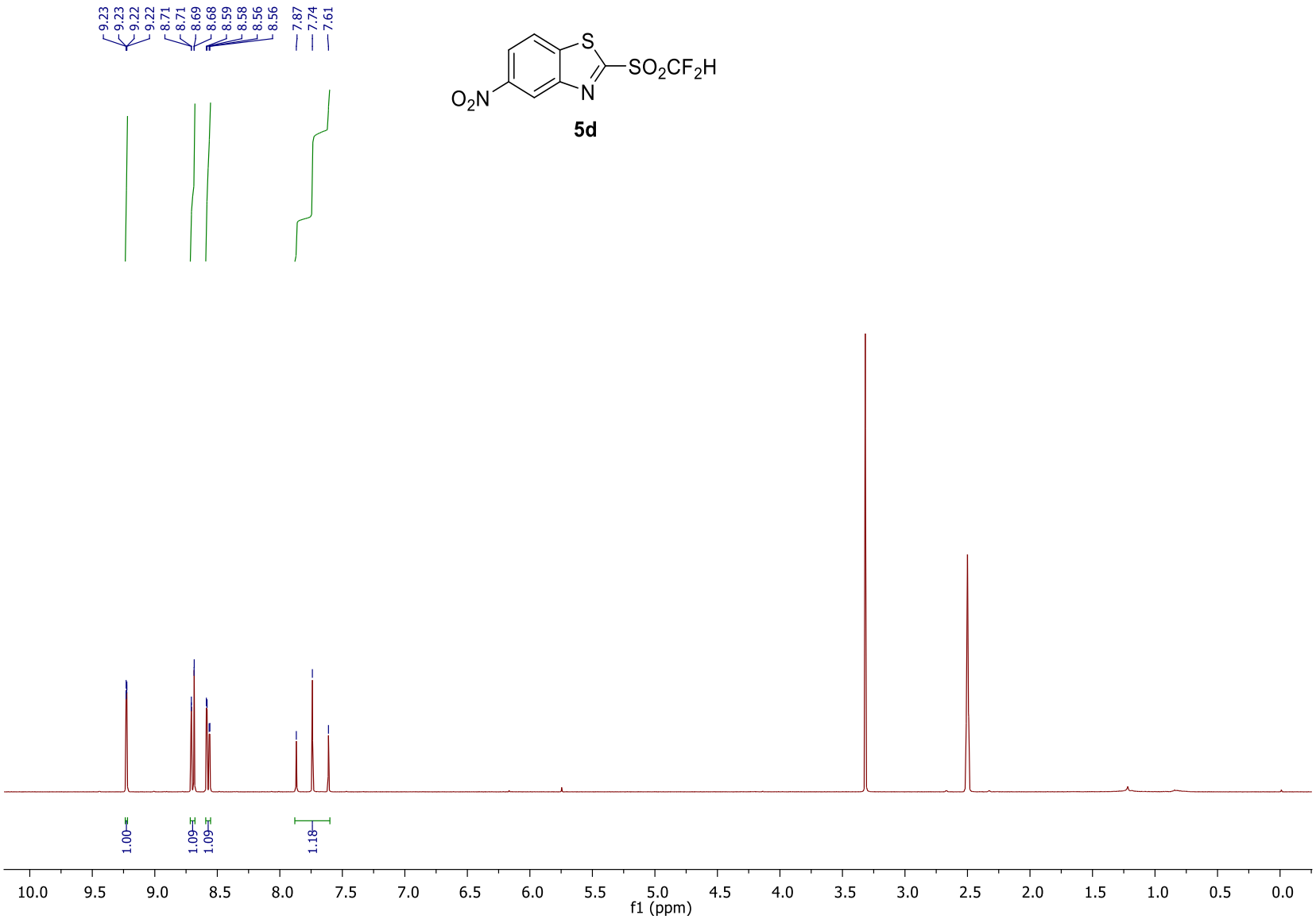

Figure S28. ^{1}H-NMR spectrum of 2-((difluoromethyl)sulfonyl)-5-nitrobenzo[*d*]thiazole (**5d**).

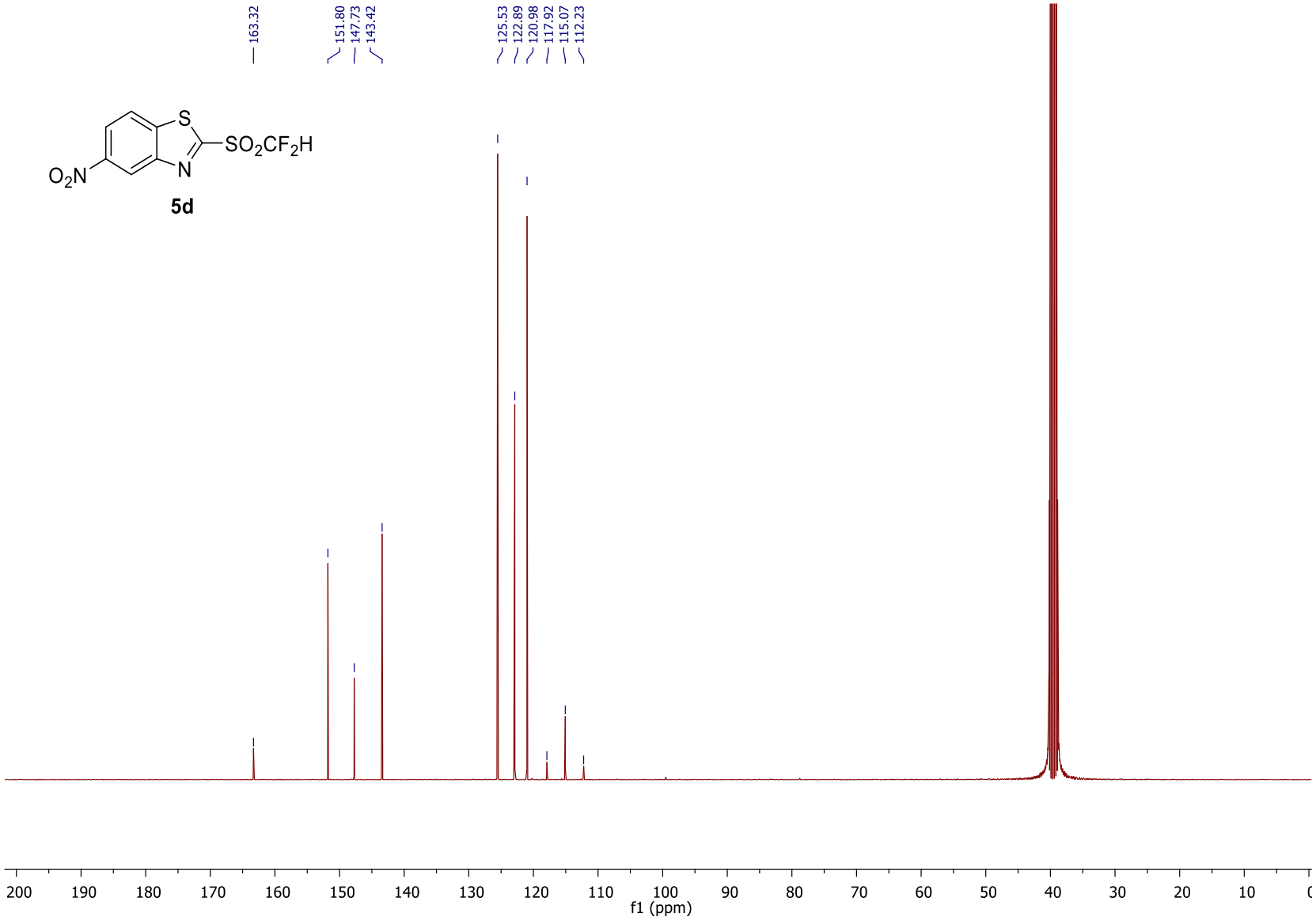

Figure S29. ^{13}C-NMR spectrum of 2-((difluoromethyl)sulfonyl)-5-nitrobenzo[*d*]thiazole (**5d**).

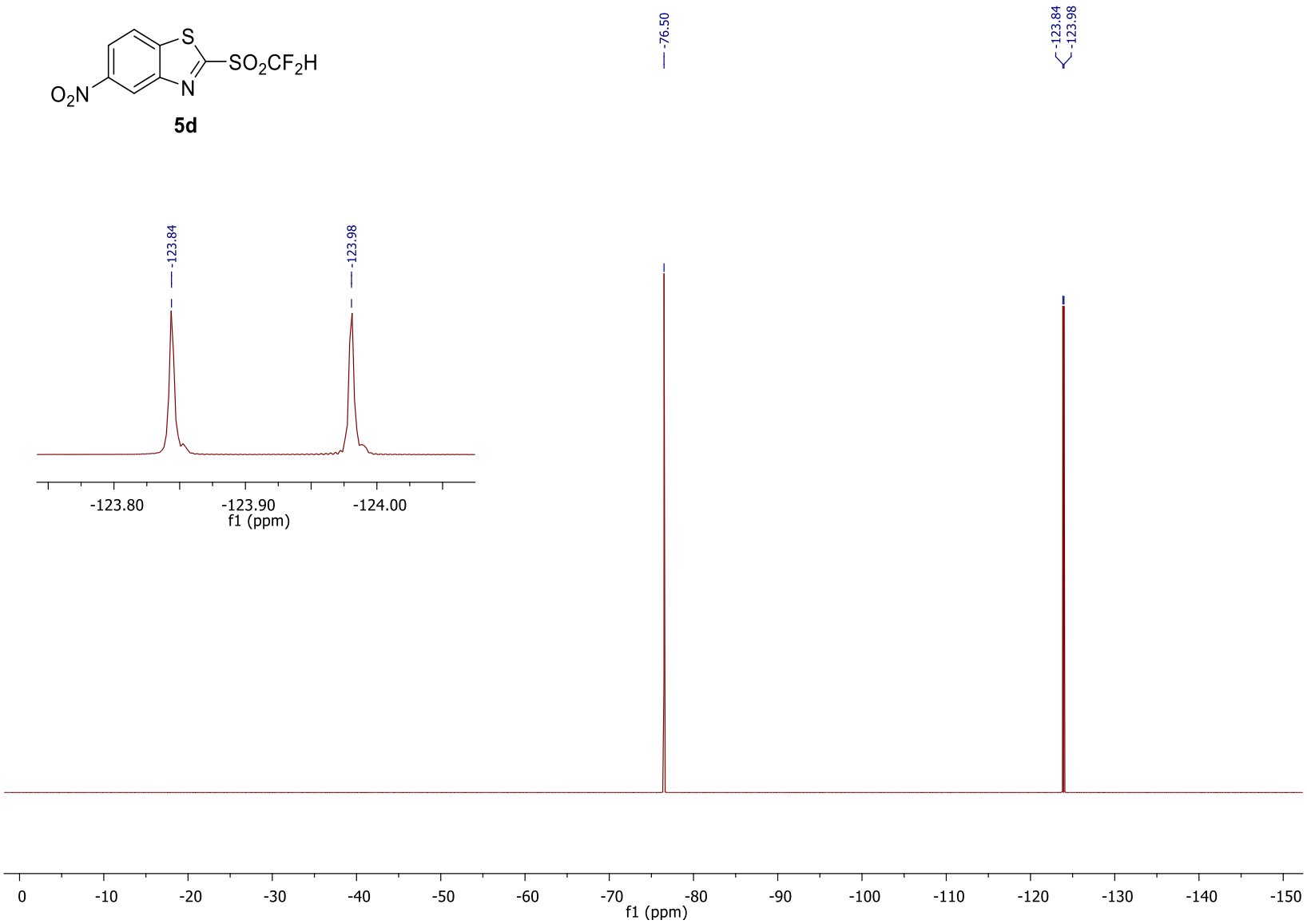

Figure S30. ^{19}F-NMR spectrum of 2-((difluoromethyl)sulfonyl)-5-nitrobenzo[*d*]thiazole (**5d**).

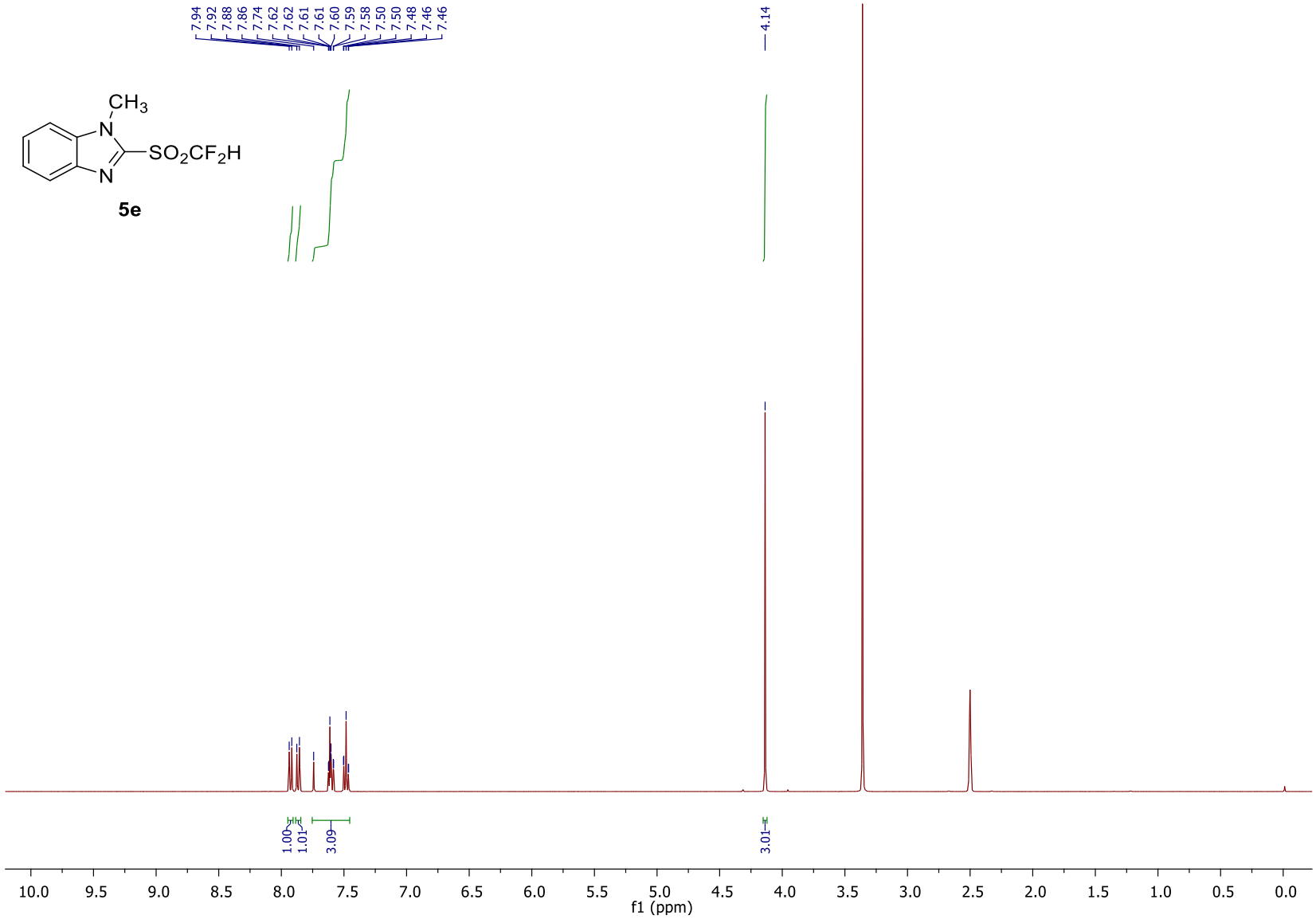

Figure S31. ^{1}H-NMR spectrum of 2-((difluoromethyl)sulfonyl)-1-methyl-1*H*-benzo[*d*]imidazole (**5e**).

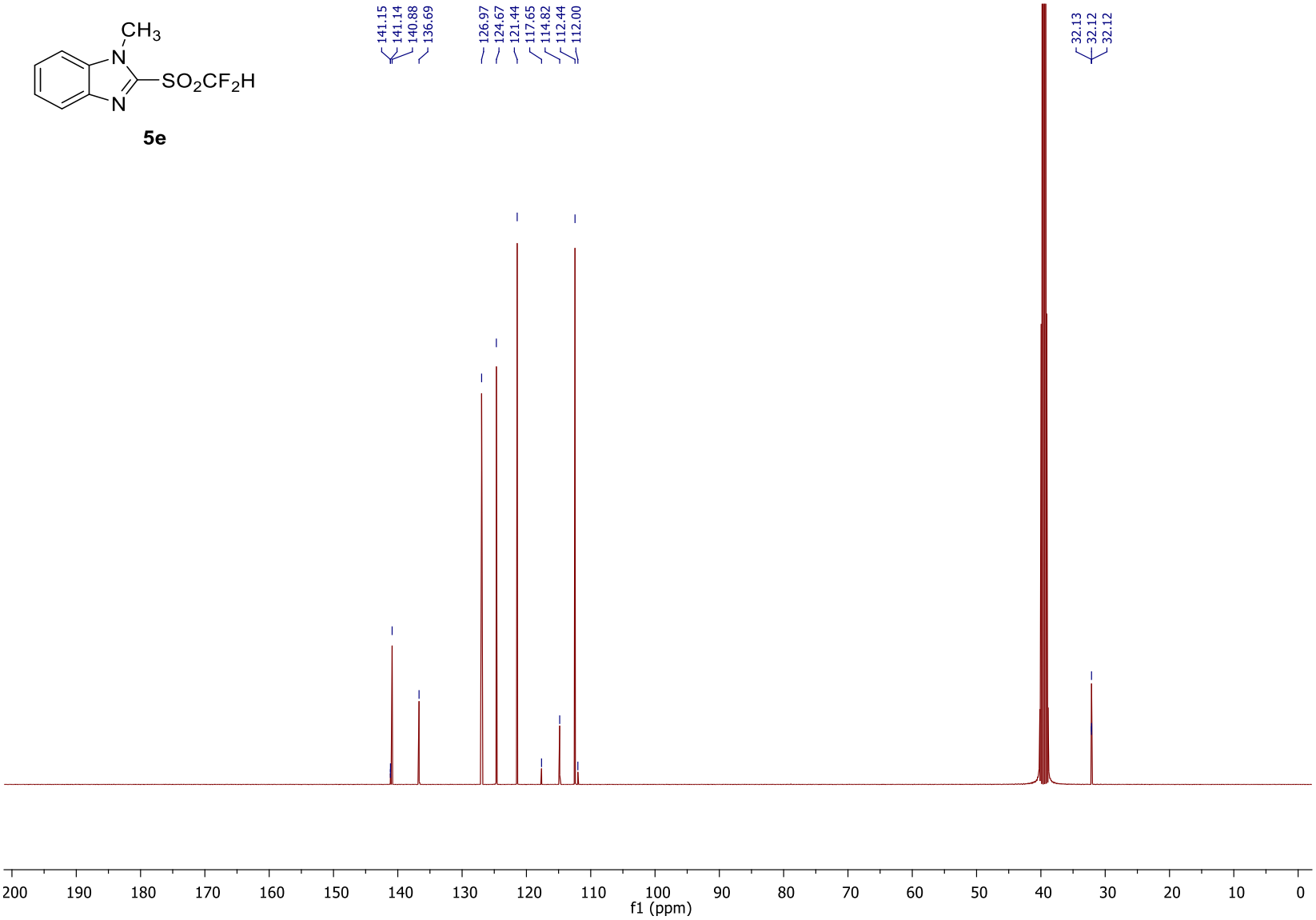

Figure S32. ^{13}C-NMR spectrum of 2-((difluoromethyl)sulfonyl)-1-methyl-1*H*-benzo[*d*]imidazole (**5e**).

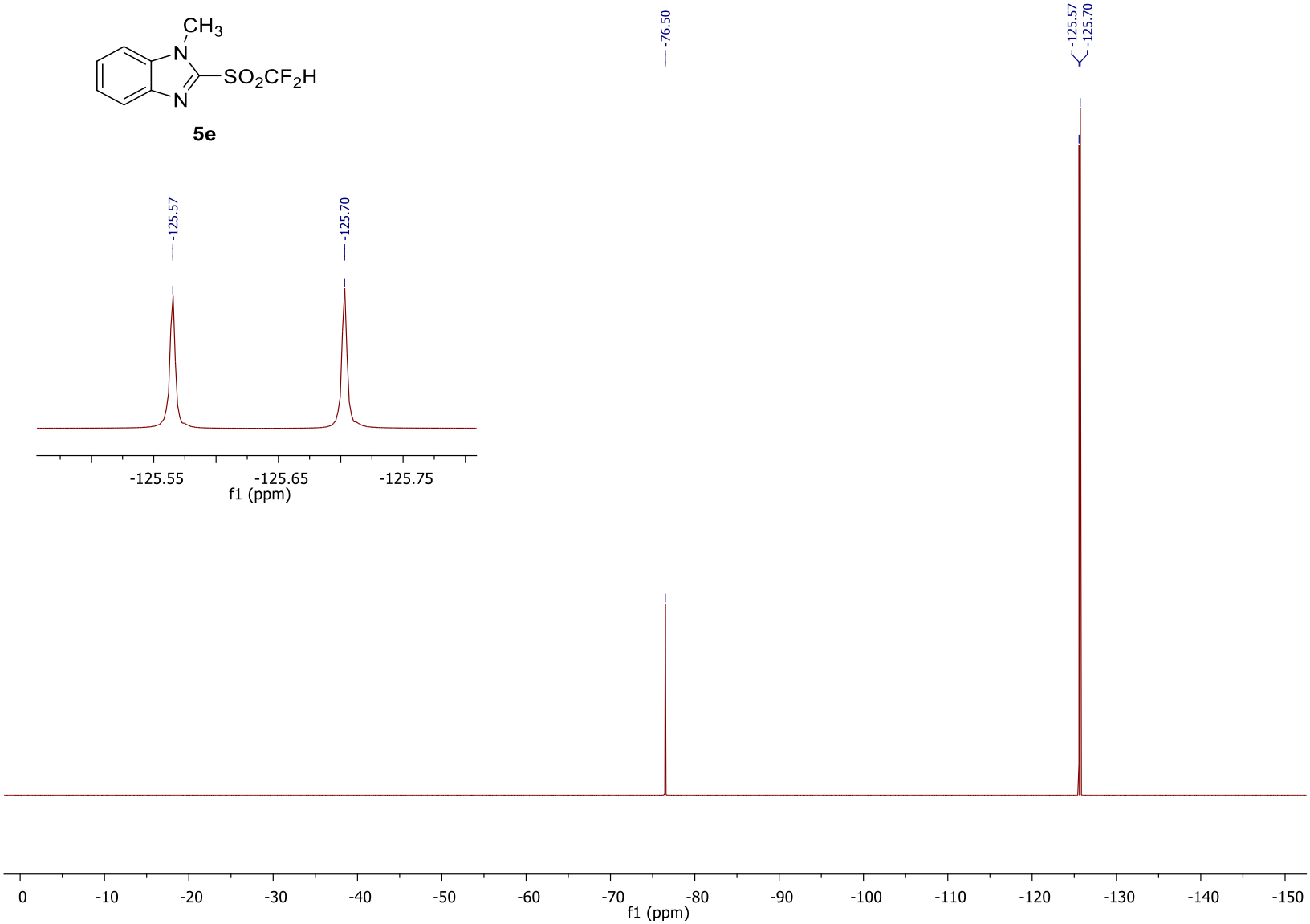

Figure S33. ^{19}F-NMR spectrum of 2-((difluoromethyl)sulfonyl)-1-methyl-1*H*-benzo[*d*]imidazole (**5e**).

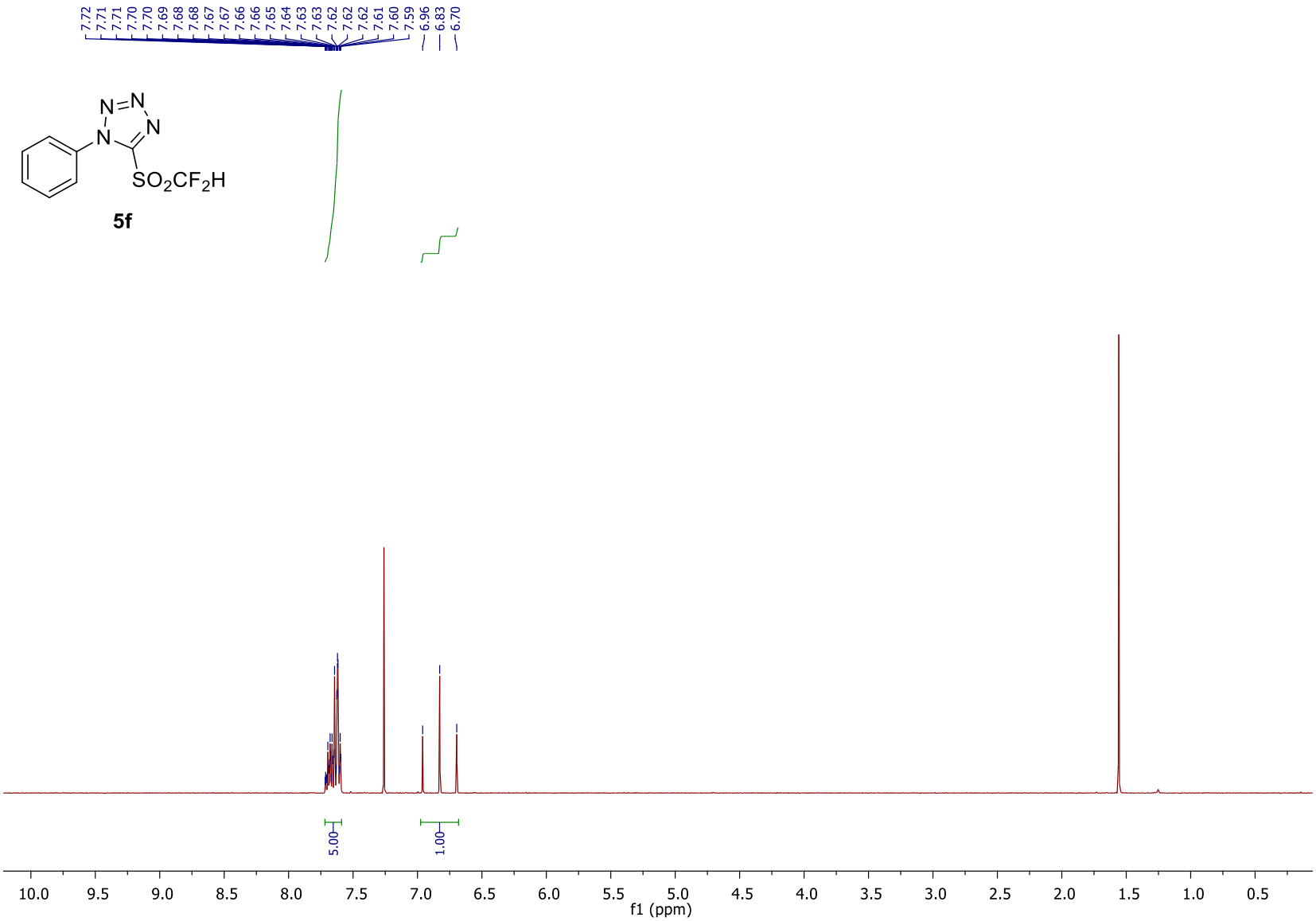

Figure S34. ^{1}H-NMR spectrum of 5-((difluoromethyl)sulfonyl)-1-phenyl-1*H*-tetrazole (**5f**).

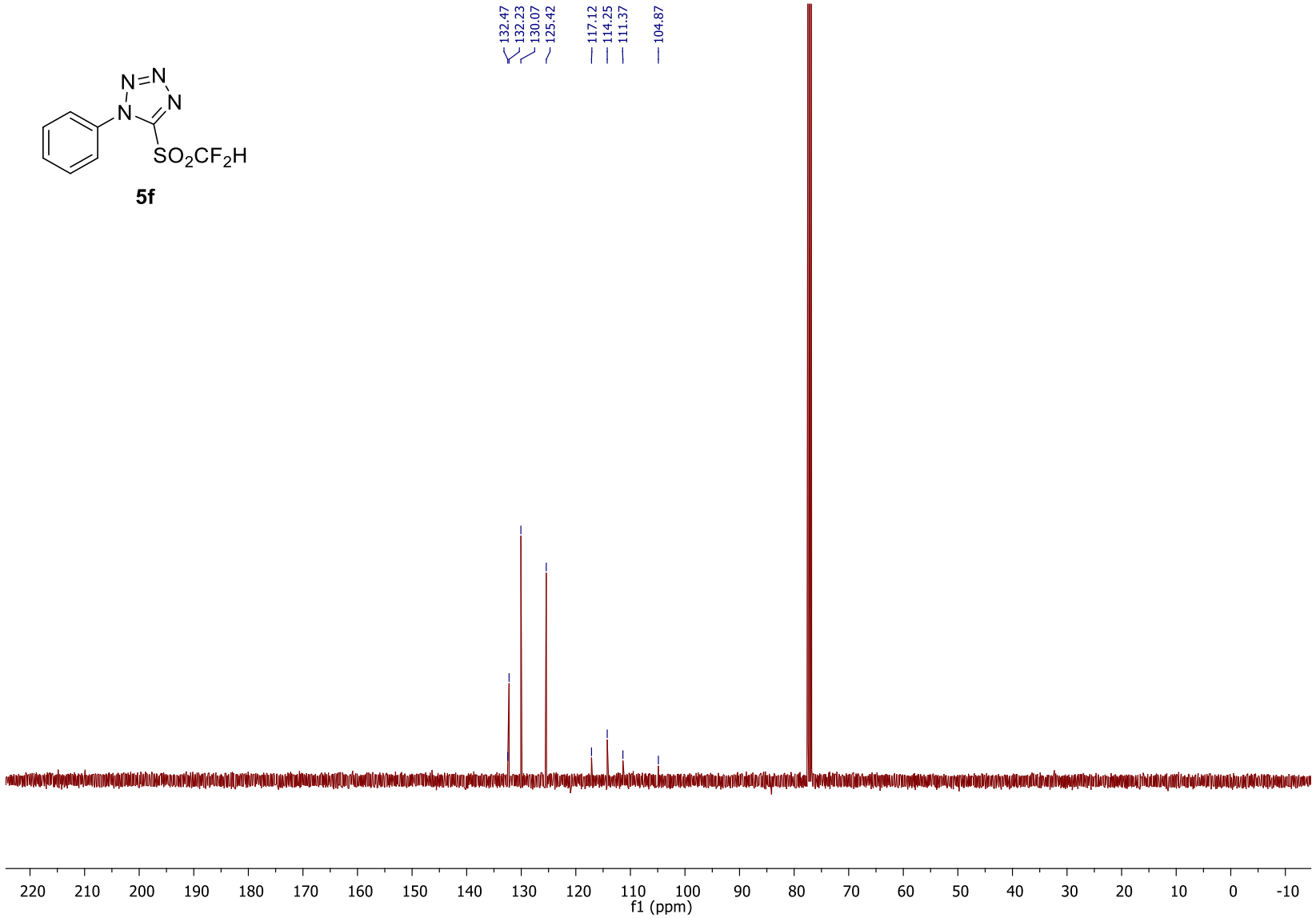

Figure S35. ^{13}C-NMR spectrum of 5-((difluoromethyl)sulfonyl)-1-phenyl-1*H*-tetrazole (**5f**).

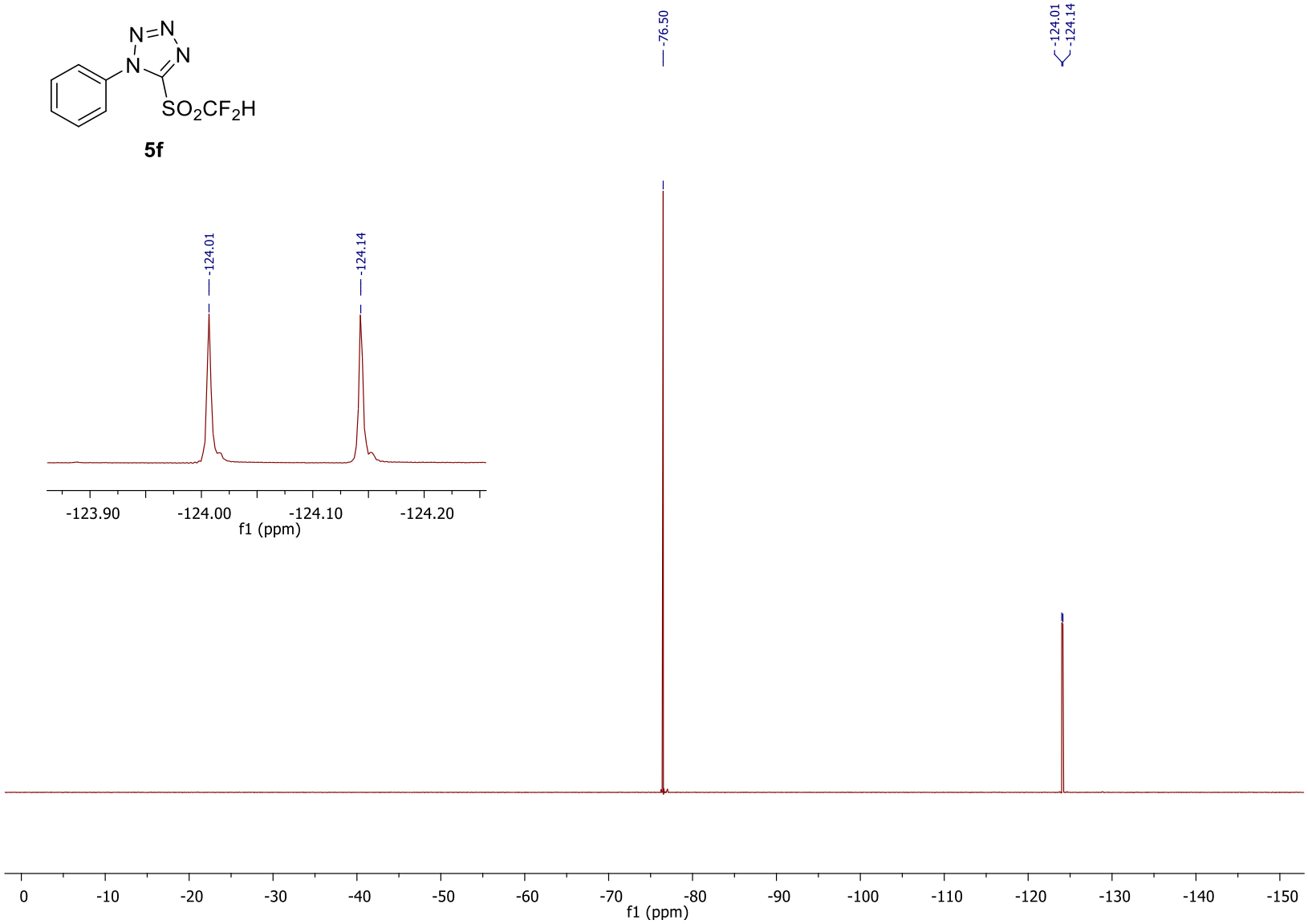

Figure S36. ^{19}F-NMR spectrum of 5-((difluoromethyl)sulfonyl)-1-phenyl-1*H*-tetrazole (**5f**).

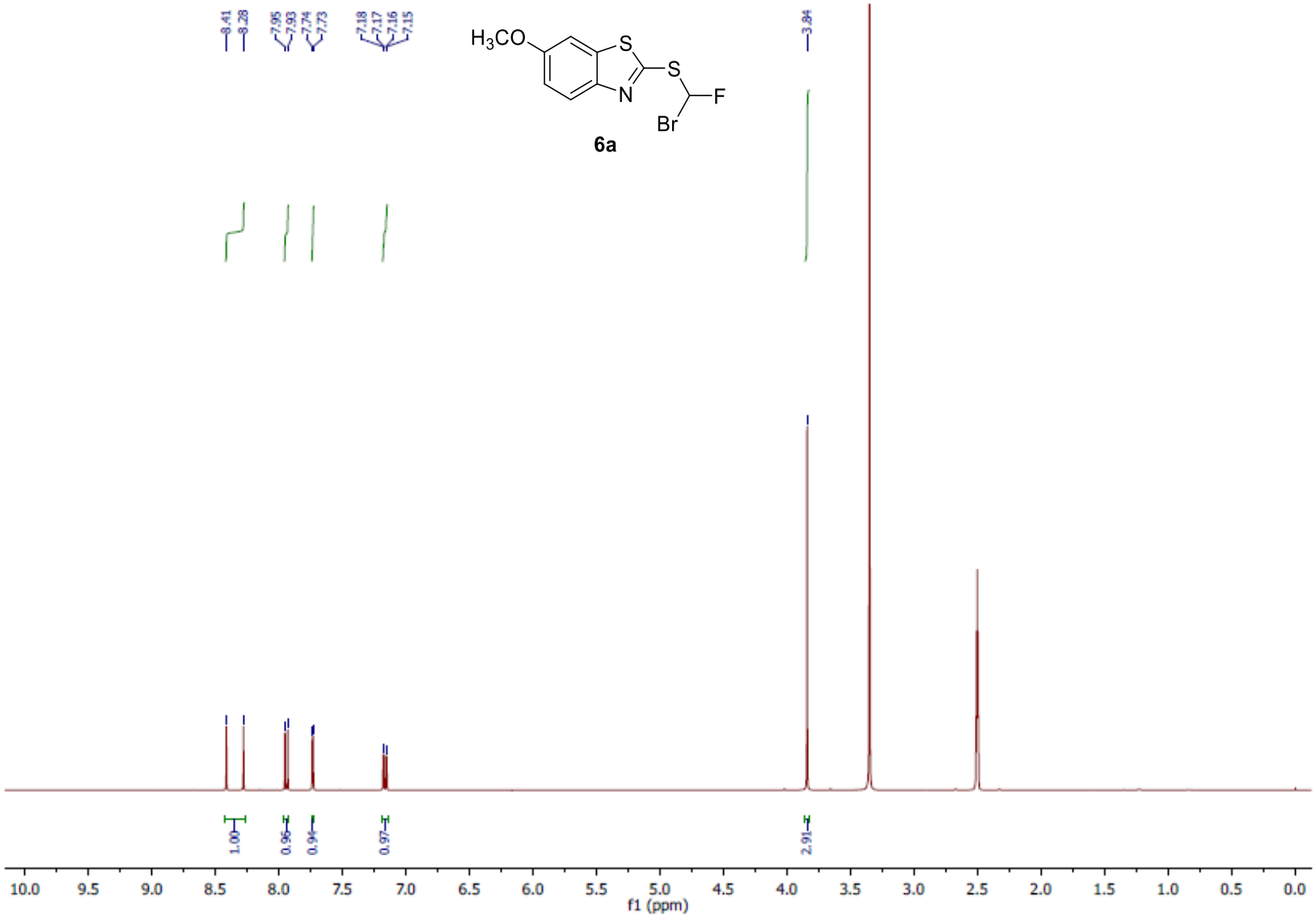

Figure S37. ^{1}H-NMR spectrum of 2-((bromofluoromethyl)thio)-6-methoxybenzo[*d*]thiazole (**6a**).

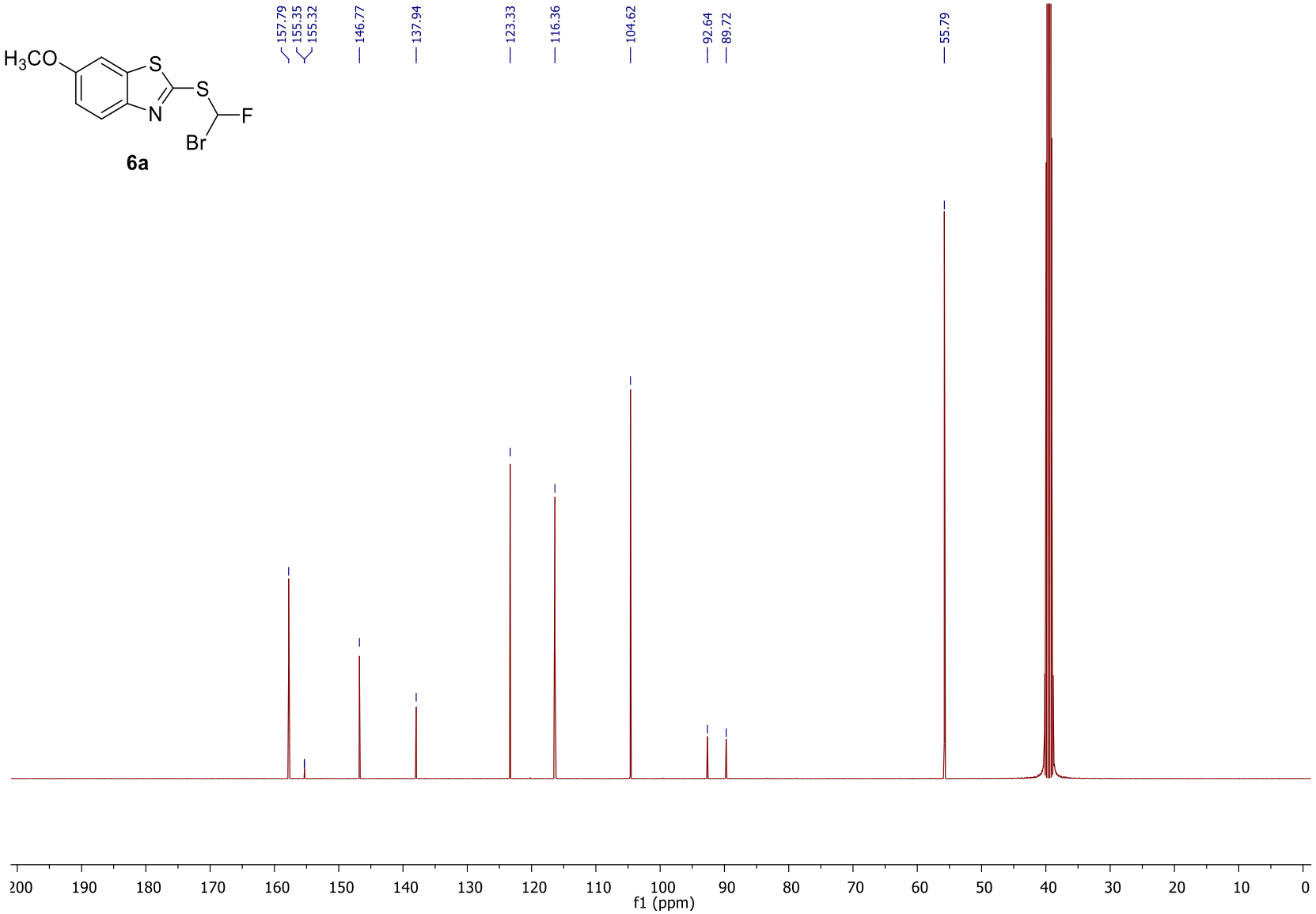

Figure S38. ^{13}C-NMR spectrum of 2-((bromofluoromethyl)thio)-6-methoxybenzo[*d*]thiazole (**6a**).

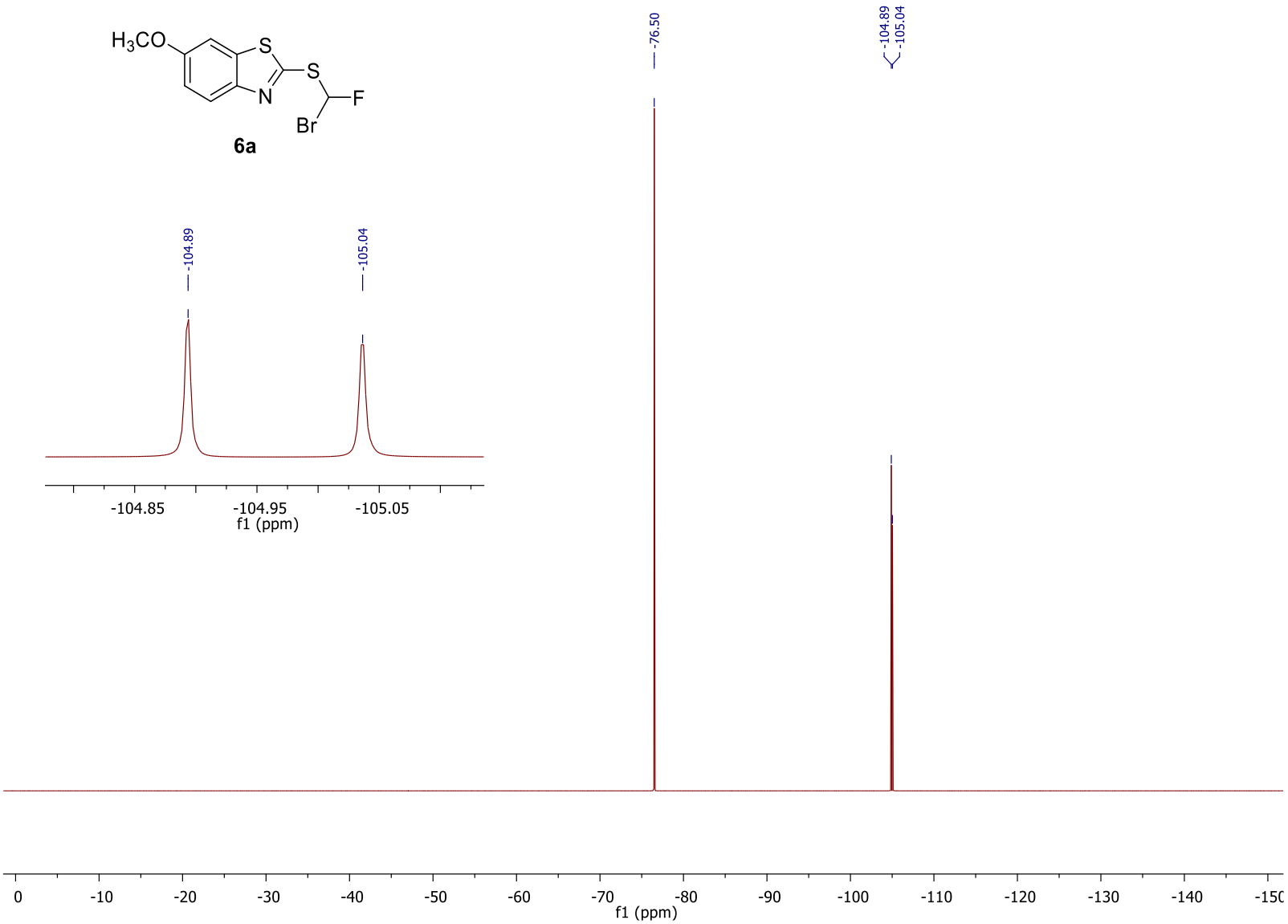

Figure S39. ^{19}F-NMR spectrum of 2-((bromofluoromethyl)thio)-6-methoxybenzo[*d*]thiazole (**6a**).

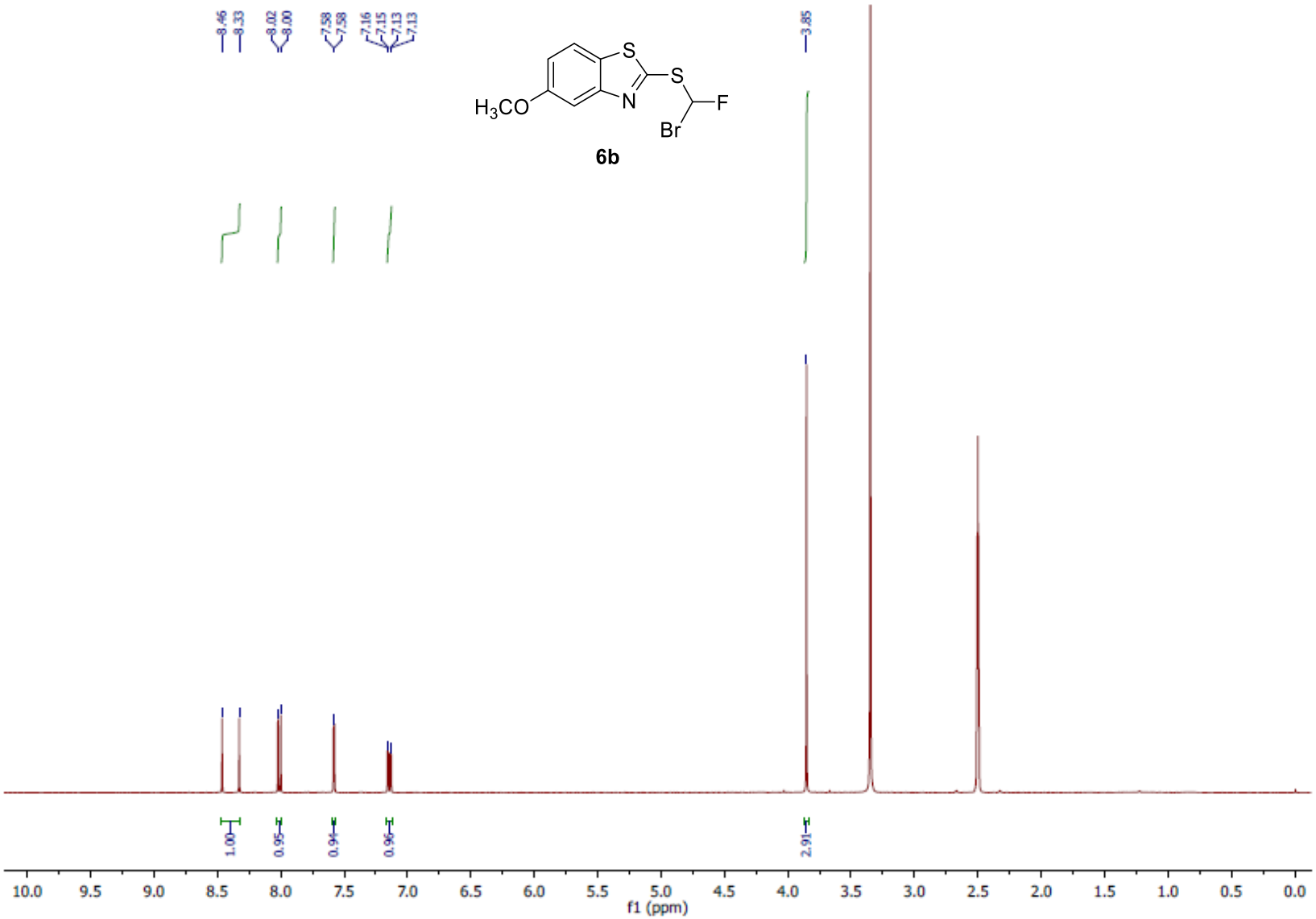

Figure S40. ^{1}H-NMR spectrum of 2-((bromofluoromethyl)thio)-5-methoxybenzo[*d*]thiazole (**6b**).

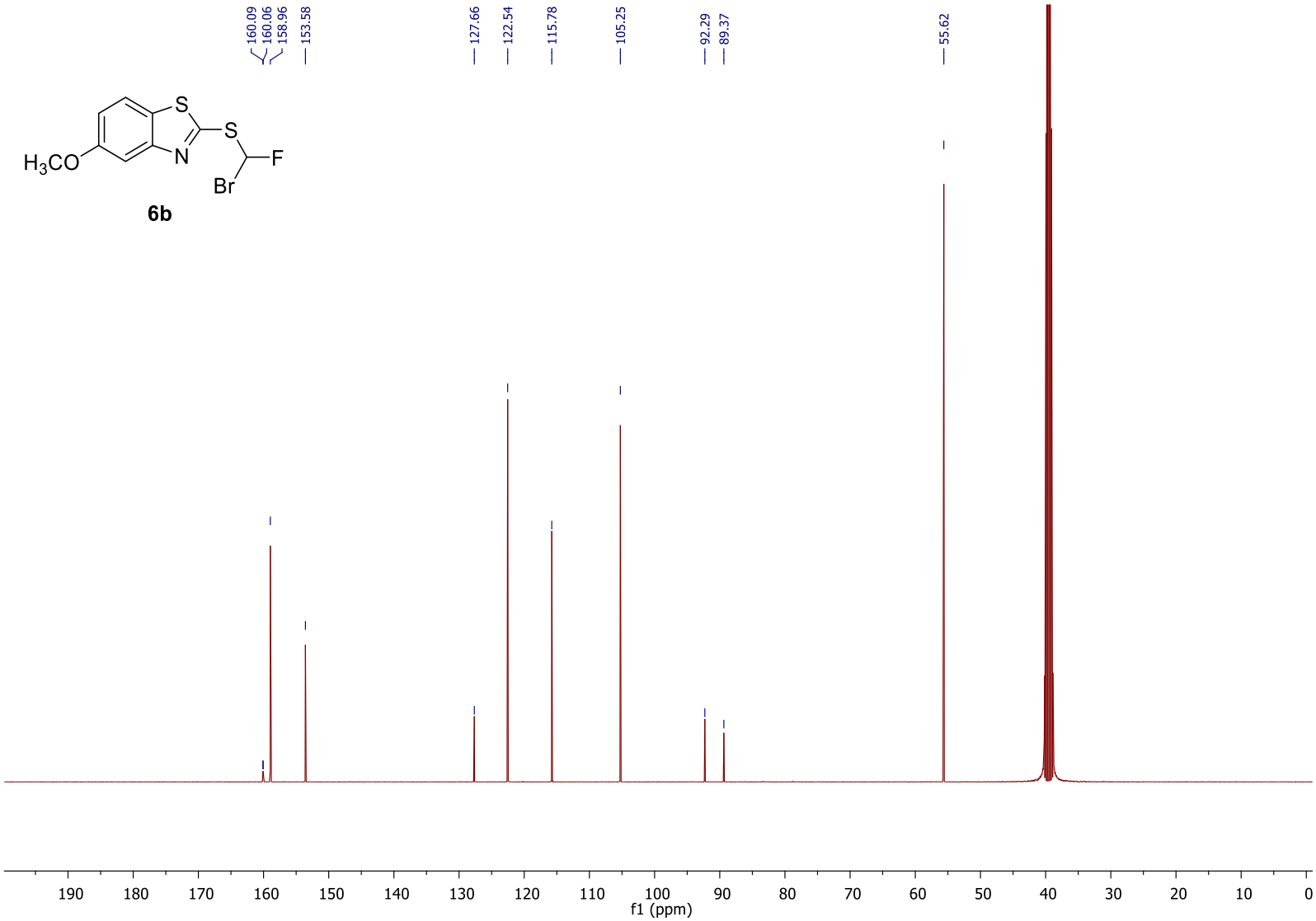

Figure S41. ^{13}C-NMR spectrum of 2-((bromofluoromethyl)thio)-5-methoxybenzo[*d*]thiazole (**6b**).

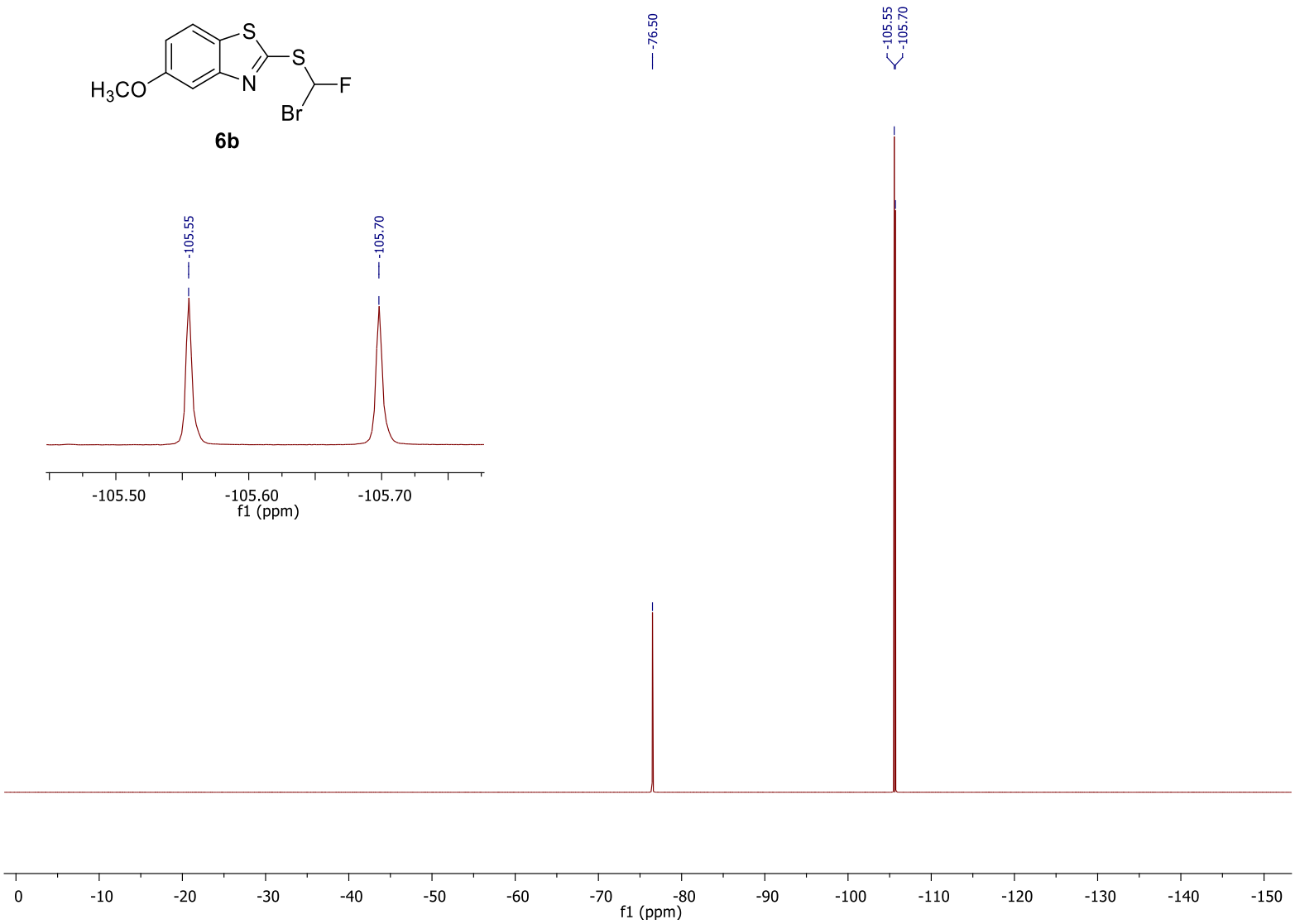

Figure S42. ^{19}F-NMR spectrum of 2-((bromofluoromethyl)thio)-5-methoxybenzo[*d*]thiazole (**6b**).

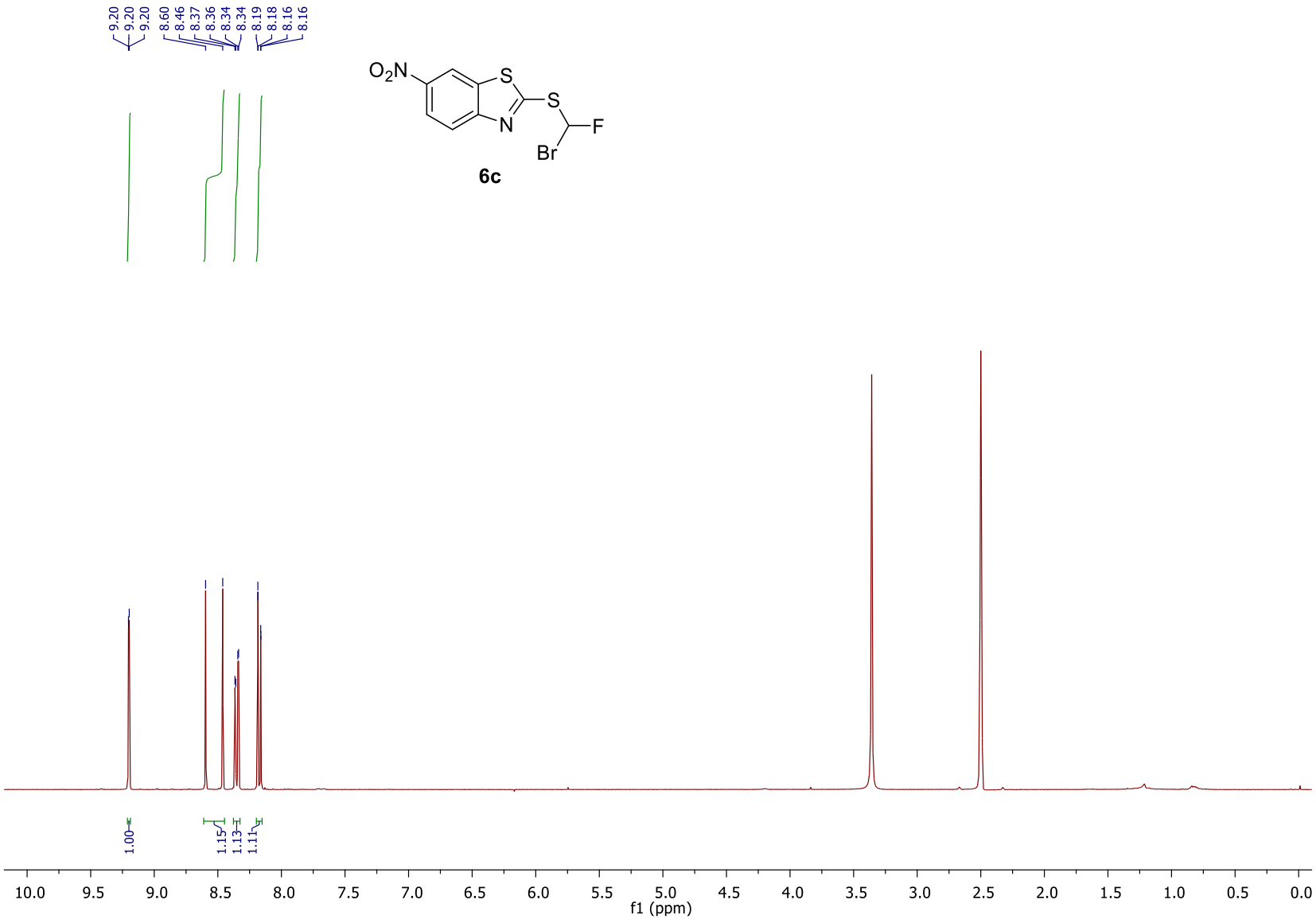

Figure S43. ^{1}H-NMR spectrum of 2-((bromofluoromethyl)thio)-6-nitrobenzo[*d*]thiazole (**6c**).

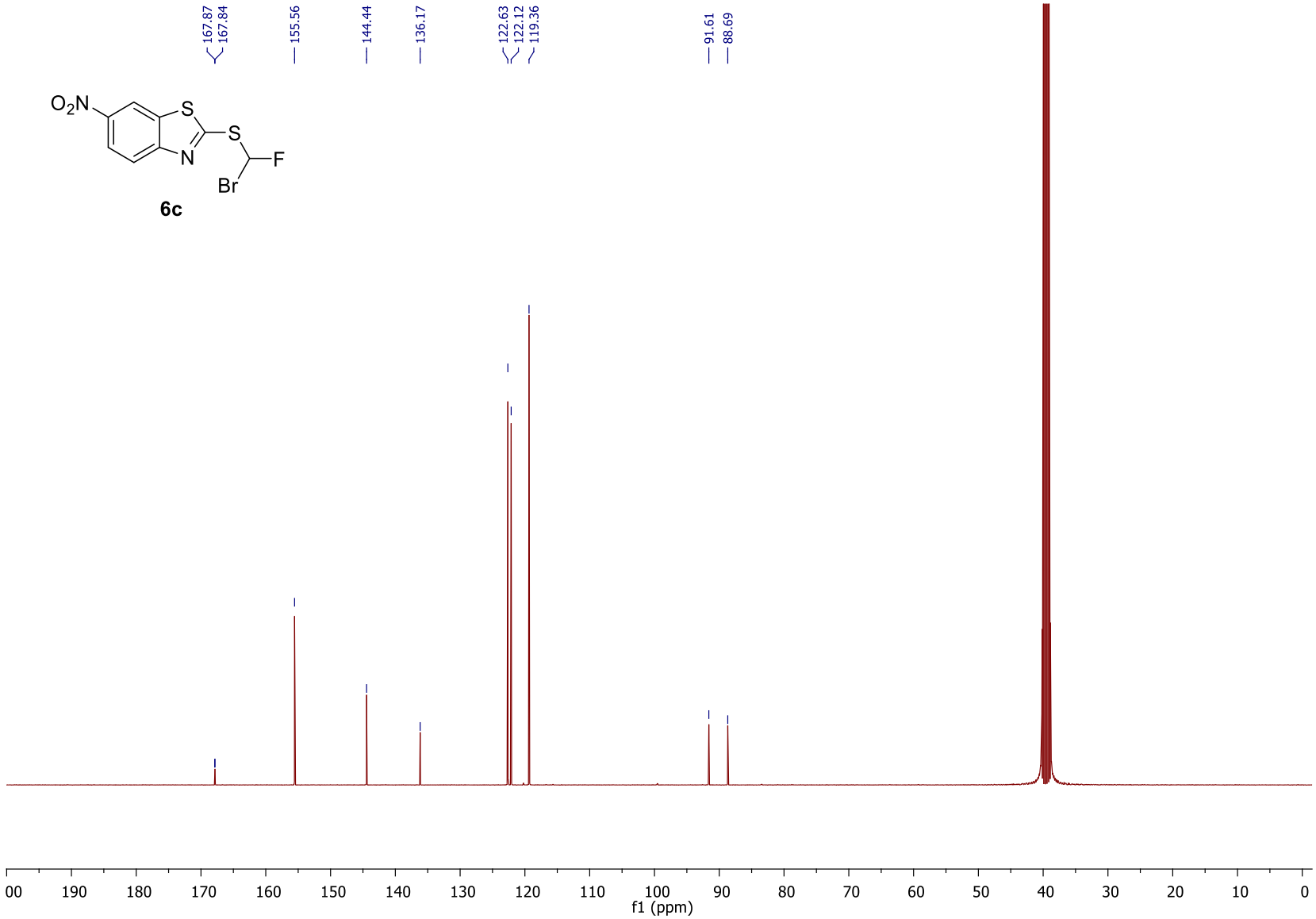

Figure S44. ^{13}C-NMR spectrum of 2-((bromofluoromethyl)thio)-6-nitrobenzo[*d*]thiazole (**6c**).

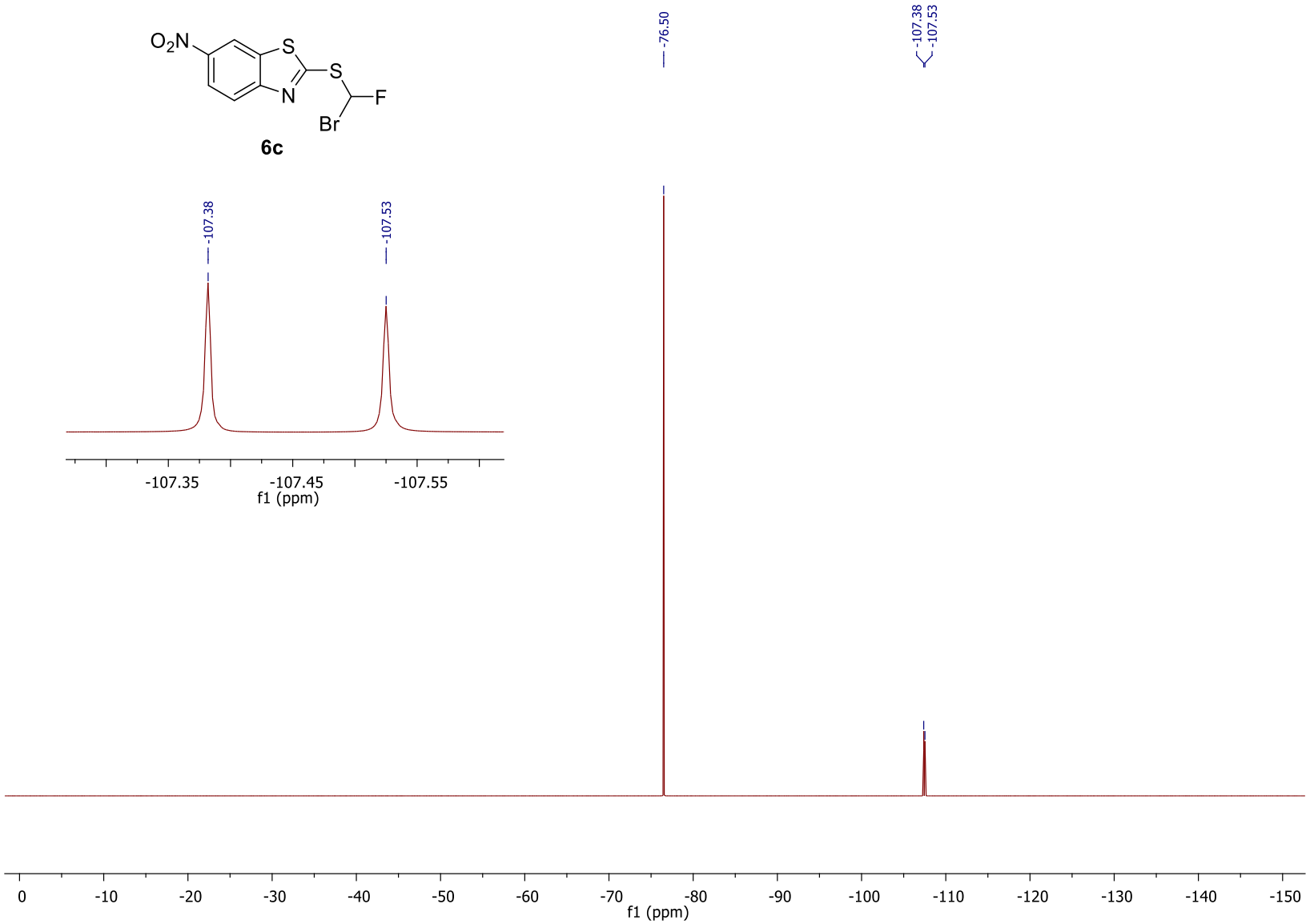

Figure S45. ^{19}F-NMR spectrum of 2-((bromofluoromethyl)thio)-6-nitrobenzo[*d*]thiazole (**6c**).

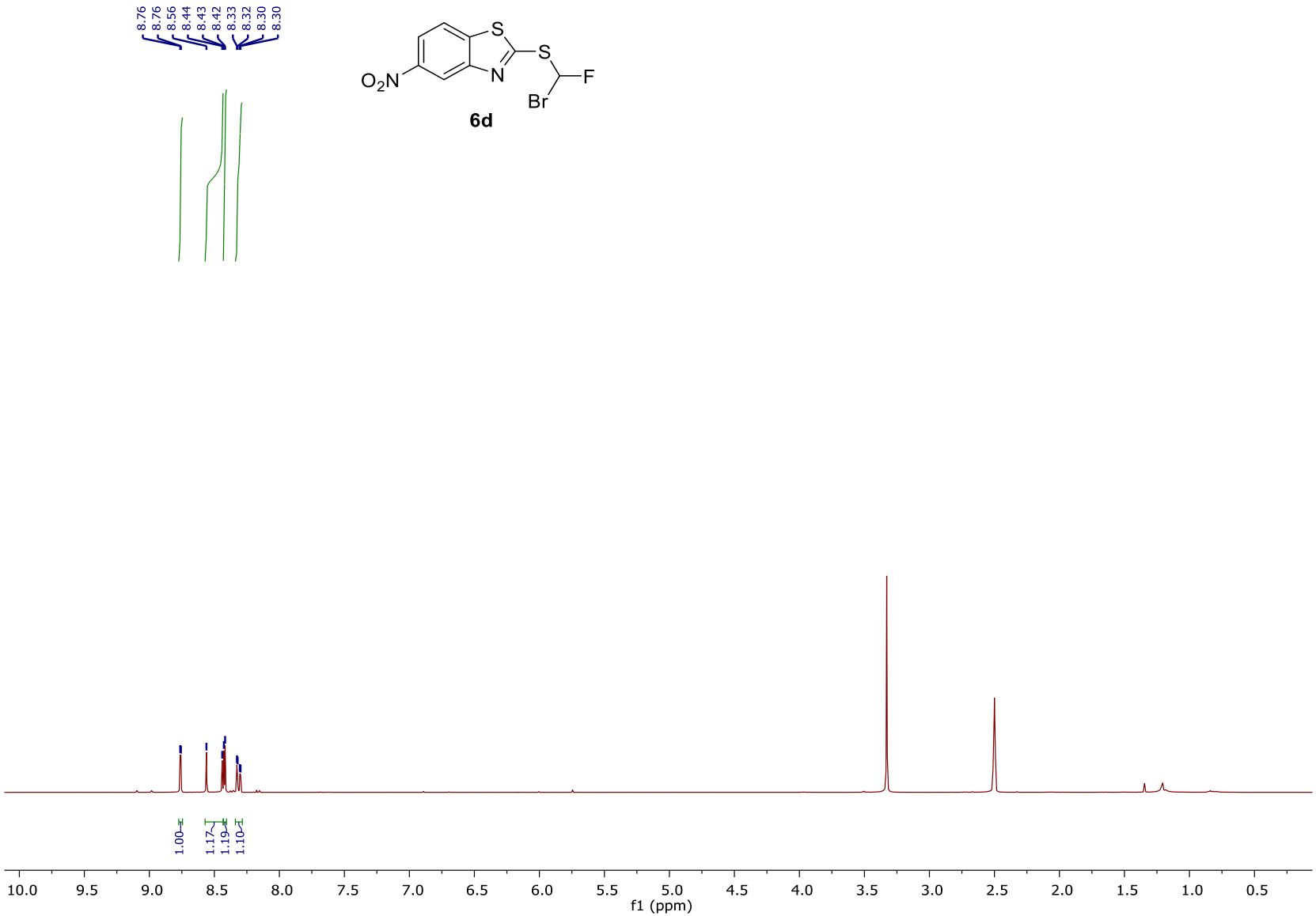

Figure S46. ^{1}H-NMR spectrum of 2-((bromofluoromethyl)thio)-5-nitrobenzo[*d*]thiazole (**6d**).

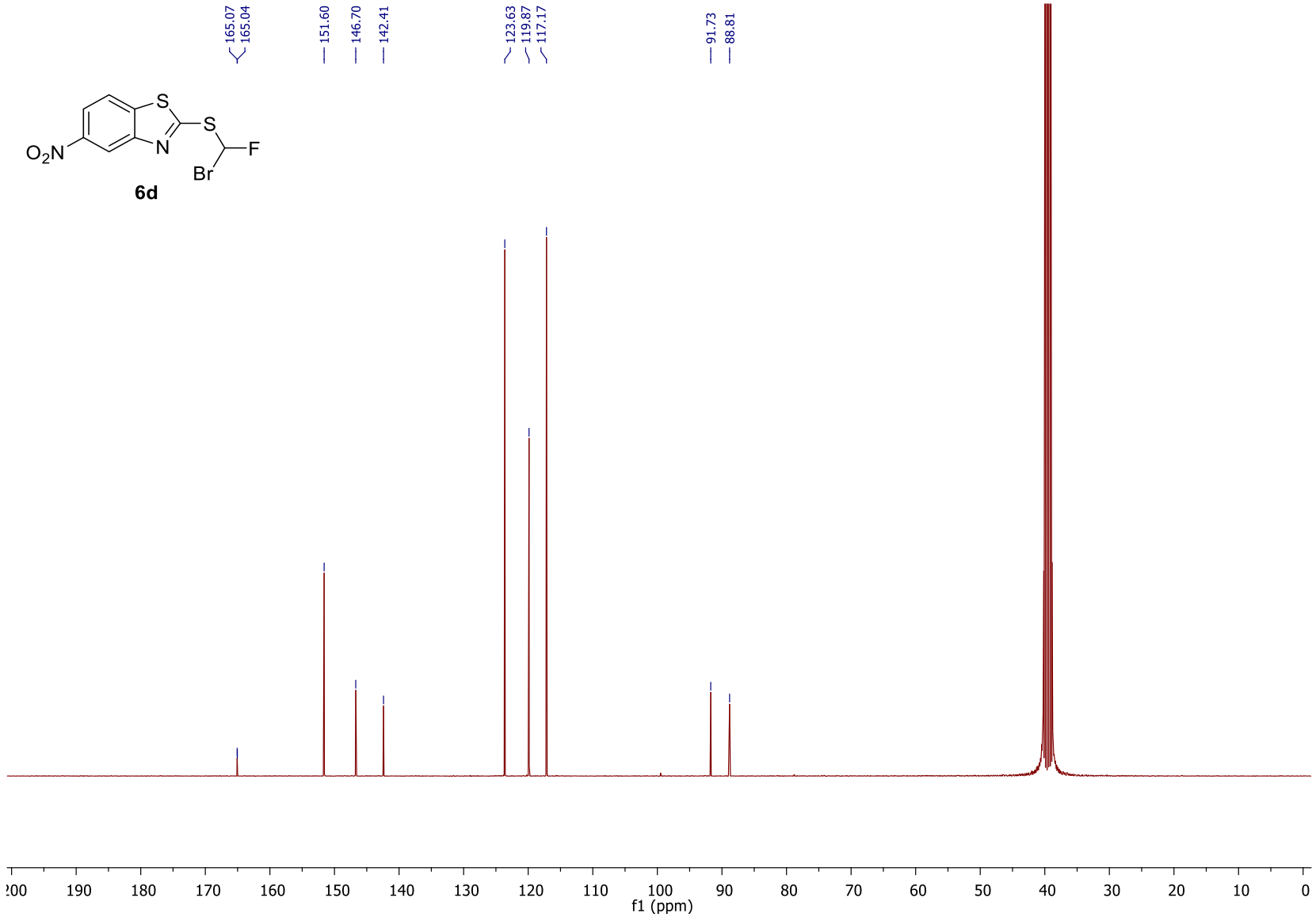

Figure S47. ^{13}C-NMR spectrum of 2-((bromofluoromethyl)thio)-5-nitrobenzo[*d*]thiazole (**6d**).

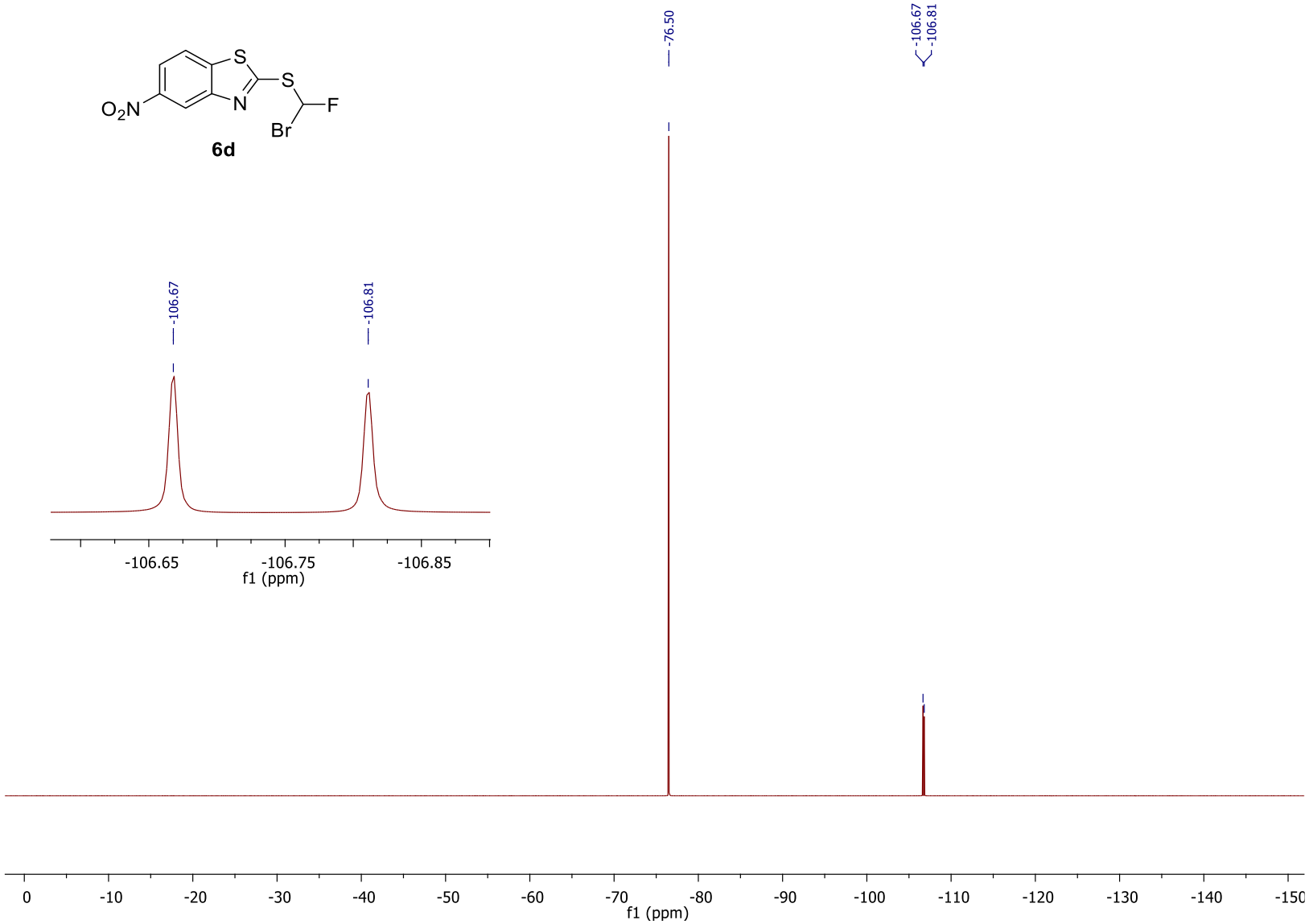

Figure S48. ^{19}F-NMR spectrum of 2-((bromofluoromethyl)thio)-5-nitrobenzo[*d*]thiazole (**6d**).

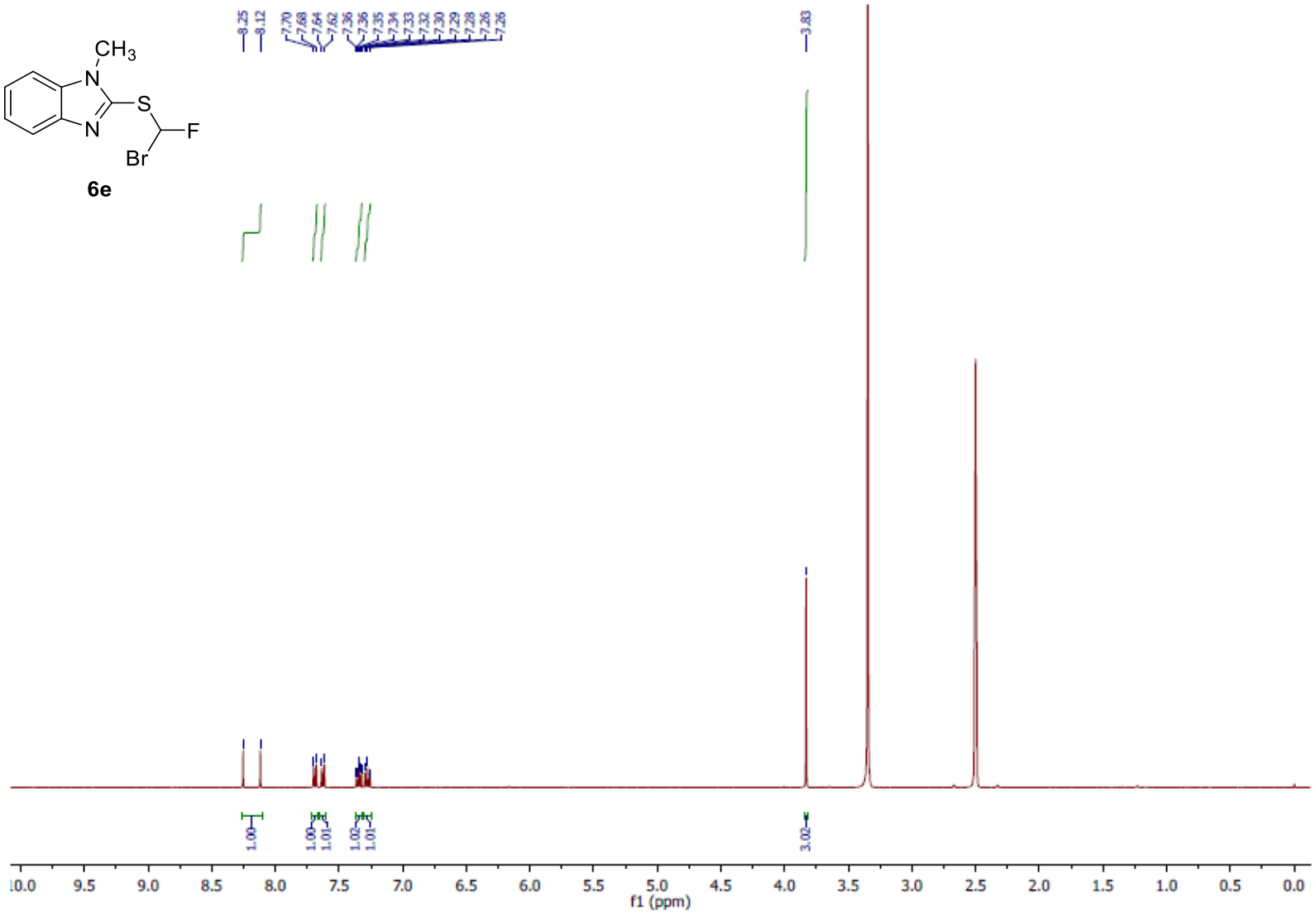

Figure S49. ^{1}H-NMR spectrum of 2-((bromofluoromethyl)thio)-1-methyl-1*H*-benzo[*d*]imidazole (**6e**).

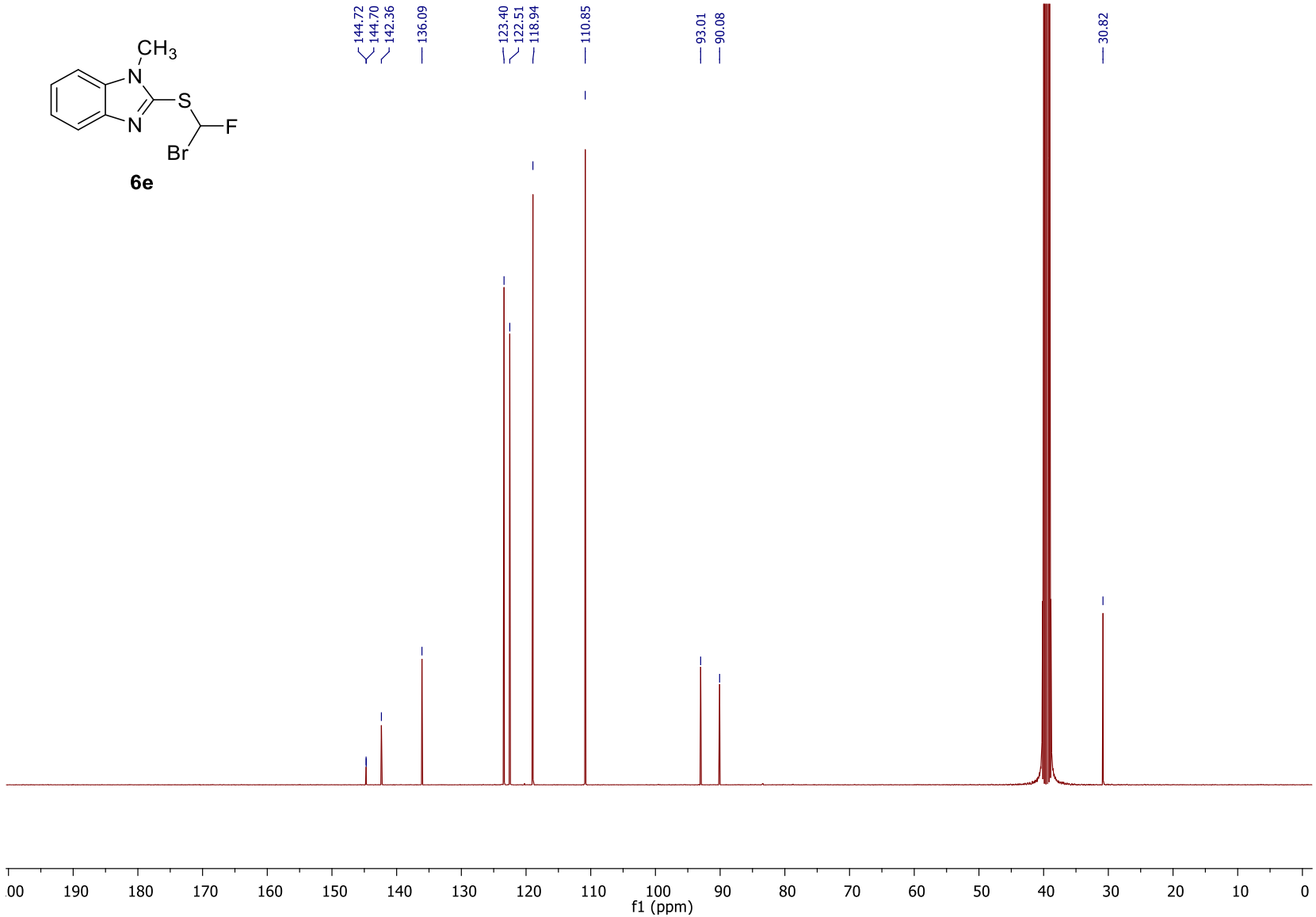

Figure S50. ^{13}C-NMR spectrum of 2-((bromofluoromethyl)thio)-1-methyl-1*H*-benzo[*d*]imidazole (**6e**).

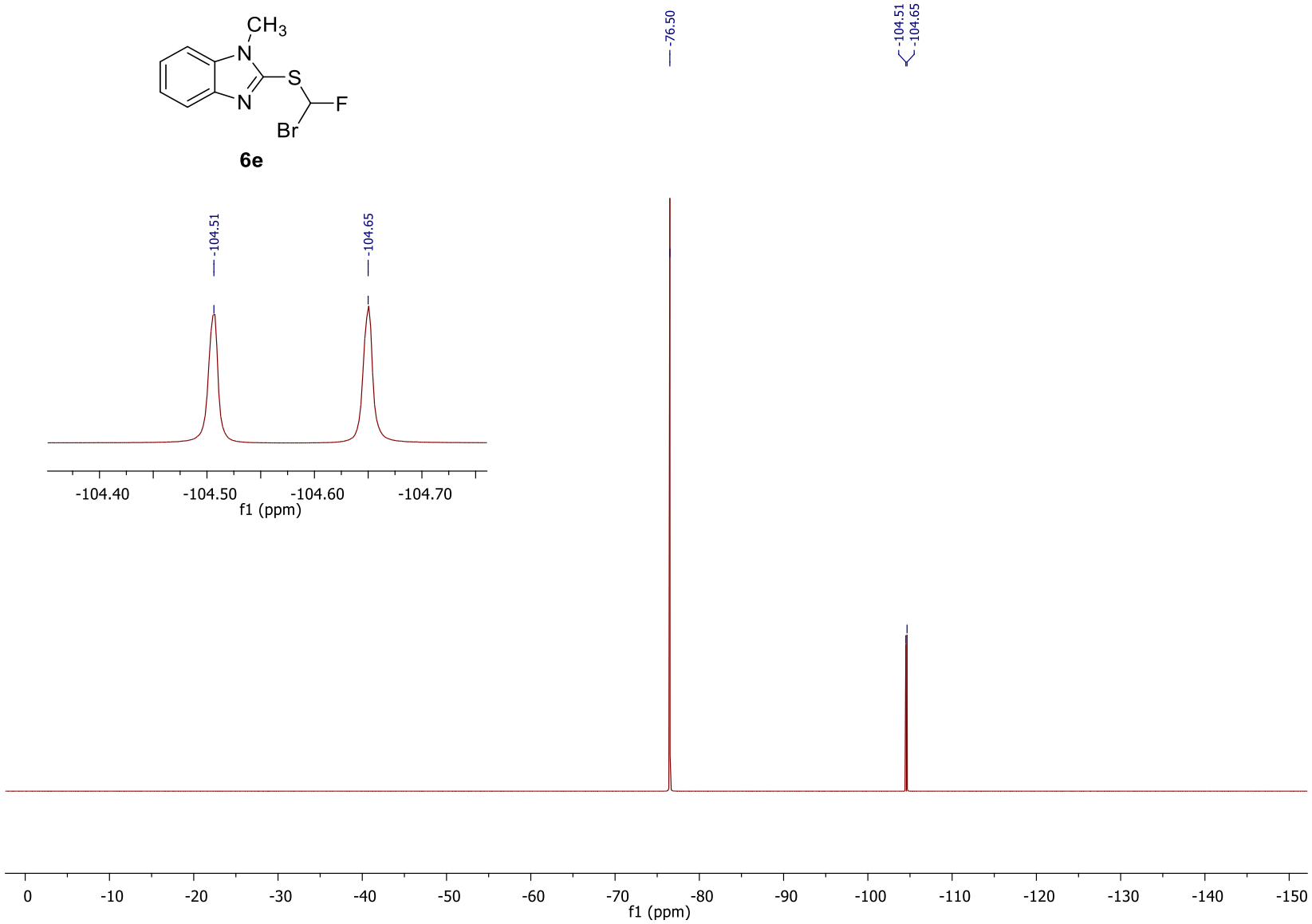

Figure S51. ^{19}F-NMR spectrum of 2-((bromofluoromethyl)thio)-1-methyl-1*H*-benzo[*d*]imidazole (**6e**).

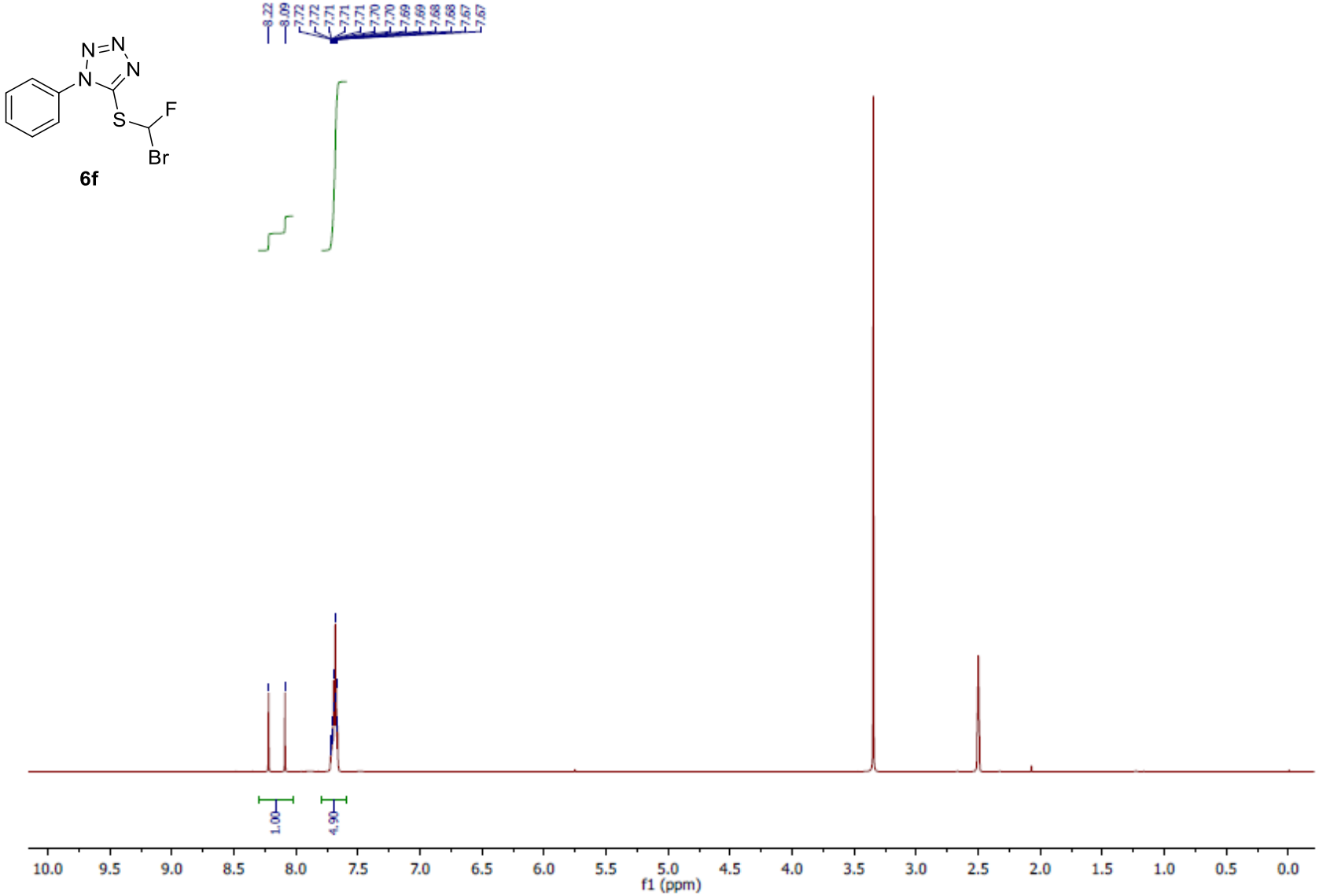

Figure S52. ^{1}H-NMR spectrum of 5-((bromofluoromethyl)thio)-1-phenyl-1*H*-tetrazole (**6f**).

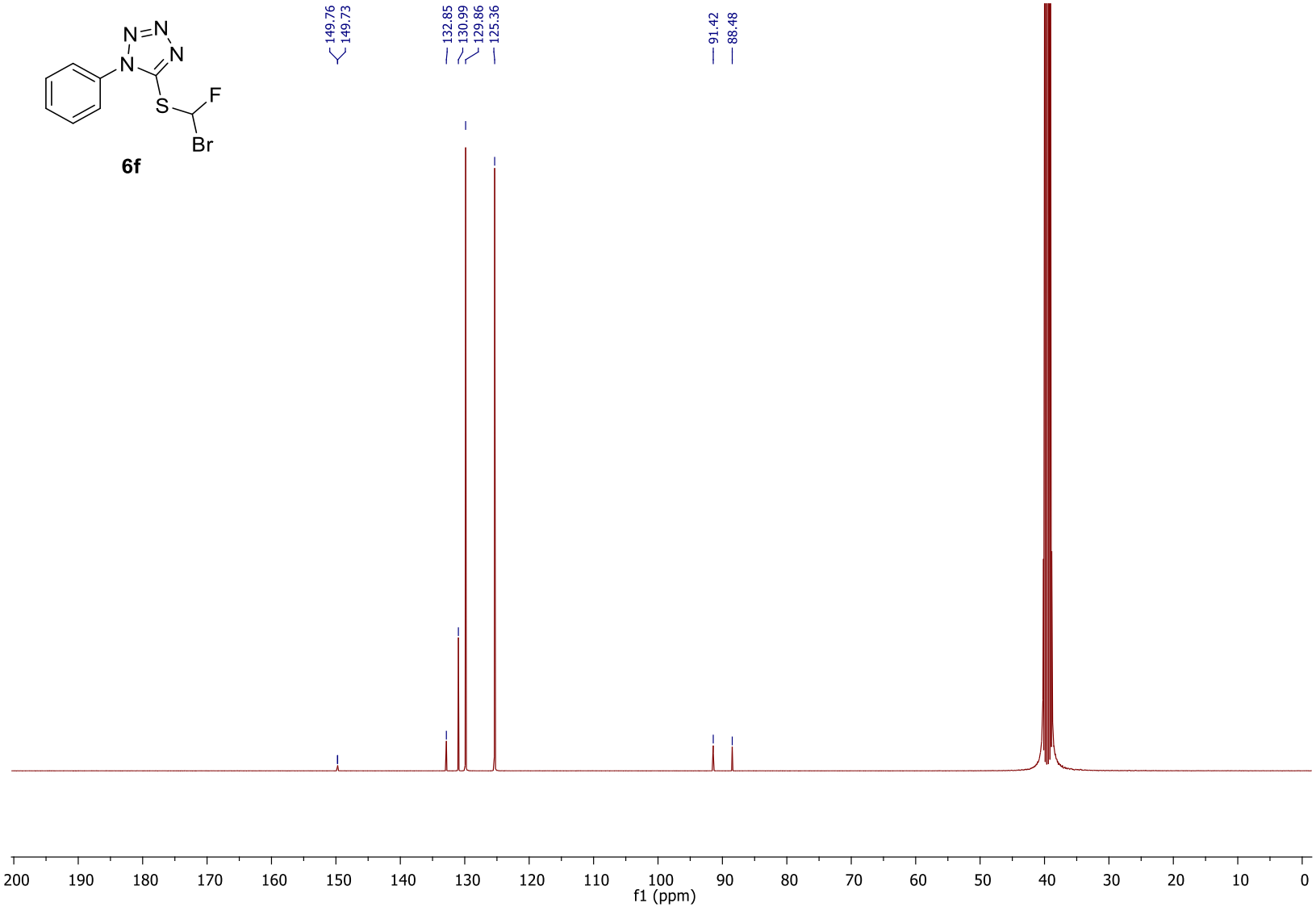

Figure S53. ^{13}C-NMR spectrum of 5-((bromofluoromethyl)thio)-1-phenyl-1*H*-tetrazole (**6f**).

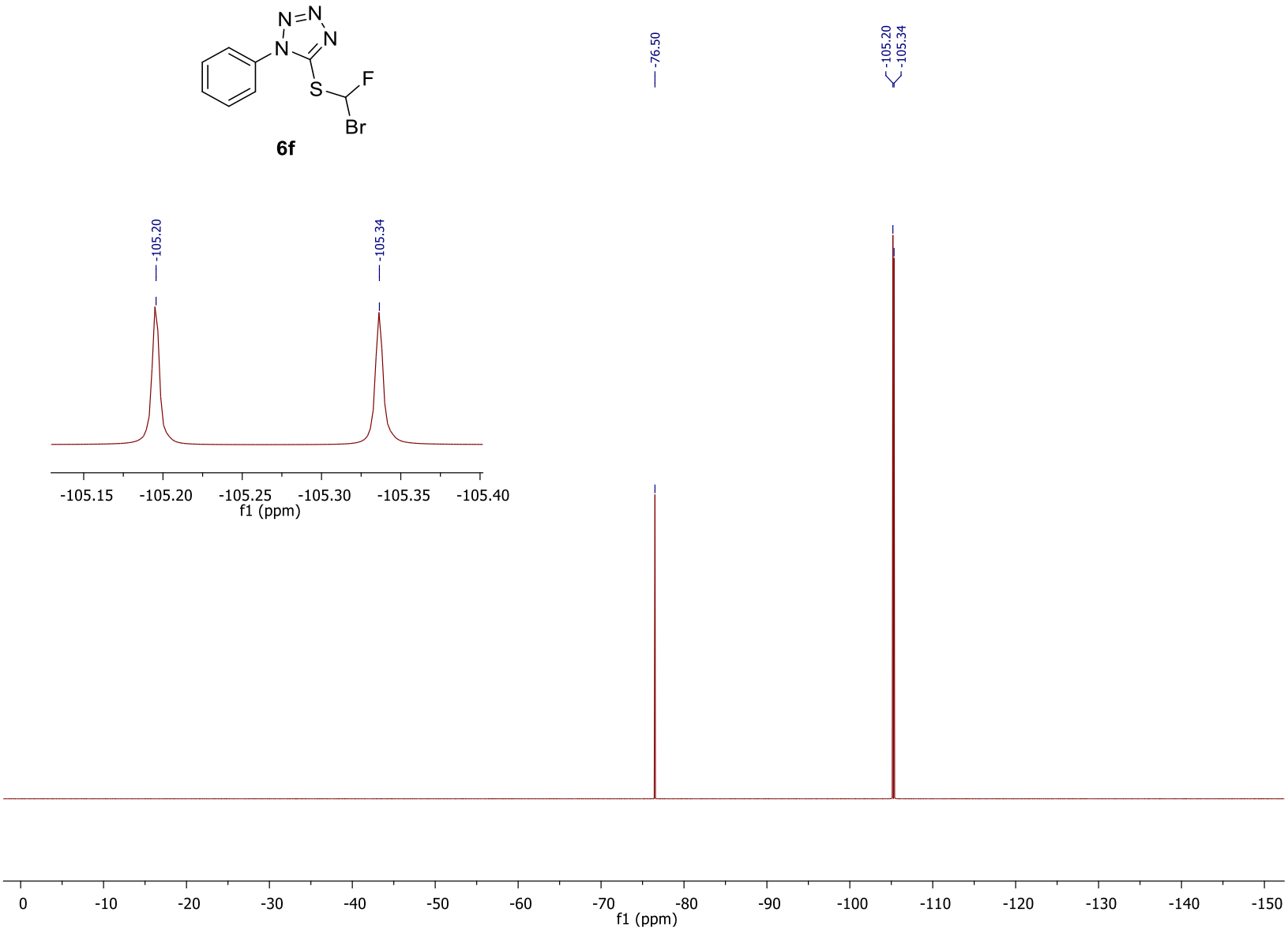

Figure S54. ^{19}F-NMR spectrum of 5-((bromofluoromethyl)thio)-1-phenyl-1*H*-tetrazole (**6f**).

2. Radiochemistry

Table S1. UPLC gradient for the analysis of the crude products **[^{18}F]4a**-**[^{18}F]4f** and **[^{18}F]5a**-**[^{18}F]5f** (gradient A)

Time (min)	HCO_2H/H_2O (0.05%, v/v)	MeCN	Flow rate (mL·min^{-1})
0	100	0	0.5
6	25	75	0.5
8	100	0	0.5

Table S2. UPLC gradient for the analysis of the crude products **[^{18}F]8a**-**[^{18}F]8g** (gradient B)

Time (min)	HCO_2H/H_2O (0.05%, v/v)	MeCN	Flow rate (mL·min^{-1})
0	100	0	0.5
6	0	100	0.5
8	100	0	0.5

2.1. General procedure for the ^{18}F-labeling of bromofluoromethyl heteroaryl-sulfides 6a-6f

Using the GE FASTlab™ synthesizer, an aliquot of [^{18}F]fluoride (150-200 MBq) was trapped on a Sep-Pak® Accell™ Plus QMA Carbonate Plus Light cartridge and eluted with a solution of Kryptofix® 222 ($K_{2.2.2}$; 7.5 mg in 600 μL of MeCN) and K_2CO_3 (1.4 mg in 150 μL of H_2O). Upon azeotropic drying, a solution of the precursors **6a** (12.3 mg, 0.04 mmol), **6b** (12.3 mg, 0.04 mmol), **6c** (6.5 mg, 0.02 mmol), **6d** (12.9 mg, 0.04 mmol), **6e** (11.0 mg, 0.04 mmol), or **6f** (11.6 mg, 0.04 mmol) in MeCN (1 mL) was transferred to the dry [^{18}F]potassium fluoride/Kryptofix® 222 ([^{18}F]KF/$K_{2.2.2}$) complex and heated to 120 °C. After 5 min of ^{18}F-labeling and dilution of the reaction mixture with H_2O, the labeled compounds **[^{18}F]4a–[^{18}F]4f** were trapped on Sep-Pak® C18 Plus Short cartridge. Subsequently, the ^{t}C18 cartridge was removed and the trapped crude products **[^{18}F]4a–[^{18}F]4f** were recovered to a 4 mL-vial *via* manual elution with MeCN (1 mL).

2.1.1. Synthesis of [^{18}F]2-((difluoromethyl)thio)-6-methoxybenzo[*d*]thiazole ([^{18}F]4a)

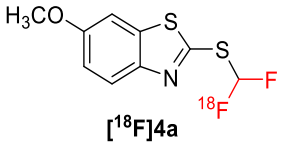

[^{18}F]4a

The implementation of the general procedure for the ^{18}F-labeling of 2-((bromofluoromethyl)thio)-6-methoxybenzo[*d*]thiazole (**6a**) (12.3 mg, 0.04 mmol) provided the labeled compound **[^{18}F]4a** in 14.2 ± 0.7% RCY (d.c. at the SOS).

The radiochemical yield (RCY) of the ^{18}F-labeling step was determined based on the activity of the recovered crude products **[^{18}F]4a–[^{18}F]4f**, on their radio-TLC and radio-UPLC purities, and the starting radioactivity, according to the following formula:

$$RCY\ (\%, d.c.) = \frac{radioTLC\ purity\ (\%)\ \times\ radioUPLC\ purity\ (\%)\ \times\ activity\ of\ the\ solution\ of\ [^{18}\mathbf{F}]\mathbf{4a}\text{–}[^{18}\mathbf{F}]\mathbf{4f}\ (d.c.)}{starting\ radioactivity\ \times\ 100}$$

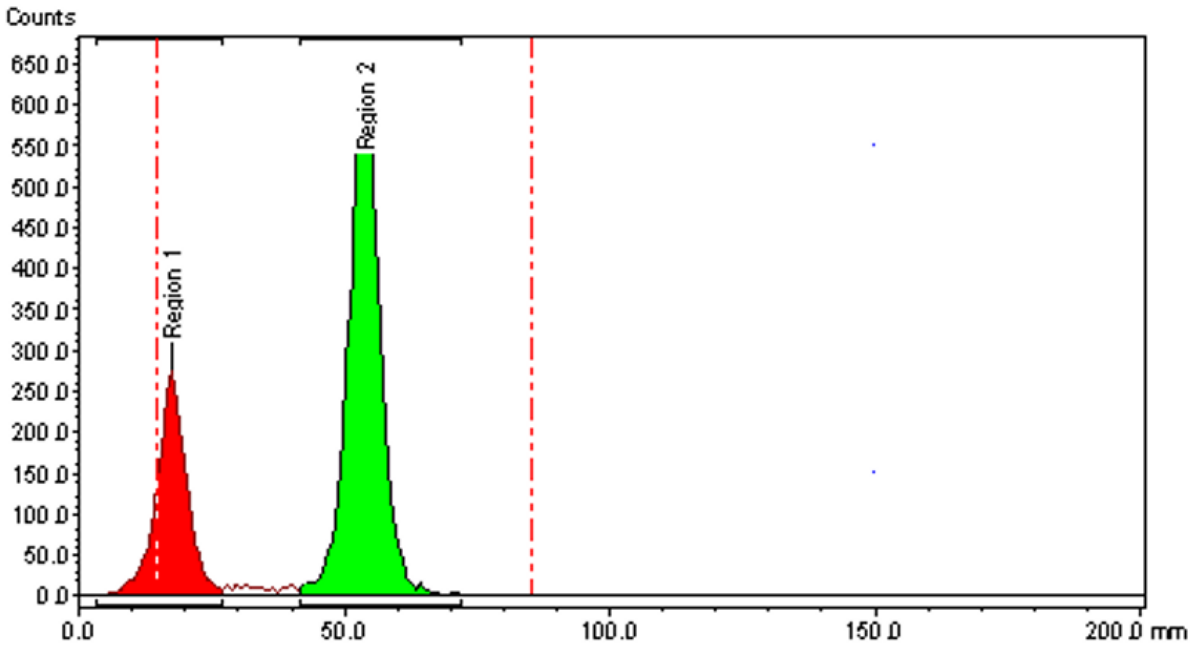

Figure S55. TLC radio-chromatogram of the crude product **[^{18}F]4a** (eluent: methanol).

Table S3. Determination of the radio-TLC purity of the crude product **[^{18}F]4a**

Retention factor (R_f, mm)	Ratio (%)
0.03	29 (impurity/by-product)
0.67	71 (desired crude product)

Table S4 furnishes more details of the RCY determination. The UPLC radio-chromatogram of the crude product **[^{18}F]4a** is depicted in Figure S56. Figure S57 represents the UPLC UV-chromatogram of the non-radioactive reference **4a**.

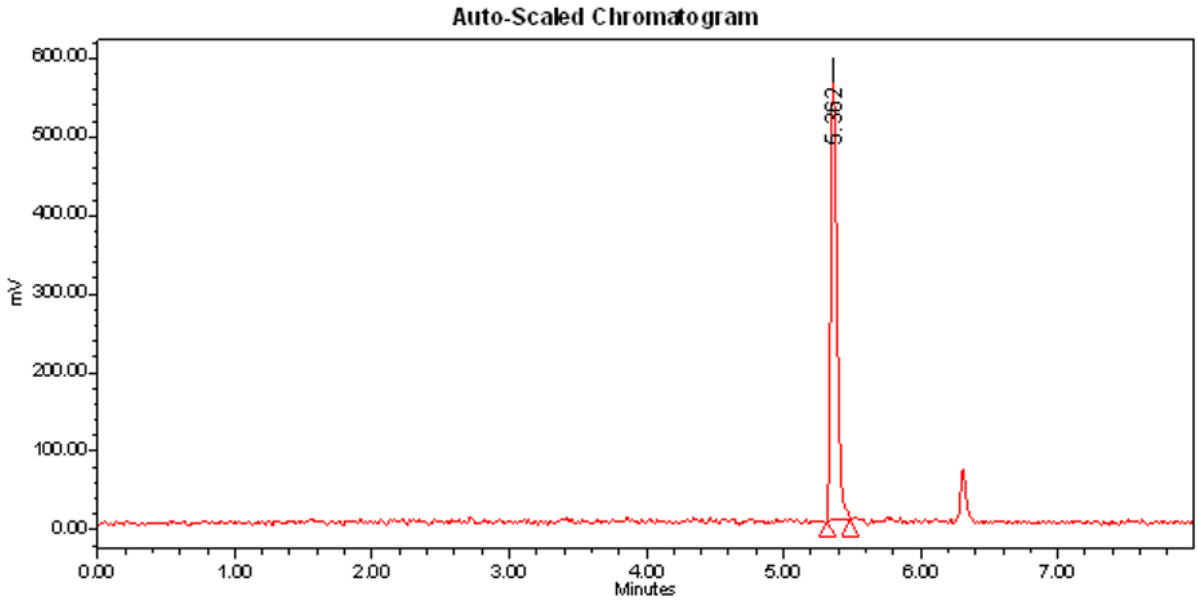

Figure S56. UPLC radio-chromatogram of the crude product **[^{18}F]4a** (gradient A).

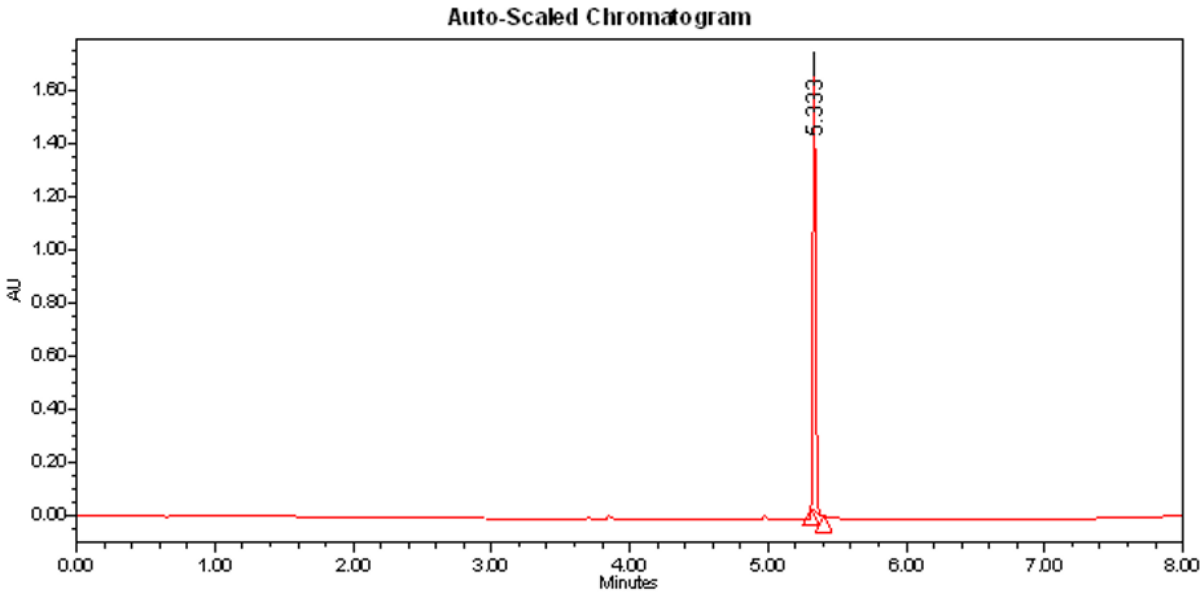

Figure S57. UPLC UV-chromatogram of the authentic reference **4a** (gradient A).

$$RCY\ (\%, d.c.) = \frac{radioTLC\ purity\ (\%)\ \times\ radioUPLC\ purity\ (\%)\ \times\ activity\ of\ the\ solution\ of\ [^{18}\mathbf{F}]\mathbf{4a}\ (d.c.)}{starting\ radioactivity\ \times\ 100}$$

$$RCY\ (\%, d.c.) = \frac{71\ \times\ 92\ \times\ 37.0}{169.4\ \times\ 100}$$

$$RCY\ (\%, d.c.) = 14.3\ \%$$

Table S4. Determination of the radiochemical yield (%) of the synthesis of **[^{18}F]4a**

Reaction	Starting activity (MBq)	Activity of the crude product [^{18}F]4a (MBq, d.c.)	Radio-TLC purity (%)	Radio-UPLC purity (%)	Radiochemical Yield (%)
1	169.4	37.0	71	92	14.3
2	144.4	28.8	74	90	13.3
3	187.9	50.9	55	100	14.9
Radiochemical Yield (%) ± Deviation					14.2 ± 0.7

2.1.2. Synthesis of [^{18}F]2-((difluoromethyl)thio)-5-methoxybenzo[*d*]thiazole ([^{18}F]4b)

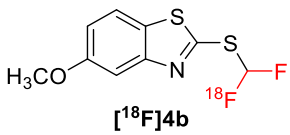

[^{18}F]4b

The implementation of the general procedure for the ^{18}F-labeling of 2-((bromofluoromethyl)thio)-5-methoxybenzo[*d*]thiazole (**6b**) (12.3 mg, 0.04 mmol) provided the labeled compound **[^{18}F]4b** in 11.8 ± 1.9% RCY (d.c. at the SOS). Table S5 furnishes more details of the RCY determination. The UPLC radio-chromatogram of the crude product **[^{18}F]4b** is depicted in Figure S58. Figure S59 represents the UPLC UV-chromatogram of the non-radioactive reference **4b**.

Table S5. Determination of the radiochemical yield (%) of the synthesis of **[^{18}F]4b**

Reaction	Starting activity (MBq)	Activity of the crude product [^{18}F]4b (MBq, d.c.)	Radio-TLC purity (%)	Radio-UPLC purity (%)	Radiochemical Yield (%)
1	187.5	41.5	42	100	9.3
2	142.2	24.2	68	100	11.6
3	173.4	30.5	67	100	11.8
4	167.4	34.2	73	97	14.5
Radiochemical Yield (%) ± Deviation					11.8 ± 1.9

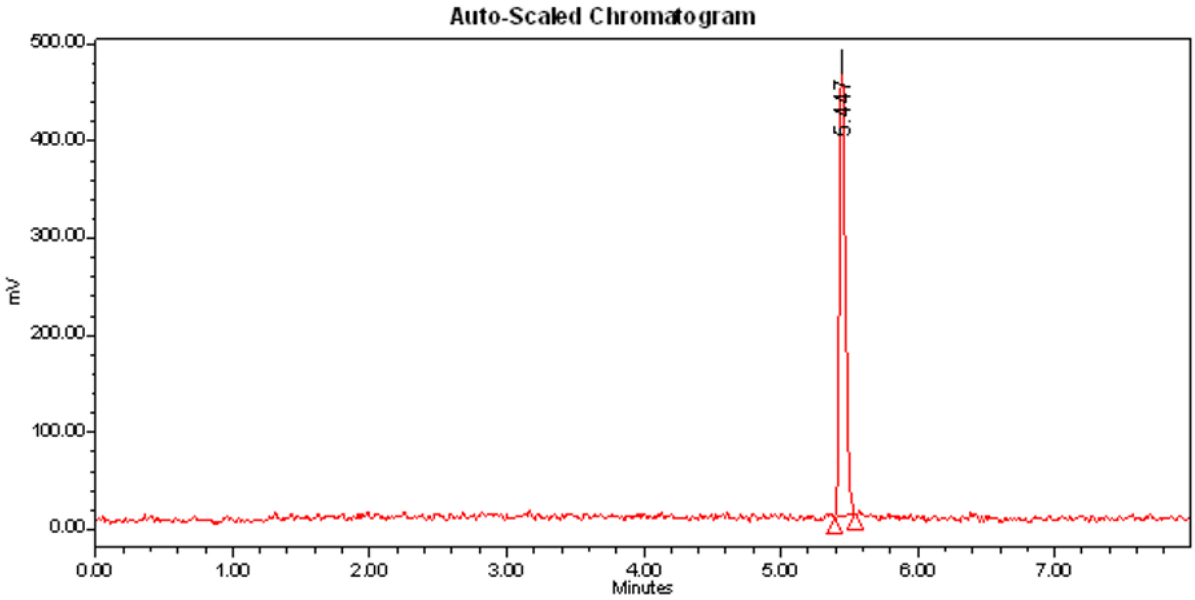

Figure S58. UPLC radio-chromatogram of the crude product **[^{18}F]4b** (gradient A).

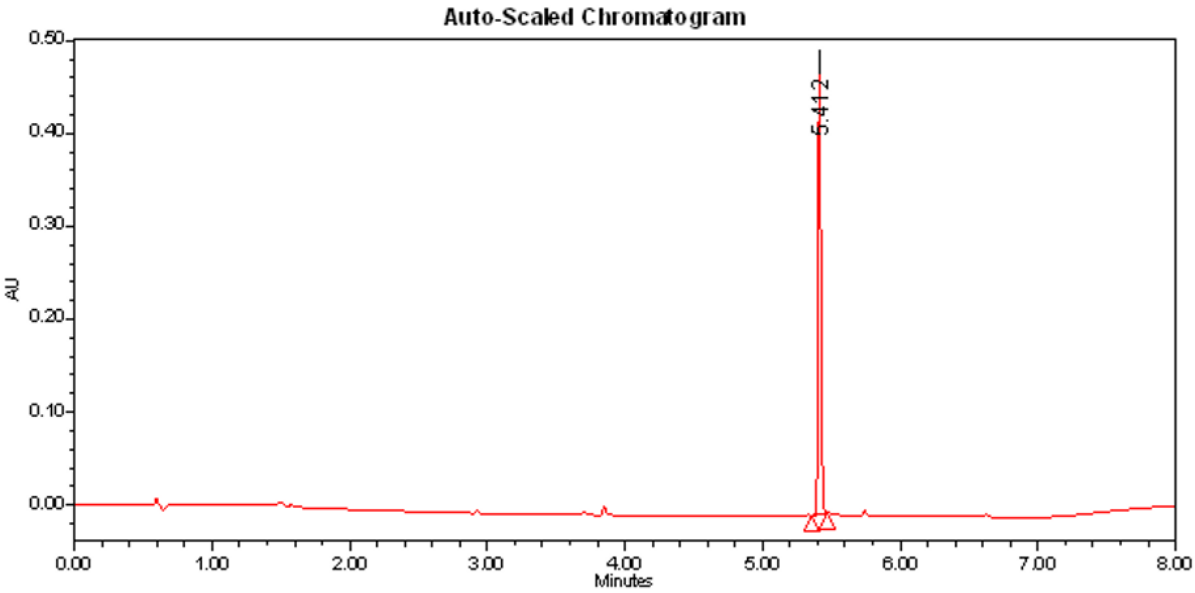

Figure S59. UPLC UV-chromatogram of the authentic reference **4b** (gradient A).

2.1.3. Synthesis of [^{18}F]2-((difluoromethyl)thio)-6-nitrobenzo[*d*]thiazole ([^{18}F]4c)

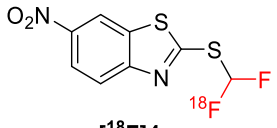

[^{18}F]4c

The implementation of the general procedure for the ^{18}F-labeling of 2-((bromofluoromethyl)thio)-6-nitrobenzo[*d*]thiazole (**6c**) (6.5 mg, 0.02 mmol) provided the labeled compound **[^{18}F]4c** in 13.6 ± 0.6% RCY (d.c. at the SOS). Table S6 furnishes more details of the RCY determination. The UPLC radio-chromatogram of the crude product **[^{18}F]4c** is depicted in Figure S60. Figure S61 represents the UPLC UV-chromatogram of the non-radioactive reference **4c**.

Table S6. Determination of the radiochemical yield (%) of the synthesis of **[^{18}F]4c**

Reaction	Starting activity (MBq)	Activity of the crude product [^{18}F]4c (MBq, d.c.)	Radio-TLC purity (%)	Radio-UPLC purity (%)	Radiochemical Yield (%)
1	150.9	32.6	75	82	13.3
2	173.1	36.1	81	86	14.5
3	196.1	37.8	70	97	13.1
Radiochemical Yield (%) ± Deviation					13.6 ± 0.6

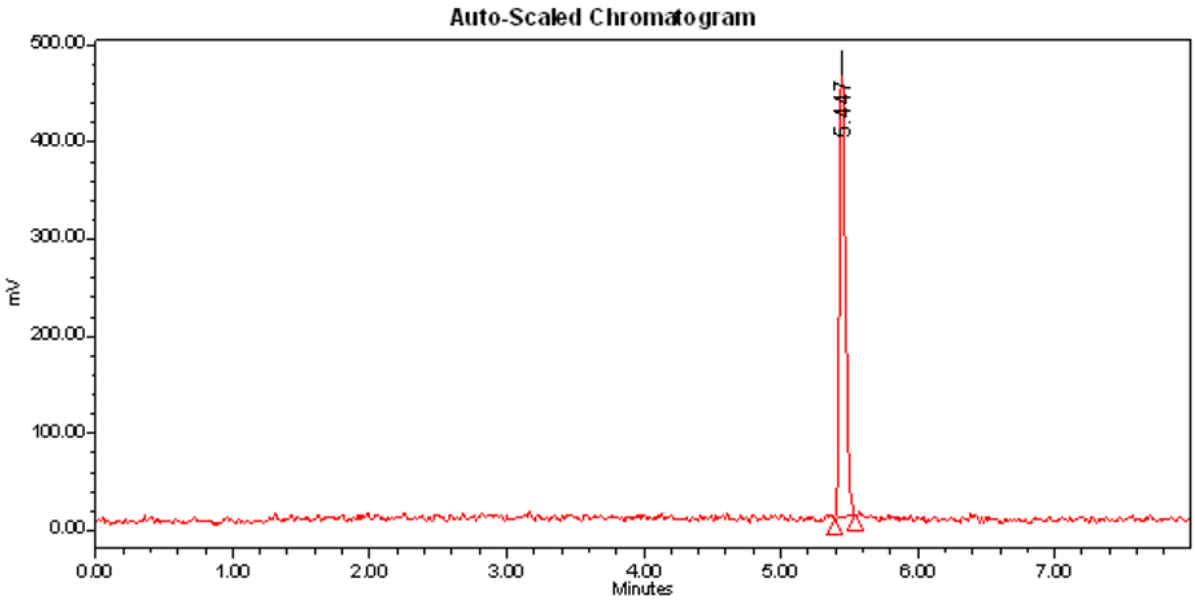

Figure S60. UPLC radio-chromatogram of the crude product **[^{18}F]4c** (gradient A).

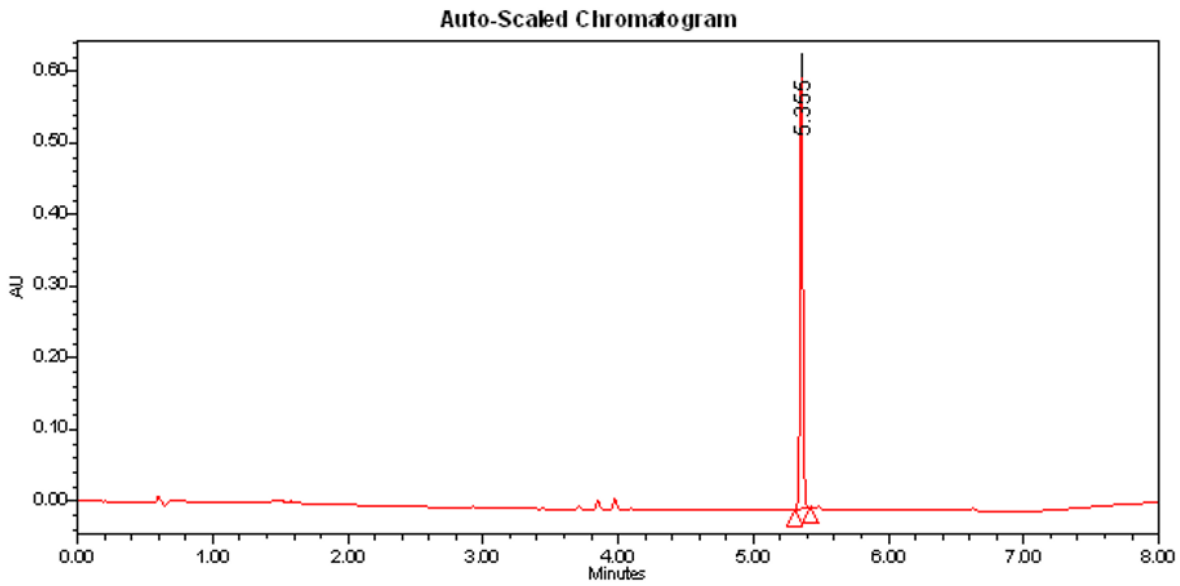

Figure S61. UPLC UV-chromatogram of the authentic reference **4c** (gradient A).

2.1.4. Synthesis of [^{18}F]2-((difluoromethyl)thio)-5-nitrobenzo[*d*]thiazole ([^{18}F]4d)

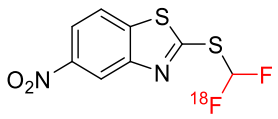

[^{18}F]4d

The implementation of the general procedure for the ^{18}F-labeling of 2-((bromofluoromethyl)thio)-5-nitrobenzo[*d*]thiazole (**6d**) (12.9 mg, 0.04 mmol) provided the labeled compound **[^{18}F]4d** in 12.7 ± 0.2% RCY (d.c. at the SOS). Table S7 furnishes more details of the RCY determination. The UPLC radio-chromatogram of the crude product **[^{18}F]4d** is depicted in Figure S62. Figure S63 represents the UPLC UV-chromatogram of the non-radioactive reference **4d**.

Table S7. Determination of the radiochemical yield (%) of the synthesis of **[^{18}F]4d**

Reaction	Starting activity (MBq)	Activity of the crude product [^{18}F]4d (MBq, d.c.)	Radio-TLC purity (%)	Radio-UPLC purity (%)	Radiochemical Yield (%)
1	196.8	62.1	46	86	12.5
2	161.4	38.7	67	79	12.7
3	180.6	34.9	75	89	12.9
Radiochemical Yield (%) ± Deviation					12.7 ± 0.2

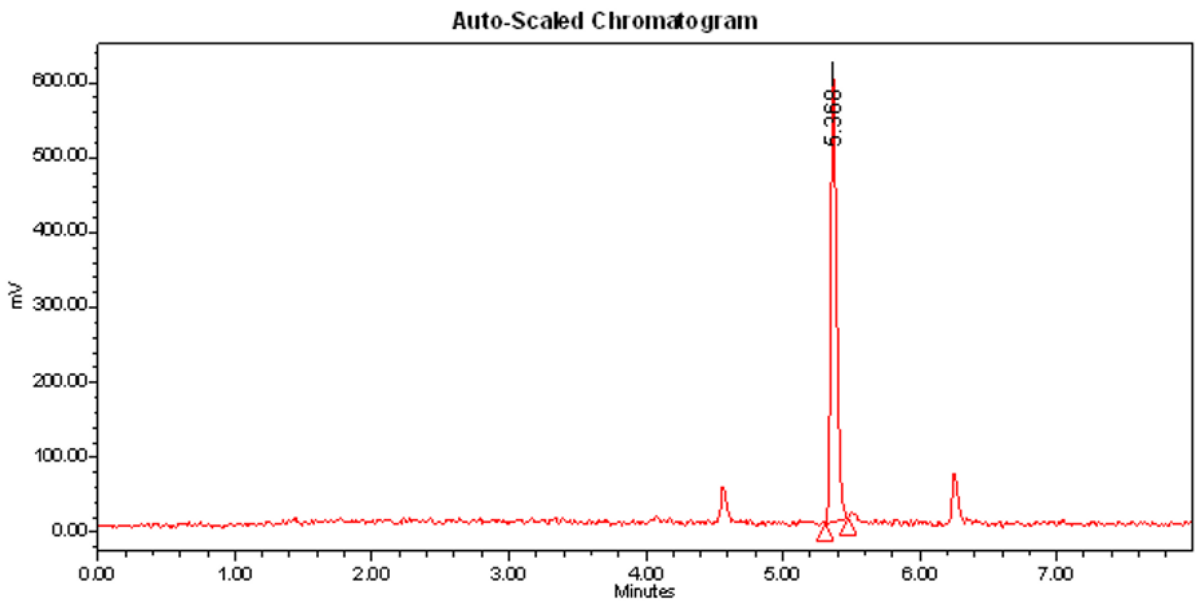

Figure S62. UPLC radio-chromatogram of the crude product **[^{18}F]4d** (gradient A).

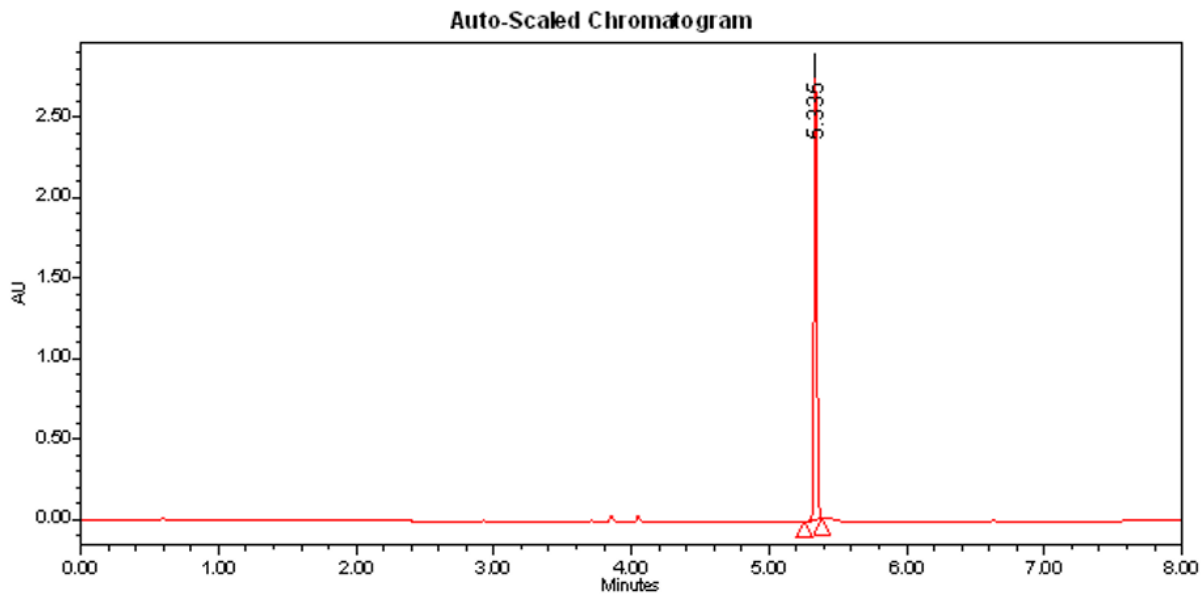

Figure S63. UPLC UV-chromatogram of the authentic reference **4d** (gradient A).

2.1.5. Synthesis of [^{18}F]2-((difluoromethyl)thio)-1-methyl-1*H*-benzo[*d*]imidazole ([^{18}F]4e)

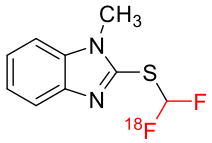

[^{18}F]4e

The implementation of the general procedure for the ^{18}F-labeling of 2-((bromofluoromethyl)thio)-1-methyl-1*H*-benzo[*d*]imidazole (**6e**) (11.0 mg, 0.04 mmol) provided the labeled compound **[^{18}F]4e** in 8.3 ± 1.9% RCY (d.c. at the SOS). Table S8 furnishes more details of the RCY determination. The UPLC radio-chromatogram of the crude product **[^{18}F]4e** is depicted in Figure S64. Figure S65 represents the UPLC UV-chromatogram of the non-radioactive reference **4e**.

Table S8. Determination of the radiochemical yield (%) of the synthesis of **[^{18}F]4e**

Reaction	Starting activity (MBq)	Activity of the crude product [^{18}F]4e (MBq, d.c.)	Radio-TLC purity (%)	Radio-UPLC purity (%)	Radiochemical Yield (%)
1	182.4	33	32	100	5.8
2	154.6	16.8	69	100	7.5
3	169.8	25.7	58	100	8.8
4	187.4	30.5	71	95	11.0
Radiochemical Yield (%) ± Deviation					8.3 ± 1.9

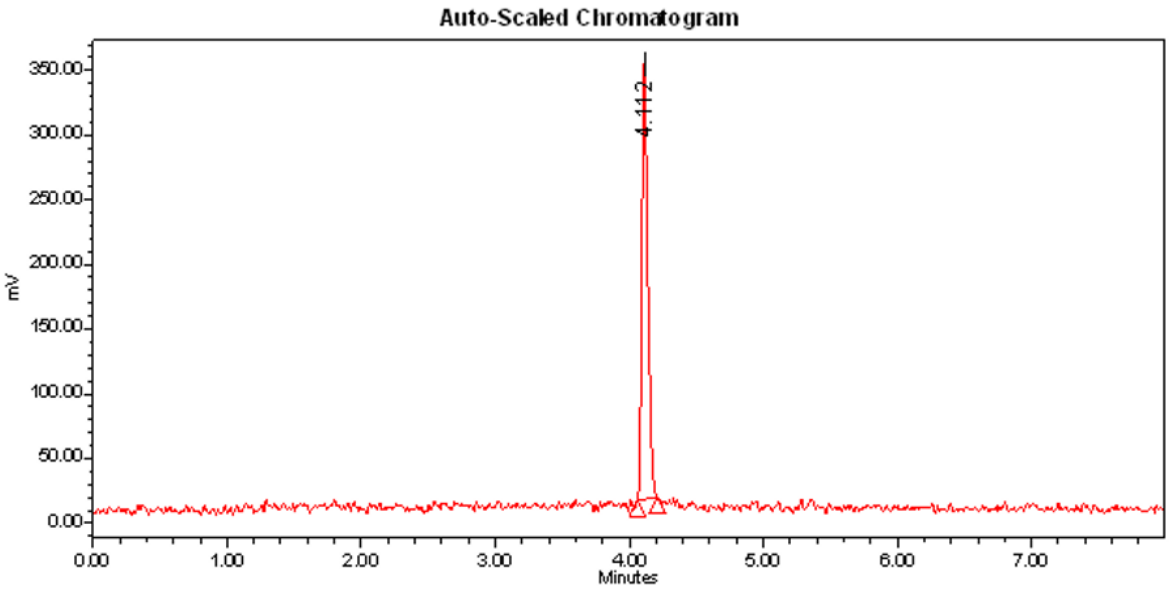

Figure S64. UPLC radio-chromatogram of the crude product **[^{18}F]4e** (gradient A).

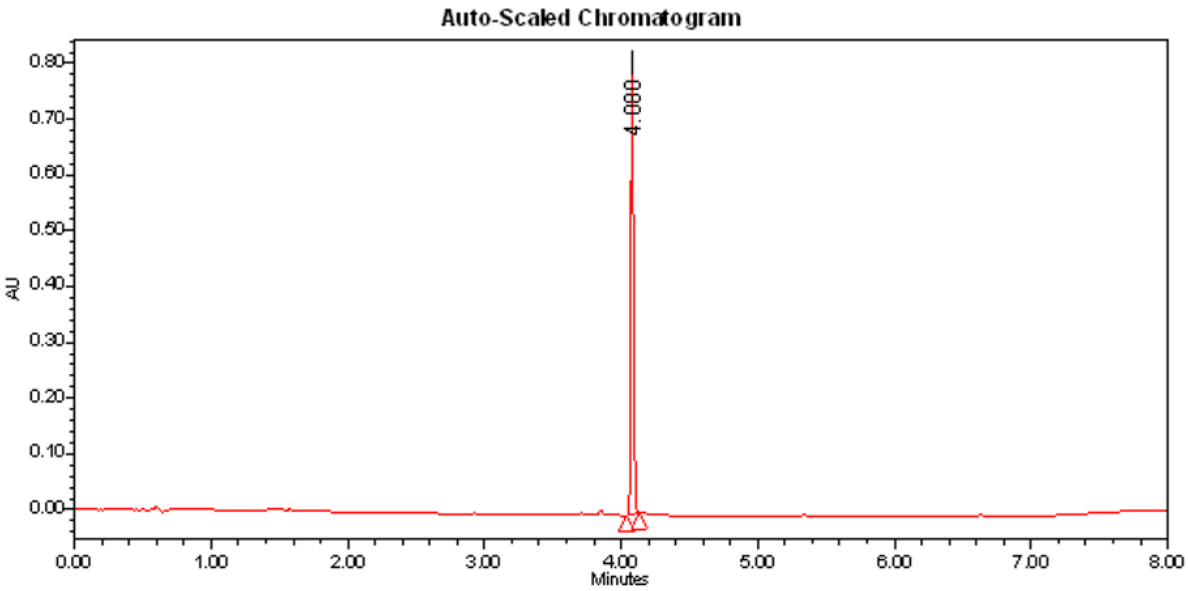

Figure S65. UPLC UV-chromatogram of the authentic reference **4e** (gradient A).

2.1.6. Synthesis of [^{18}F]5-((difluoromethyl)thio)-1-phenyl-1*H*-tetrazole ([^{18}F]4f)

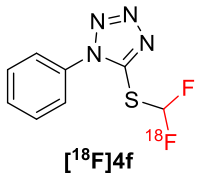

[^{18}F]4f

The implementation of the general procedure for the ^{18}F-labeling of 5-((bromofluoromethyl)thio)-1-phenyl-1*H*-tetrazole (**6f**) (11.6 mg, 0.04 mmol) provided the labeled compound **[^{18}F]4f** in 14.8 ± 0.8% RCY (d.c. at the SOS). Table S9 furnishes more details of the RCY determination. The UPLC radio-chromatogram of the crude product **[^{18}F]4f** is depicted in Figure S66. Figure S67 represents the UPLC UV-chromatogram of the non-radioactive reference **4f**.

Table S9. Determination of the radiochemical yield (%) of the synthesis of **[^{18}F]4f**

Reaction	Starting activity (MBq)	Activity of the crude product [^{18}F]4f (MBq, d.c.)	Radio-TLC purity (%)	Radio-UPLC purity (%)	Radiochemical Yield (%)
1	130.2	26.8	81	96	16.0
2	190.4	38.4	74	95	14.2
3	195.8	39.3	75	95	14.3
Radiochemical Yield (%) ± Deviation					14.8 ± 0.8

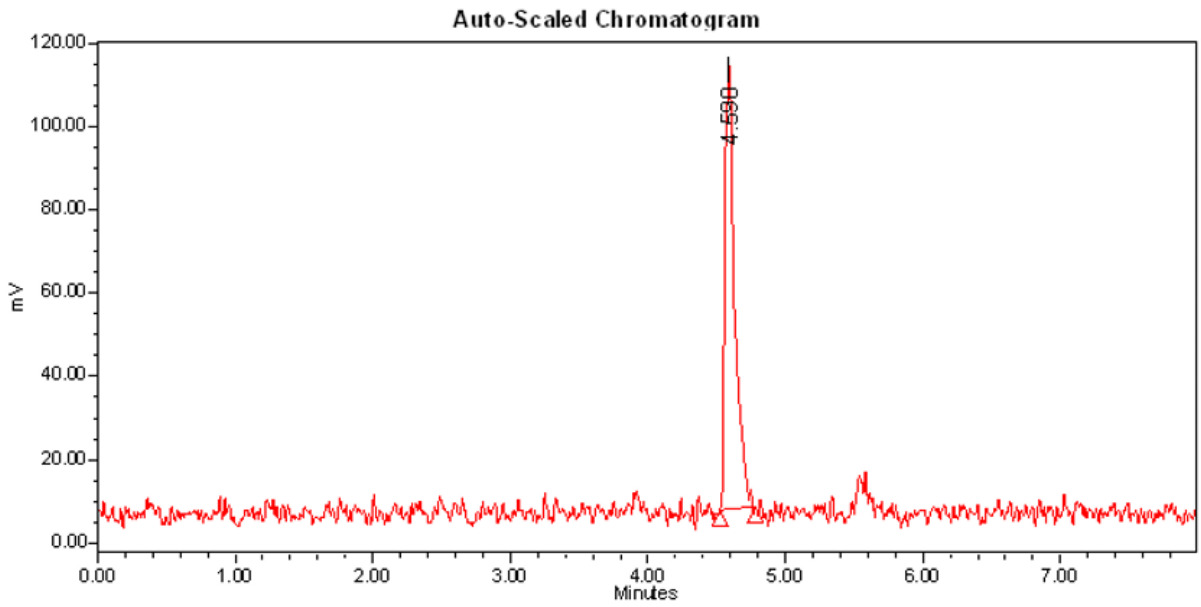

Figure S66. UPLC radio-chromatogram of the crude product **[^{18}F]4f** (gradient A).

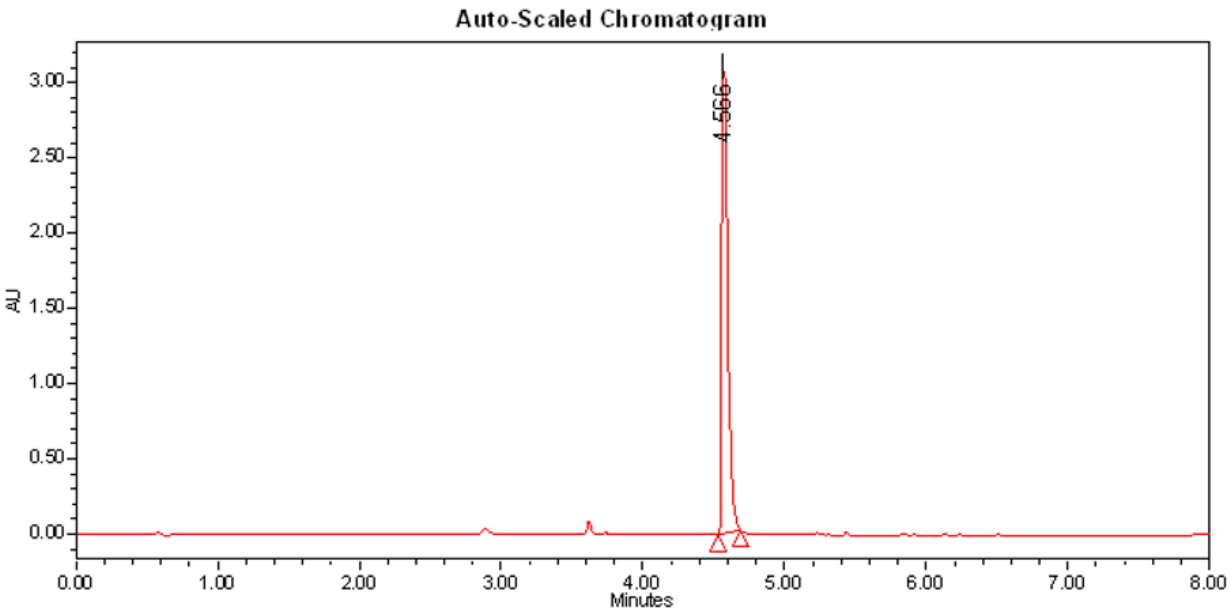

Figure S67. UPLC UV-chromatogram of the authentic reference **4f** (gradient A).

2.2. Optimization of the conditions for the oxidation of the [^{18}F]difluoromethyl heteroaryl-sulfide [^{18}F]4a

2.2.1. Synthesis of [^{18}F]2-((difluoromethyl)sulfonyl)-6-methoxybenzo[*d*]thiazole ([^{18}F]5a)

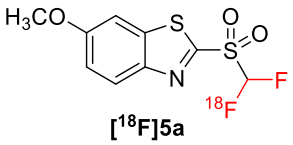

[^{18}F]5a

A solution containing $NaIO_4$ and $RuCl_3{\cdot}xH_2O$ in H_2O (1 mL) was transferred to the ^{t}C18 cartridge and the oxidation of the trapped crude products **[^{18}F]4a** (10-20 MBq) was carried out in solid-phase for 5 min at room temperature. Afterwards, the corresponding [^{18}F]difluoromethyl heteroaryl-sulfone **[^{18}F]5a** was manually eluted from the ^{t}C18 cartridge with MeCN (1 mL) to a 4 mL-vial.

The RCY of the oxidation step was determined based on the activity of the crude products **[^{18}F]4a** and **[^{18}F]5a**, and on their radio-TLC and radio-UPLC purities, according to the following equation:

$$RCY\ (\%, d.c.) = \frac{radioTLC\ purity\ (\%)\ \times\ radioUPLC\ purity\ (\%)\ \times\ activity\ of\ the\ solution\ of\ [^{18}\mathbf{F}]\mathbf{5a}\ (d.c.)}{activity\ of\ the\ solution\ of\ [^{18}\mathbf{F}]\mathbf{4a}\ \times\ 100}$$

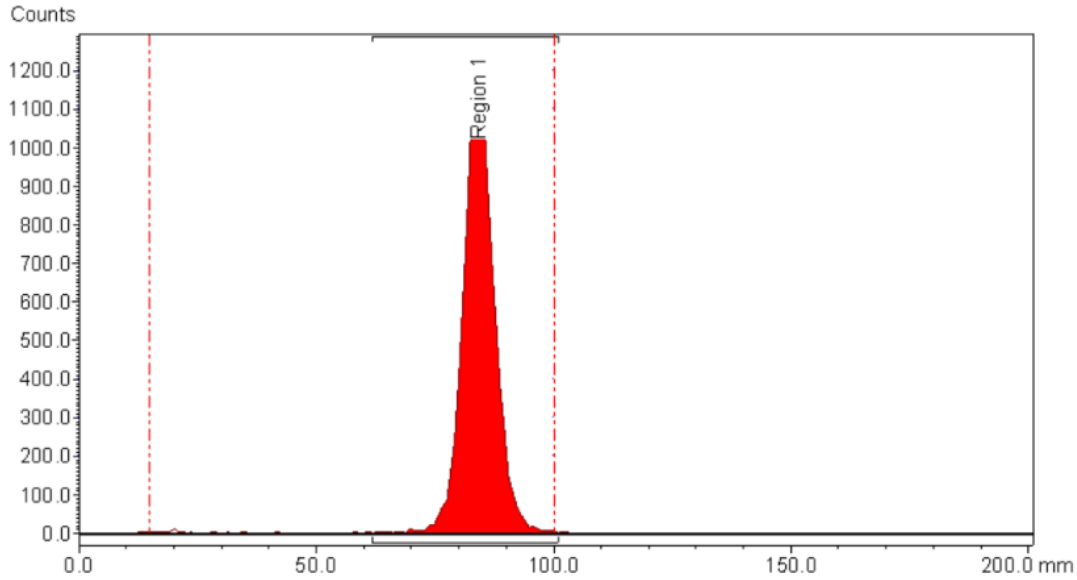

Figure S68. TLC radio-chromatogram of the crude product **[^{18}F]5a** (eluent: methanol).

Table S10. Determination of the radio-TLC purity of the crude product **[^{18}F]5a**

Retention factor (R_f, mm)	Ratio (%)
0	0 (impurity/by-product)
0.78	100 (desired crude product)

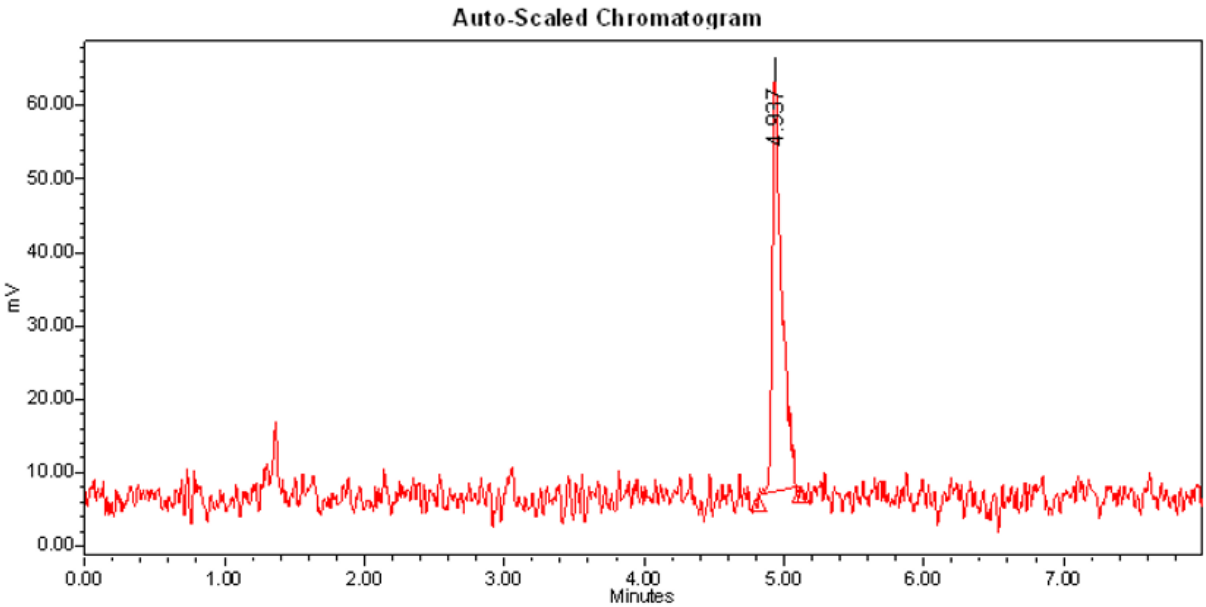

Figure S69. UPLC radio-chromatogram of the crude product **[^{18}F]5a** (gradient A).

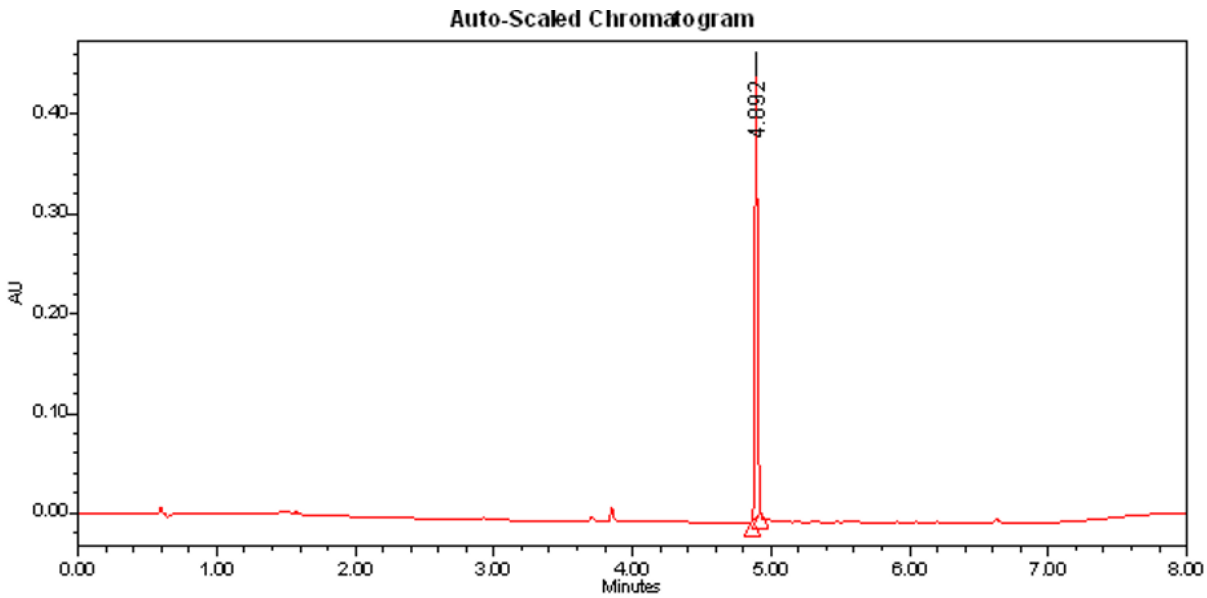

Figure S70. UPLC UV-chromatogram of the authentic reference **5a** (gradient A).

$$RCY\ (\%, d.c.) = \frac{radioTLC\ purity\ (\%)\ \times\ radioUPLC\ purity\ (\%)\ \times\ activity\ of\ the\ solution\ of\ [^{18}\mathbf{F}]\mathbf{5a}\ (d.c.)}{activity\ of\ the\ solution\ of\ [^{18}\mathbf{F}]\mathbf{4a}\ (d.c.)\ \times\ 100}$$

$$RCY\ (\%, d.c.) = \frac{100\ \times\ 92\ \times\ 12.0}{15.6\ \times\ 100}$$

$$RCY\ (\%, d.c.) =\ 70.6\ \%$$

According to the reported conditions for the oxidation of the [^{18}F]difluoromethyl heteroaryl-sulfide **[^{18}F]1'**, the following table summarizes the results of the different optimization tests conducted in the **[^{18}F]4a**.

Standard reaction conditions for the oxidation of [^{18}F]4a: [^{18}F]difluoromethyl heteroaryl-sulfide **[^{18}F]4a** (10-20 MBq), $NaIO_4$ (mmol), $RuCl_3{\cdot}xH_2O$ (mmol), H_2O (1 mL), rt, 5 min.

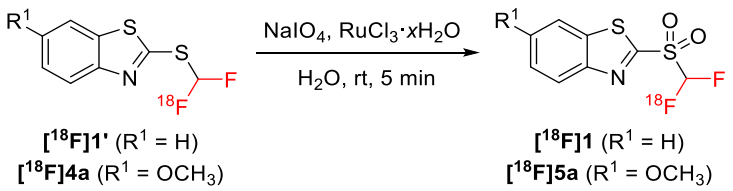

Entry	Substrate	$NaIO_4$ (mmol)	$RuCl_3{\cdot}xH_2O$ (mmol)	RCY (%)[a]
1	**[^{18}F]1'**	0.24	0.008	82.9 ± 7.9 (n=3)[b]
2	**[^{18}F]4a**	0.24	0.008	32.1
3	**[^{18}F]4a**	0.24	0.016	59.6
4	**[^{18}F]4a**	**0.72**	**0.016**	**70.9 ± 6.1 (n=3)**[b]

[a] All RCYs were decay-corrected at the SOS. [b] Full consumption of the substrates.

The best conditions for the oxidation of the substrate **[^{18}F]4a** were: [^{18}F]difluoromethyl heteroaryl-sulfide **[^{18}F]4a** (10-20 MBq), $NaIO_4$ (0.72 mmol), $RuCl_3{\cdot}xH_2O$ (0.016 mmol), H_2O (1 mL), rt, 5 min.

The implementation of the optimized procedure for the oxidation of [^{18}F]2-((difluoromethyl)thio)-5-methoxybenzo[*d*]thiazole (**[^{18}F]4a**) (10-20 MBq) provided the labeled compound **[^{18}F]5a** in 70.9 ± 6.1% RCY (d.c. at the SOS). Table S11 furnishes more details of the RCY determination. The UPLC radio-

chromatogram of the crude product **[^{18}F]5a** is depicted in Figure S69. Figure S70 represents the UPLC UV-chromatogram of the non-radioactive reference **5a**.

Table S11. Determination of the radiochemical yield (%) of the synthesis of **[^{18}F]5a**

Reaction	Activity of the crude product [^{18}F]4a (MBq)	Activity of the crude product [^{18}F]5a (MBq, d.c.)	Radio-TLC purity (%)	Radio-UPLC purity (%)	Radiochemical Yield (%)
1	15.6	12.0	100	92	70.6
2	12.7	10.3	99	98	78.5
3	13.6	11.5	100	75	63.6
Radiochemical Yield (%) ± Deviation					70.9 ± 6.1

2.3. General procedure for oxidation of the [^{18}F]difluoromethyl heteroaryl-sulfides [^{18}F]4a-[^{18}F]4f

A solution containing $NaIO_4$ (153.9 mg, 0.072 mmol) and $RuCl_3{\cdot}xH_2O$ (3.4 mg, 0.016 mmol) in H_2O (1 mL) was transferred to the ^{t}C18 cartridge and the oxidation of the trapped crude products **[^{18}F]4a–[^{18}F]4f** (10-20 MBq) was carried out in solid-phase for 5 min at room temperature. Afterwards, the corresponding [^{18}F]difluoromethyl heteroaryl-sulfones **[^{18}F]5a–[^{18}F]5f** were manually eluted from the ^{t}C18 cartridge with MeCN (1 mL) to a 4 mL-vial.

2.3.1. Synthesis of [^{18}F]2-((difluoromethyl)sulfonyl)-5-methoxybenzo[*d*]thiazole ([^{18}F]5b)

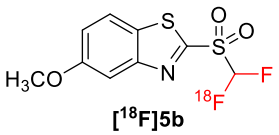

[^{18}F]5b

The implementation of the general procedure for the oxidation of [^{18}F]2-((difluoromethyl)thio)-5-methoxybenzo[*d*]thiazole (**[^{18}F]4b**) (10-20 MBq) provided the labeled compound **[^{18}F]5b** in 70.6 ± 5.1% RCY (d.c. at the SOS). Table S12 furnishes more details of the RCY determination. The UPLC radio-chromatogram of the crude product **[^{18}F]5b** is depicted in Figure S71. Figure S72 represents the UPLC UV-chromatogram of the non-radioactive reference **5b**.

Table S12. Determination of the radiochemical yield (%) of the synthesis of **[^{18}F]5b**

Reaction	Activity of the crude product [^{18}F]4b (MBq)	Activity of the crude product [^{18}F]5b (MBq, d.c.)	Radio-TLC purity (%)	Radio-UPLC purity (%)	Radiochemical Yield (%)
1	17.4	13.1	99	85	63.5
2	16.2	13.7	99	87	72.9
3	14.9	11.2	100	100	75.4
Radiochemical Yield (%) ± Deviation					70.6 ± 5.1

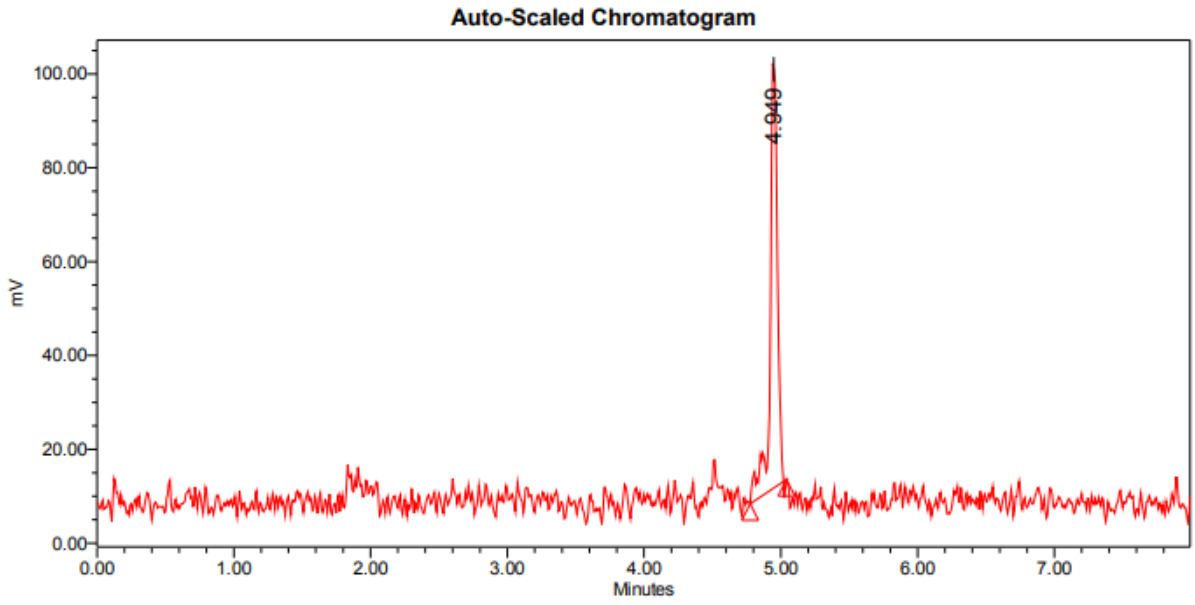

Figure S71. UPLC radio-chromatogram of the crude product **[^{18}F]5b** (gradient A).

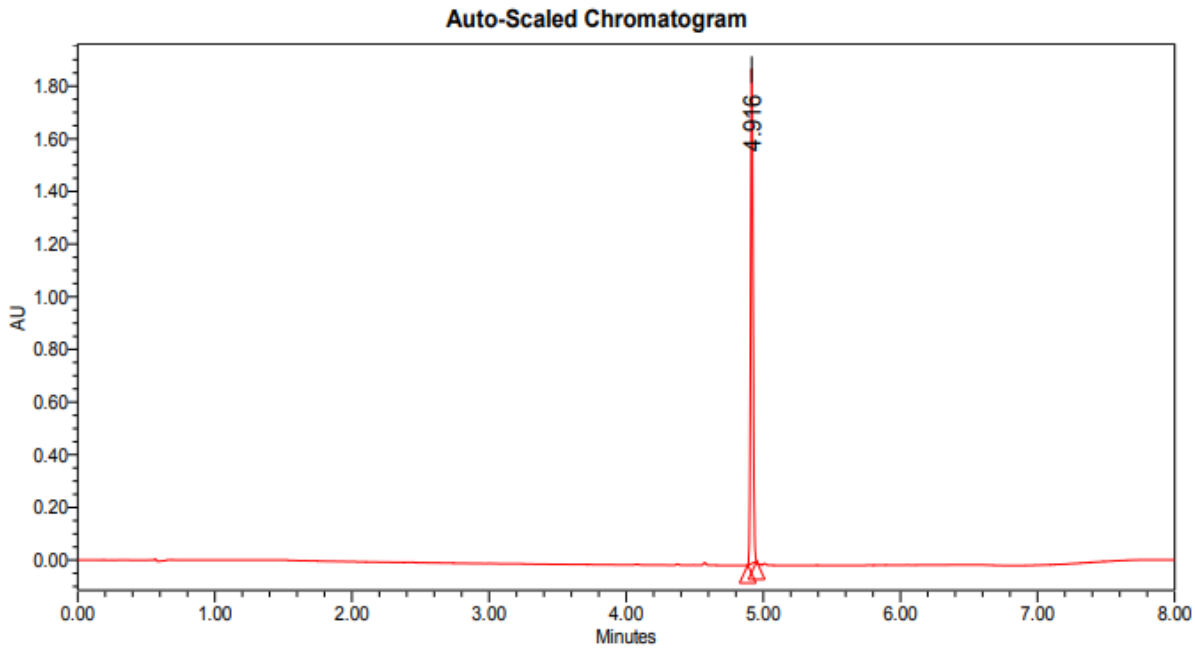

Figure S72. UPLC UV-chromatogram of the authentic reference **5b** (gradient A).

2.3.2. Synthesis of [^{18}F]2-((difluoromethyl)sulfonyl)-6-nitrobenzo[*d*]thiazole ([^{18}F]5c)

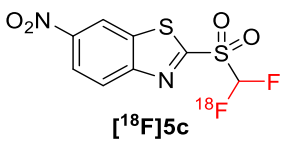

[^{18}F]5c

The implementation of the general procedure for the oxidation of [^{18}F]2-((difluoromethyl)thio)-6-nitrobenzo[*d*]thiazole (**[^{18}F]4c**) (10-20 MBq) provided the labeled compound **[^{18}F]5c** in 88.2 ± 0.2% RCY (d.c. at the SOS). Table S13 furnishes more details of the RCY determination. The UPLC radio-chromatogram of the crude product **[^{18}F]5c** is depicted in Figure S73. Figure S74 represents the UPLC UV-chromatogram of the non-radioactive reference **5c**.

Table S13. Determination of the radiochemical yield (%) of the synthesis of **[^{18}F]5c**

Reaction	Activity of the crude product [^{18}F]4c (MBq)	Activity of the crude product [^{18}F]5c (MBq, d.c.)	Radio-TLC purity (%)	Radio-UPLC purity (%)	Radiochemical Yield (%)
1	15.9	14.1	100	100	88.4
2	14.2	12.6	100	99	88
3	14.8	13.4	100	97	88.1
Radiochemical Yield (%) ± Deviation					88.2 ± 0.2

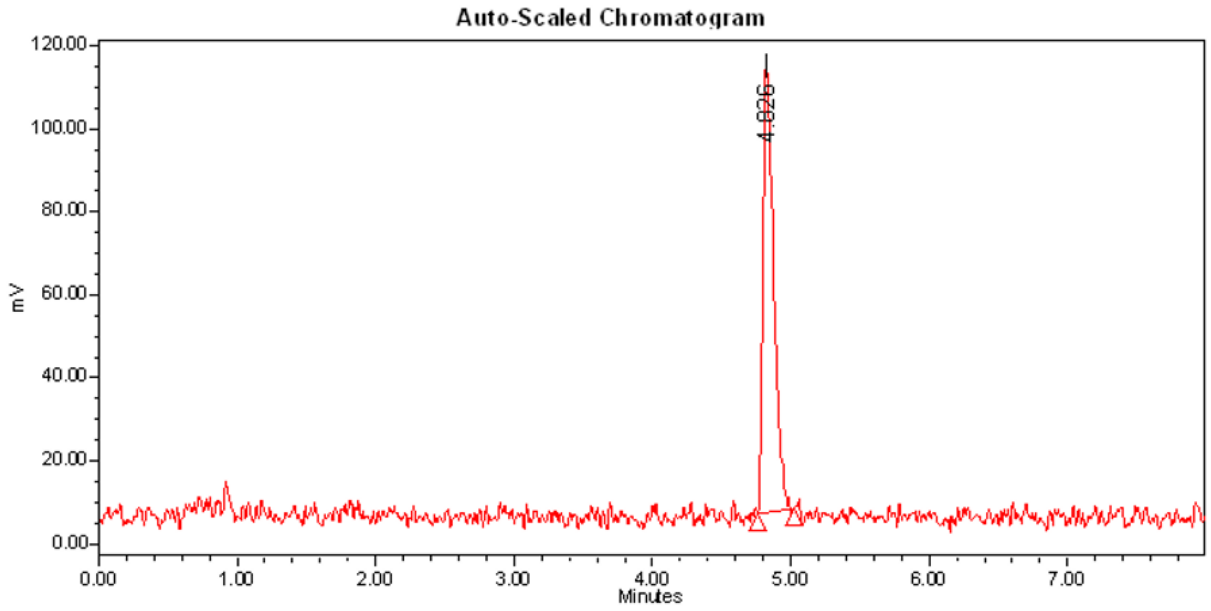

Figure S73. UPLC radio-chromatogram of the crude product **[^{18}F]5c** (gradient A).

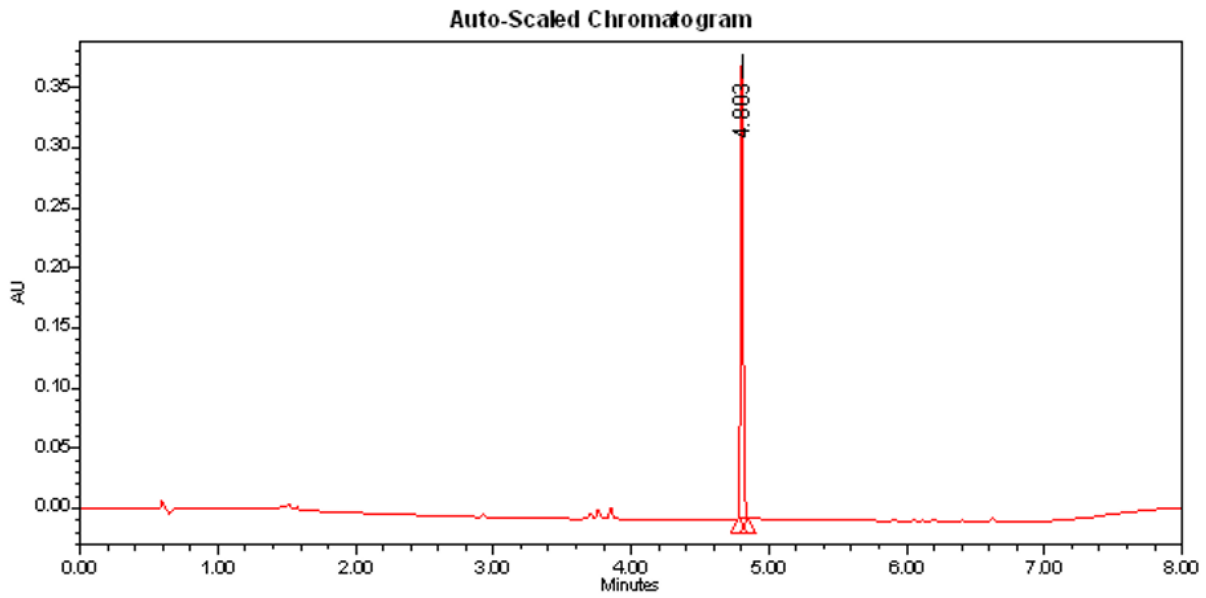

Figure S74. UPLC UV-chromatogram of the authentic reference **5c** (gradient A).

2.3.3. Synthesis of [^{18}F]2-((difluoromethyl)sulfonyl)-5-nitrobenzo[*d*]thiazole ([^{18}F]5d)

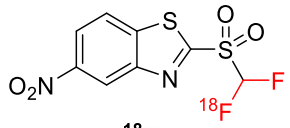

[^{18}F]5d

The implementation of the general procedure for the oxidation of [^{18}F]2-((difluoromethyl)thio)-5-nitrobenzo[*d*]thiazole (**[^{18}F]4d**) (10-20 MBq) provided the labeled compound **[^{18}F]5d** in 88.4 ± 2.8% RCY (d.c. at the SOS). Table S14 furnishes more details of the RCY determination. The UPLC radio-chromatogram of the crude product **[^{18}F]5d** is depicted in Figure S75. Figure S76 represents the UPLC UV-chromatogram of the non-radioactive reference **5d**.

Table S14. Determination of the radiochemical yield (%) of the synthesis of **[^{18}F]5d**

Reaction	Activity of the crude product [^{18}F]4d (MBq)	Activity of the crude product [^{18}F]5d (MBq, d.c.)	Radio-TLC purity (%)	Radio-UPLC purity (%)	Radiochemical Yield (%)
1	13.9	13.3	99	97	92.1
2	15.0	14.6	99	89	85.6
3	15.9	15.1	99	93	87.6
Radiochemical Yield (%) ± Deviation					88.4 ± 2.8

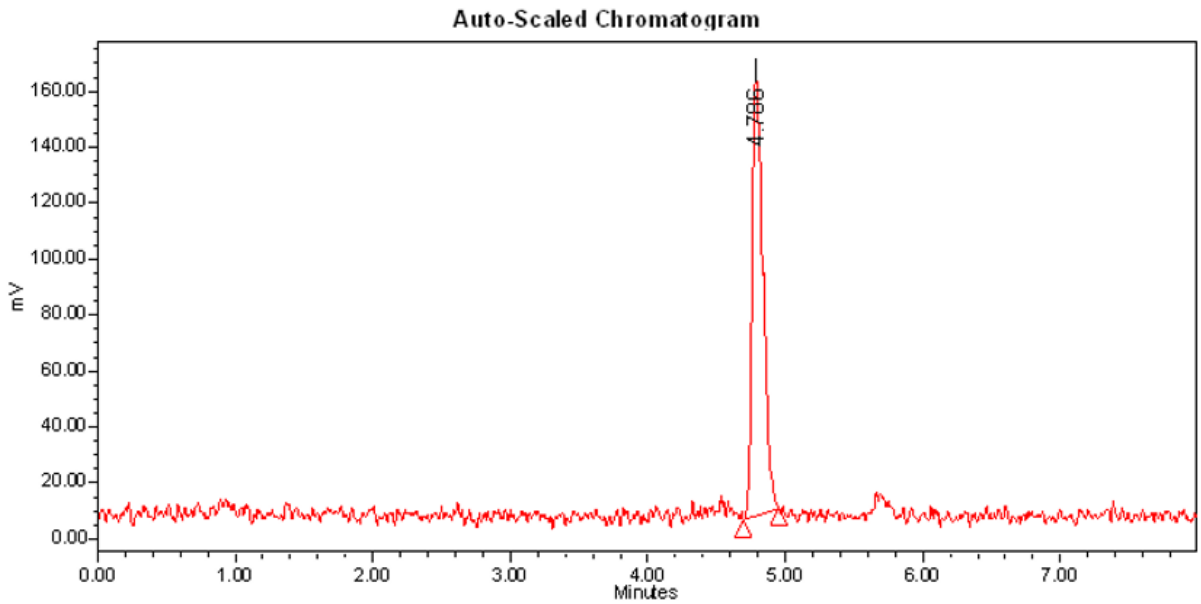

Figure S75. UPLC radio-chromatogram of the crude product **[^{18}F]5d** (gradient A).

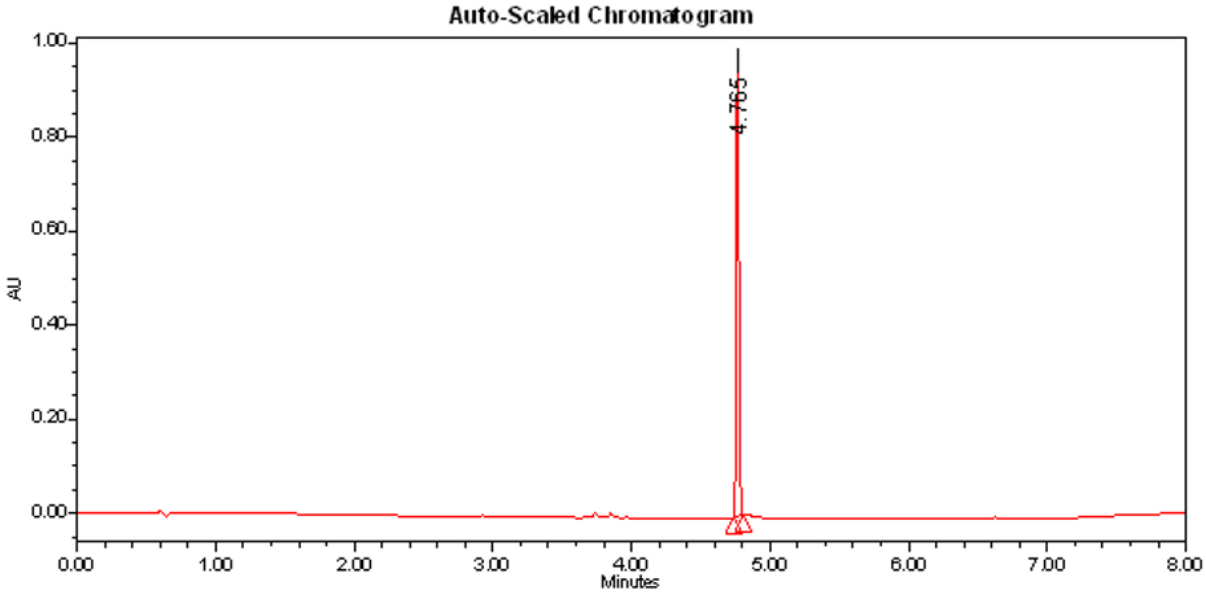

Figure S76. UPLC UV-chromatogram of the authentic reference **5d** (gradient A).

2.3.4. Synthesis of [^{18}F]2-((difluoromethyl)sulfonyl)-1-methyl-1*H*-benzo[*d*]imidazole ([^{18}F]5e)

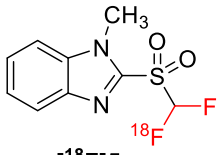

[^{18}F]5e

The implementation of the general procedure for the oxidation of [^{18}F]2-((difluoromethyl)thio)-1-methyl-1*H*-benzo[*d*]imidazole (**[^{18}F]4e**) (10-20 MBq) provided the labeled compound **[^{18}F]5e** in 86.1 ± 3.0% RCY (d.c. at the SOS). Table S15 furnishes more details of the RCY determination. The UPLC radio-chromatogram of the crude product **[^{18}F]5e** is depicted in Figure S77. Figure S78 represents the UPLC UV-chromatogram of the non-radioactive reference **5e**.

Table S15. Determination of the radiochemical yield (%) of the synthesis of **[^{18}F]5e**

Reaction	Activity of the crude product [^{18}F]4e (MBq)	Activity of the crude product [^{18}F]5e (MBq, d.c.)	Radio-TLC purity (%)	Radio-UPLC purity (%)	Radiochemical Yield (%)
1	13.7	12.4	100	100	90.2
2	17.4	16.0	93	97	83.1
3	14.7	13.2	100	95	85
Radiochemical Yield (%) ± Deviation					86.1 ± 3.0

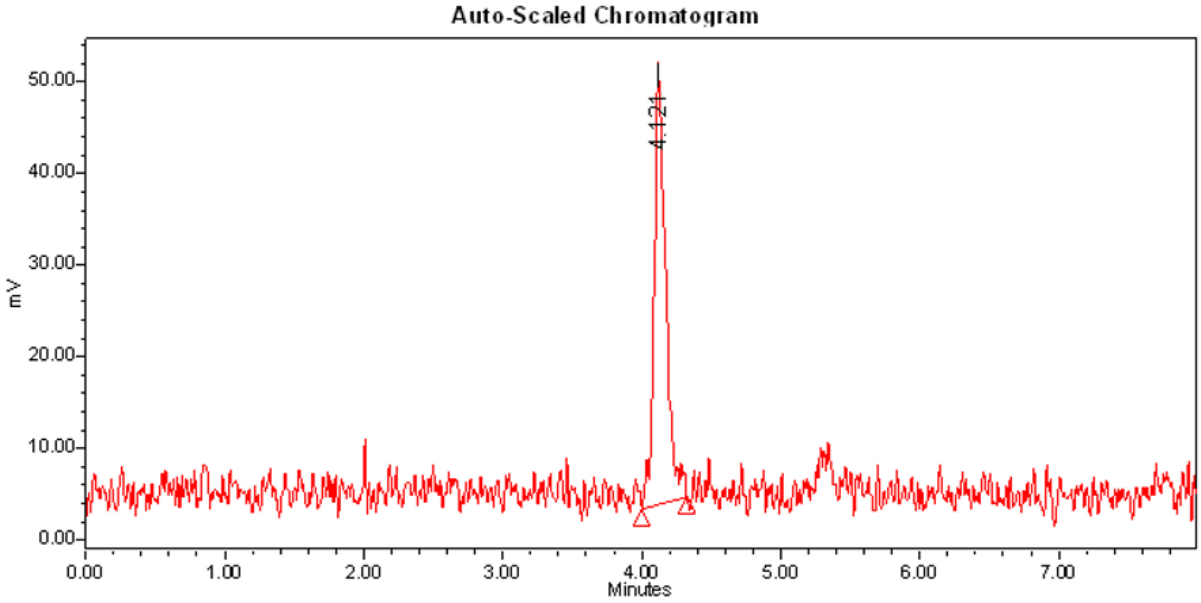

Figure S77. UPLC radio-chromatogram of the crude product **[^{18}F]5e** (gradient A).

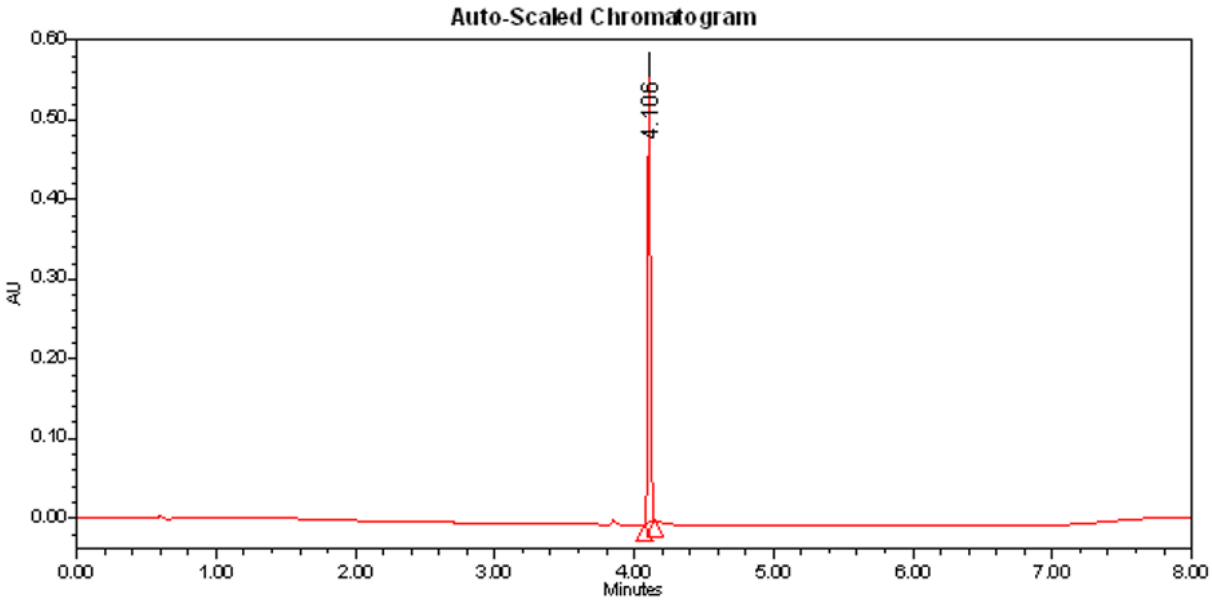

Figure S78. UPLC UV-chromatogram of the authentic reference **5e** (gradient A).

2.3.5. Synthesis of [^{18}F]5-((difluoromethyl)sulfonyl)-1-phenyl-1*H*-tetrazole ([^{18}F]5f)

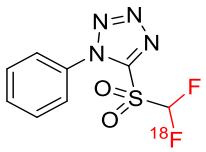

[^{18}F]5f

The implementation of the general procedure for the oxidation of [^{18}F]5-((difluoromethyl)thio)-1-phenyl-1*H*-tetrazole (**[^{18}F]4f**) (10-20 MBq) provided the labeled compound **[^{18}F]5f** in 91.9 ± 2.8% RCY (d.c. at the SOS). Table S16 furnishes more details of the RCY determination. The UPLC radio-chromatogram of the crude product **[^{18}F]5f** is depicted in Figure S79. Figure S80 represents the UPLC UV-chromatogram of the non-radioactive reference **5f**.

Table S16. Determination of the radiochemical yield (%) of the synthesis of **[^{18}F]5f**

Reaction	Activity of the crude product [^{18}F]4f (MBq)	Activity of the crude product [^{18}F]5f (MBq, d.c.)	Radio-TLC purity (%)	Radio-UPLC purity (%)	Radiochemical Yield (%)
1	15.4	13.7	100	100	88.7
2	16.1	14.7	100	100	91.4
3	15.7	15.0	100	100	95.6
Radiochemical Yield (%) ± Deviation					91.9 ± 2.8

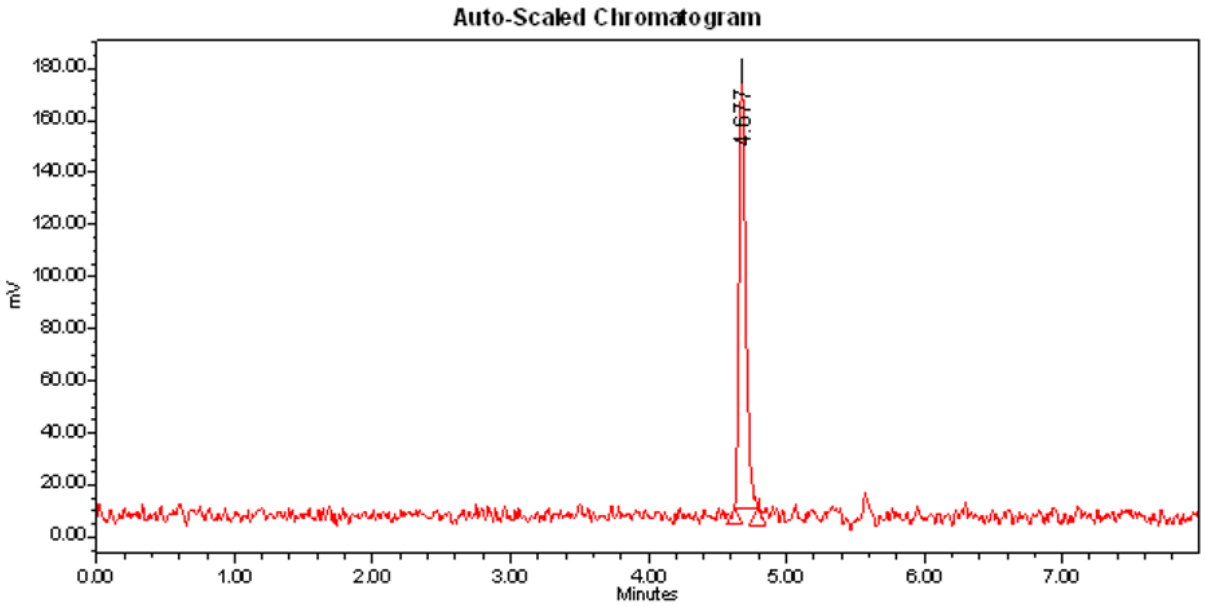

Figure S79. UPLC radio-chromatogram of the crude product **[^{18}F]5f** (gradient A).

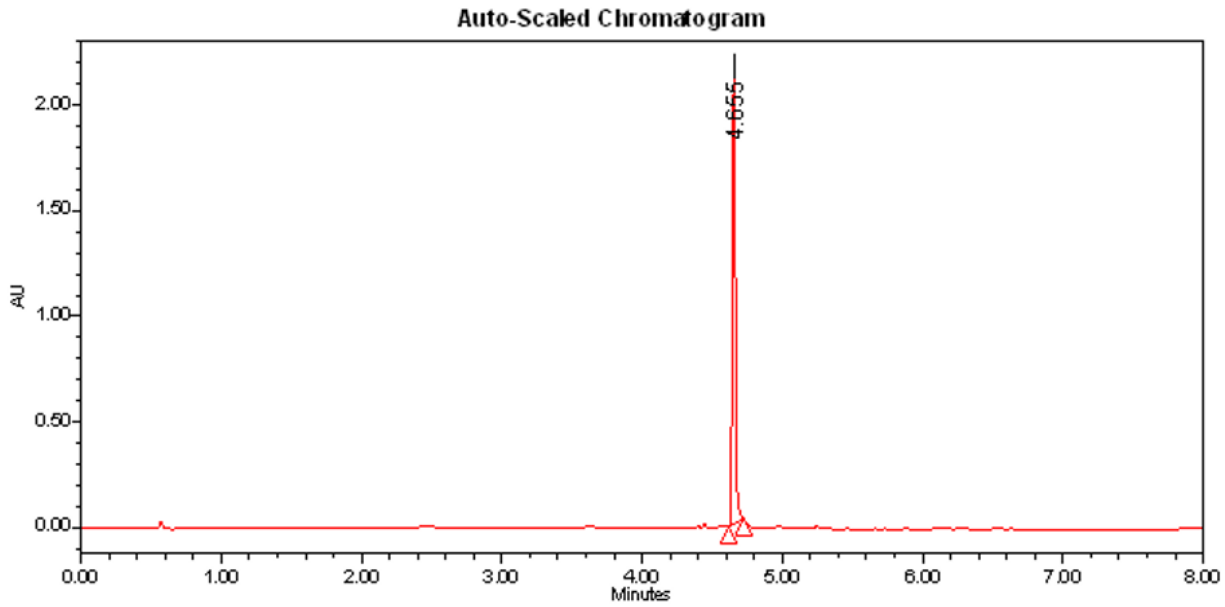

Figure S80. UPLC UV-chromatogram of the authentic reference **5f** (gradient A).

2.4. Two-step radiosyntheses of the [^{18}F]difluoromethyl heteroaryl-sulfones [^{18}F]5a-[^{18}F]5f from the precursors 6a-6f

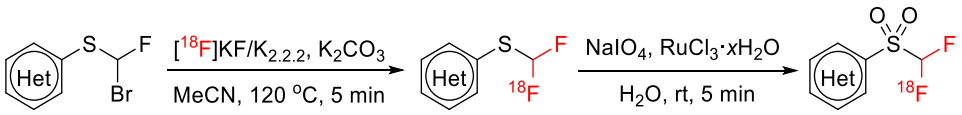

6a-6f **[^{18}F]4a-[^{18}F]4f** **[^{18}F]5a-[^{18}F]5f**

The overall RCY of the ^{18}F-labeling step of **6a-6f** and the oxidation of **[^{18}F]4a-[^{18}F]4f** was determined based on the activity of the recovered crude products **[^{18}F]5a–[^{18}F]5f**, on their radio-TLC and radio-UPLC purities, and the starting radioactivity, according to the following formula:

$$RCY\ (\%, d.c.) = \frac{radioTLC\ purity\ (\%)\ \times\ radioUPLC\ purity\ (\%)\ \times\ activity\ of\ the\ solution\ of\ [^{18}\mathbf{F}]\mathbf{5a}\text{–}[^{18}\mathbf{F}]\mathbf{5f}\ (d.c.)}{starting\ radioactivity\ \times\ 100}$$

Table S17. Determination of the radiochemical yield (%) of the synthesis of **[^{18}F]5a** from the precursor **6a**

Reaction	Starting activity (MBq)	Activity of the crude product [^{18}F]5a (MBq, d.c.)	Radio-TLC purity (%)	Radio-UPLC purity (%)	Radiochemical Yield (%)
1	100	11.0	98	93	10.0
2	98.6	11.8	98	95	11.1
3	131.8	13.6	99	89	9.1
Radiochemical Yield (%) ± Deviation					10.1 ± 0.8

Table S18. Determination of the radiochemical yield (%) of the synthesis of **[^{18}F]5b** from the precursor **6b**

Reaction	Starting activity (MBq)	Activity of the crude product [^{18}F]5b (MBq, d.c.)	Radio-TLC purity (%)	Radio-UPLC purity (%)	Radiochemical Yield (%)
1	92.2	9.3	98	87	8.6
2	112.0	10.1	98	85	7.5
3	110.0	11.5	99	86	8.9
Radiochemical Yield (%) ± Deviation					8.3 ± 0.6

Table S19. Determination of the radiochemical yield (%) of the synthesis of **[^{18}F]5c** from the precursor **6c**

Reaction	Starting activity (MBq)	Activity of the crude product [^{18}F]5c (MBq, d.c.)	Radio-TLC purity (%)	Radio-UPLC purity (%)	Radiochemical Yield (%)
1	112.8	14.6	100	99	12.8
2	101.3	12.1	100	98	11.7
3	122.9	14.5	100	98	11.6
Radiochemical Yield (%) ± Deviation					12 ± 0.5

Table S20. Determination of the radiochemical yield (%) of the synthesis of **[^{18}F]5d** from the precursor **6d**

Reaction	Starting activity (MBq)	Activity of the crude product [^{18}F]5d (MBq, d.c.)	Radio-TLC purity (%)	Radio-UPLC purity (%)	Radiochemical Yield (%)
1	115.1	12.9	100	97	10.9
2	108.9	12.5	100	97	11.1
3	98.2	11.7	100	98	11.7
Radiochemical Yield (%) ± Deviation					11.2 ± 0.3

Table S21. Determination of the radiochemical yield (%) of the synthesis of **[^{18}F]5e** from the precursor **6e**

Reaction	Starting activity (MBq)	Activity of the crude product [^{18}F]5e (MBq, d.c.)	Radio-TLC purity (%)	Radio-UPLC purity (%)	Radiochemical Yield (%)
1	106.8	8.2	100	98	7.5
2	99.1	7.4	99	96	7.1
3	105.3	7.6	99	96	6.9
Radiochemical Yield (%) ± Deviation					7.2 ± 0.2

Table S22. Determination of the radiochemical yield (%) of the synthesis of **[^{18}F]5f** from the precursor **6f**

Reaction	Starting activity (MBq)	Activity of the crude product [^{18}F]5f (MBq, d.c.)	Radio-TLC purity (%)	Radio-UPLC purity (%)	Radiochemical Yield (%)
1	116.8	15.8	100	100	13.5
2	111.3	14.6	100	100	13.1
3	110.6	15.6	100	100	14.1
Radiochemical Yield (%) ± Deviation					13.6 ± 0.4

2.5. Fully automated radiosyntheses of the labeled compounds [^{18}F]5a, [^{18}F]5c, and [^{18}F]5f

2.5.1. Layout of the FASTlab™ cassette for the radiosyntheses of the labeled compounds [^{18}F]5a, [^{18}F]5c, and [^{18}F]5f

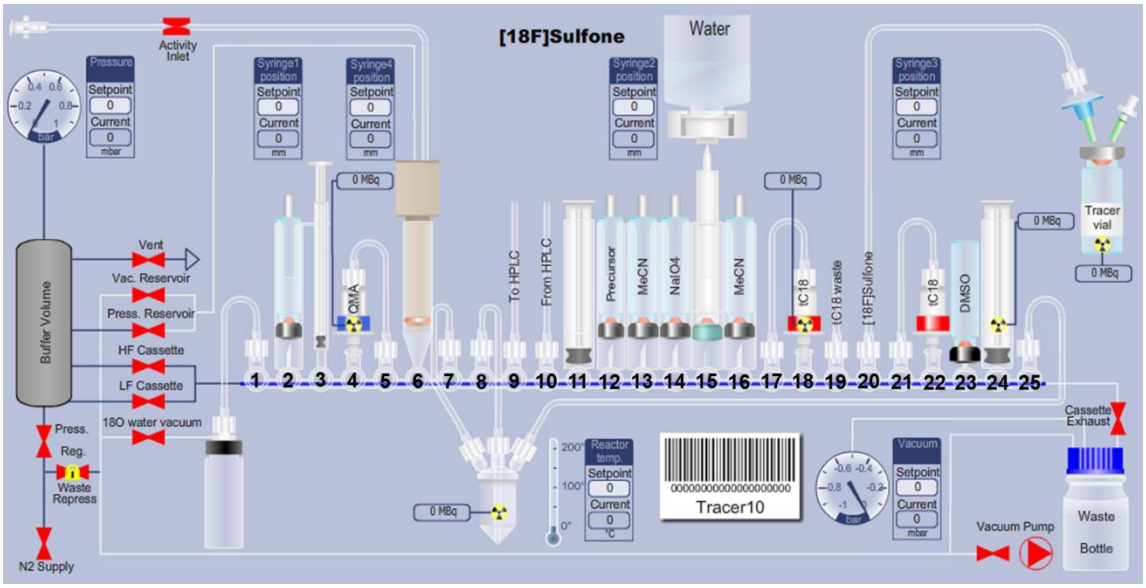

Figure S81. Layout of the FASTlab™ cassette for the radiosyntheses of the labeled compounds **[^{18}F]5a**, **[^{18}F]5c**, and **[^{18}F]5f**.

Table S23. Location of the reagents, solvents, and materials in the manifold of the FASTlab™ cassette

Manifold position	Reagents, solvents, and materials	Details
V1	Silicone tubing connected to [^{18}O]H_2O recovery vial	14 cm
V2	$K_{2.2.2}$® (7.5 mg) in MeCN (600 μL) and K_2CO_3 (1.4 mg) in H_2O (150 μL)	11 mm vial (volume = 750 μL)
V3	Syringe S1 (part of the manifold)	Maximum volume = 1 mL
V4	Sep-Pak® Accell™ Plus QMA Carbonate Plus Light Cartridge with silicone tubing at position V5	46 mg (40 μm) (Waters)
V5	Silicone tubing connected to the Sep-Pak® Accell™ Plus QMA Carbonate Plus Light Cartridge at position V4	14 cm
V6	[^{18}O]H_2O/[^{18}F]F^- inlet conical reservoir (part of the manifold)	Maximum volume = 5 mL
V7	Silicone tubing connected to the cyclic olefin copolymer (COC) reactor (left-hand side)	14 cm
V8	Silicone tubing connected to the COC reactor (central port)	14 cm
V9	Outlet "to HPLC loop" *via* silicone tubing connected to a Sterifix® Paed filter (B. Braun)	30 cm
V10	Inlet "from HPLC loop" enabling the recovery of the purified labeled compounds **[^{18}F]5a, [^{18}F]5c**, and **[^{18}F]5f** after semi-preparative HPLC purification	30 cm
V11	Syringe S2 (part of the manifold)	Maximum volume = 6 mL
V12	Precursors **6a** (12.3 mg, 40 μmol), **6c** (6.5 mg, 20 μmol), or **6f** (11.6 mg, 40 μmol) solubilized in MeCN	11 mm vial (volume = 1 mL)

V13	MeCN	13 mm vial (volume = 4 mL)
V14	$NaIO_4$ (153.9 mg) and $RuCl_3 \cdot xH_2O$ (3.4 mg) solubilized in H_2O	13 mm vial (volume = 4 mL)
V15	Water bag spike	Volume = 100 mL
V16	MeCN	13 mm vial (volume = 4 mL)
V17	Silicone tubing connected to the Sep-Pak® C18 Plus Short Cartridge at position V18	14 cm
V18	Sep-Pak® C18 Plus Short Cartridge with silicone tubing at position V17	400 mg (37-55 μm)
V19	Outlet waste bottle	21 cm
V20	Final outlet vial for collection of the labeled compounds **[^{18}F]5a, [^{18}F]5c**, and **[^{18}F]5f** after semi-preparative HPLC purification and reformulation	50 cm
V21	Silicone tubing connected to the Sep-Pak® C18 Plus Short Cartridge at position V22	14 cm
V22	Sep-Pak® C18 Plus Short Cartridge with silicone tubing at position V21	400 mg (37-55 μm)
V23	Anhydrous DMSO	13 mm vial (volume = 4 mL)
V24	Syringe S3 (part of the manifold)	Maximum volume = 6 mL
V25	Silicone tubing connected to the COC reactor (right-hand side) and vent valve for the reactor	42 cm

The RCY of the fully automated radiosyntheses of the [^{18}F]difluoromethyl heteroaryl-sulfones **[^{18}F]5a**, **[^{18}F]5c**, and **[^{18}F]5f** was determined based on the radioactivity of the **[^{18}F]5a**, **[^{18}F]5c**, or **[^{18}F]5f** present in DMSO solution and the radioactivity trapped on the QMA carbonate cartridge, according to the following formula:

$$RCY\ (\%, d.c.) = \frac{activity\ of\ the\ solution\ of\ [^{18}\mathbf{F}]\mathbf{5a}, [^{18}\mathbf{F}]\mathbf{5c}, \text{or}\ [^{18}\mathbf{F}]\mathbf{5f}\ \text{in DMSO}\ (d.c.)}{activity\ trapped\ on\ the\ QMA\ carbonate\ cartridge\ \times\ 100}$$

Table S24. Determination of the radiochemical yield (%) of the synthesis of **[^{18}F]5a** from the precursor **6a**

Reaction	Starting activity (GBq)	Activity of the isolated product [^{18}F]5a (GBq, d.c.)	Radiochemical Yield (%)
1	135.0	4.0	3.0
2	137.3	3.7	2.7
3	148.9	4.3	2.9
Radiochemical Yield (%) ± Deviation			2.9 ± 0.1

Table S25. Determination of the radiochemical yield (%) of the synthesis of **[^{18}F]5c** from the precursor **6c**

Reaction	Starting activity (GBq)	Activity of the isolated product [^{18}F]5c (GBq, d.c.)	Radiochemical Yield (%)
1	134.3	6.3	4.7
2	146.9	8.5	5.8
3	135.3	8.2	6.1
4	127.6	7.5	5.9
5	147.6	9.0	6.1
Radiochemical Yield (%) ± Deviation			5.7 ± 0.5

Table S26. Determination of the radiochemical yield (%) of the synthesis of **[^{18}F]5f** from the precursor **6f**

Reaction	Starting activity (GBq)	Activity of the isolated product [^{18}F]5a (GBq, d.c.)	Radiochemical Yield (%)
1	140.1	10.2	7.3
2	130.9	9.7	7.4
3	124.9	11.6	9.3
Radiochemical Yield (%) ± Deviation			8.0 ± 0.9

2.5.2. Calibration curves of the difluoromethyl heteroaryl-sulfones 5a, 5c, and 5f for determination of the molar activity of [^{18}F]5a, [^{18}F]5c, and [^{18}F]5f

The fully automated radiosyntheses of the sulfones **[^{18}F]5a**, **[^{18}F]5c**, or **[^{18}F]5f** were performed on a commercially available FASTlab™ synthesizer (GE Healthcare), using the optimized conditions for the labeling of precursors **6a** (12.3 mg, 0.04 mmol), **6c** (6.5 mg, 0.02 mmol), or **6f** (11.6 mg, 0.04 mmol), and the oxidation of the labeled compounds **[^{18}F]4a**, **[^{18}F]4c**, and **[^{18}F]4f**. The molar activity of the [^{18}F]difluoromethyl heteroaryl-sulfones was determined using an aliquot of each reformulated solution (3 μL). After injection of an aliquot in UPLC, the radioactive peak of **[^{18}F]5a**, **[^{18}F]5c**, and **[^{18}F]5f** associated to the non-radioactive sulfones **5a**, **5c**, and **5f**, respectively, were collected and counted in an ionization chamber. The PDA UV area under the peak of the non-radioactive sulfones **5a**, **5c**, and **5f** at 258 nm, 290 nm, and 244 nm, respectively, enabled the determination of the corresponding amount (in μmol) of the difluoromethyl heteroaryl-sulfones using the calibration curves described in Figures S82-S84. The molar activity was calculated by the ratio between the radioactivity of the **[^{18}F]5a**, **[^{18}F]5c**, and **[^{18}F]5f** and the corresponding amount of non-radioactive compound, according to the following formula:

$$Molar\ activity\ (GBq \cdot \mu mol^{-1}) = \frac{activity\ of\ the\ collected\ UPLC\ peak\ of\ [^{18}\mathbf{F}]\mathbf{5a},\ [^{18}\mathbf{F}]\mathbf{5f},\ \text{or}\ [^{18}\mathbf{F}]\mathbf{5f}}{amount\ of\ \mathbf{5a},\ \mathbf{5c},\ or\ \mathbf{5f}\ associated\ to\ the\ radioactive\ peak}$$

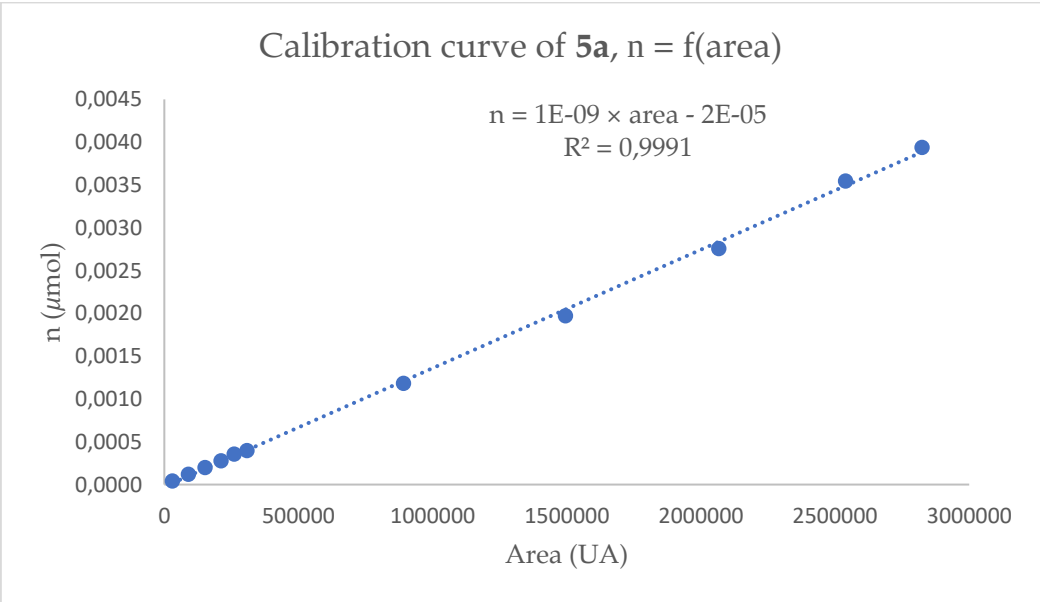

Figure S82. Calibration curve of the difluoromethyl heteroaryl-sulfone **5a** (wavelength: 258 nm).

Table S27. Determination of the molar activity of **[^{18}F]5a**

Reaction	Activity of the radioactive peak of [^{18}F]5a (GBq)	Area under the peak of 5a (UA) at 258 nm	Amount of 5a (μmol)	Molar activity (GBq· μmol^{-1})
1	4.552×10^{-3}	40425	3.146×10^{-5}	145
2	4.454×10^{-3}	38473	2.876×10^{-5}	155
3	5.175×10^{-3}	50000	4.471×10^{-5}	116
Molar activity (GBq· μmol^{-1}) ± Deviation				139 ± 17

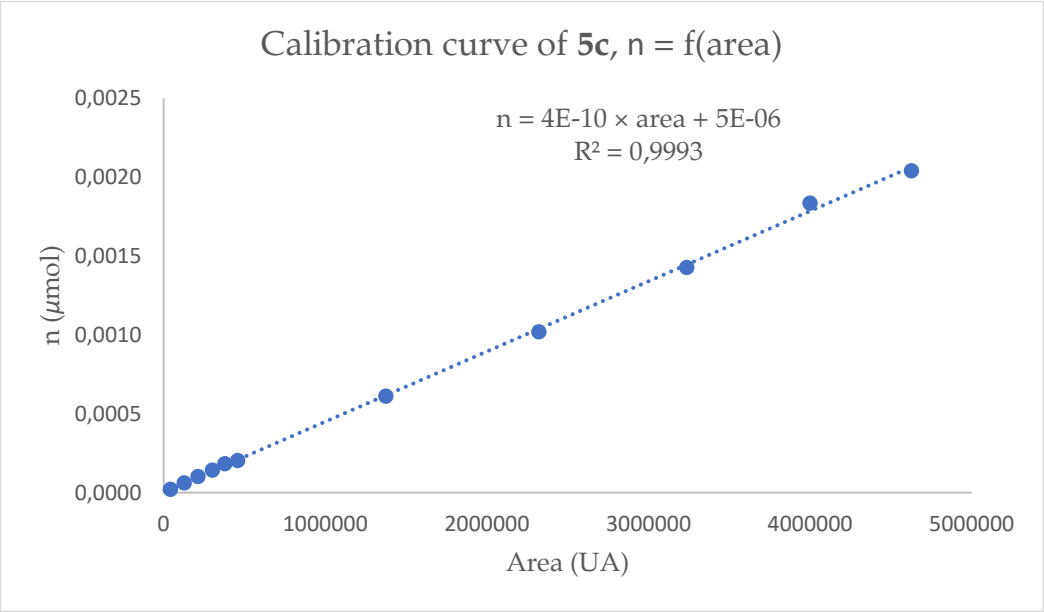

Figure S83. Calibration curve of the difluoromethyl heteroaryl-sulfone **5c** (wavelength: 290 nm).

Table S28. Determination of the molar activity of **[^{18}F]5c**

Reaction	Activity of the radioactive peak of [^{18}F]5c (GBq)	Area under the peak of 5c (UA) at 290 nm	Amount of 5c (μmol)	Molar activity (GBq· μmol^{-1})
1	4.863×10^{-3}	247987	1.150×10^{-4}	42
2	2.662×10^{-3}	90325	4.489×10^{-5}	59
3	8.242×10^{-3}	244309	1.134×10^{-4}	73
4	2.038×10^{-3}	65547	3.387×10^{-5}	60
5	2.524×10^{-3}	66094	3.412×10^{-5}	74
Molar activity (GBq· μmol^{-1}) ± Deviation				62 ± 12

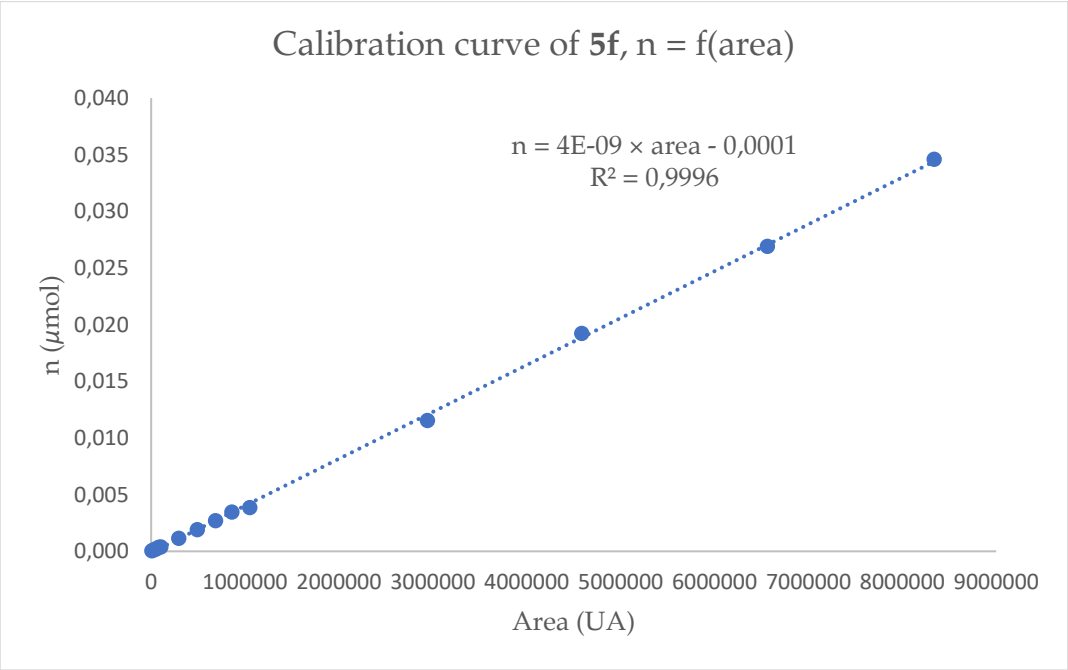

Figure S84. Calibration curve of the difluoromethyl heteroaryl-sulfone **5f** (wavelength: 244 nm).

Table S29. Determination of the molar activity of **[^{18}F]5f**

Reaction	Activity of the radioactive peak of [^{18}F]5f (GBq)	Area under the peak of 5f (UA) at 244 nm	Amount of 5f (μmol)	Molar activity (GBq· μmol^{-1})
1	1.702×10^{-2}	57459	1.378×10^{-4}	124
2	1.193×10^{-2}	57048	1.361×10^{-4}	88
3	1.435×10^{-2}	51785	1.143×10^{-4}	126
Molar activity (GBq· μmol^{-1}) ± Deviation				113 ± 17

2.6. Optimization of the conditions for the photocatalytic C-H ^{18}F-difluoromethylation with the reagents [^{18}F]5a, [^{18}F]5c, and [^{18}F]5f

The propensity of the reagents **[^{18}F]5a**, **[^{18}F]5c**, and **[^{18}F]5f** to undergo the desired photocatalytic C-H ^{18}F-difluoromethylation reaction was carried out using 2-amino-9-((2-hydroxyethoxy)methyl)-9*H*-purin-6-ol (acyclovir, **7e**) as a model substrate.

2.6.1. Synthesis of [^{18}F]2-amino-8-(difluoromethyl)-9-((2-hydroxyethoxy)methyl)-9*H*-purin-6-ol ([^{18}F]8e)

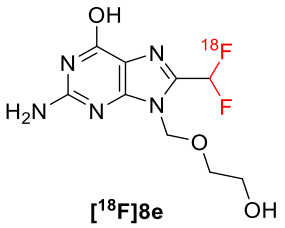

[^{18}F]8e

A solution of 2-amino-9-((2-hydroxyethoxy)methyl)-9*H*-purin-6-ol (acyclovir, **7e**) and *fac*-Ir^{III}(ppy)$_3$ in DMSO (200 μL) was prepared. Next, a solution of **[^{18}F]5a**, **[^{18}F]5c**, or **[^{18}F]5f** in DMSO (30-40 MBq, 50 μL) was added. The solution was injected in a 100 μL-microchip pumped with DMSO at a flow rate and irradiated under blue LED (470 nm, 2 W), at a temperature of 35 °C. An aliquot of the crude product **[^{18}F]8e** was then analyzed by radio-TLC and radio-UPLC for radiochemical yield (RCY) determination.

Figure S85. Instrument used for the C-H ^{18}F-difluoromethylation reaction of the heteroarenes (FlowStart Evo, FutureChemistry).

The RCY of the C-H ^{18}F-difluoromethylation reactions was determined according to the following formula:

$$RCY\ (\%) = \frac{radioTLC\ purity\ (\%) \times radioUPLC\ purity\ (\%)}{100}$$

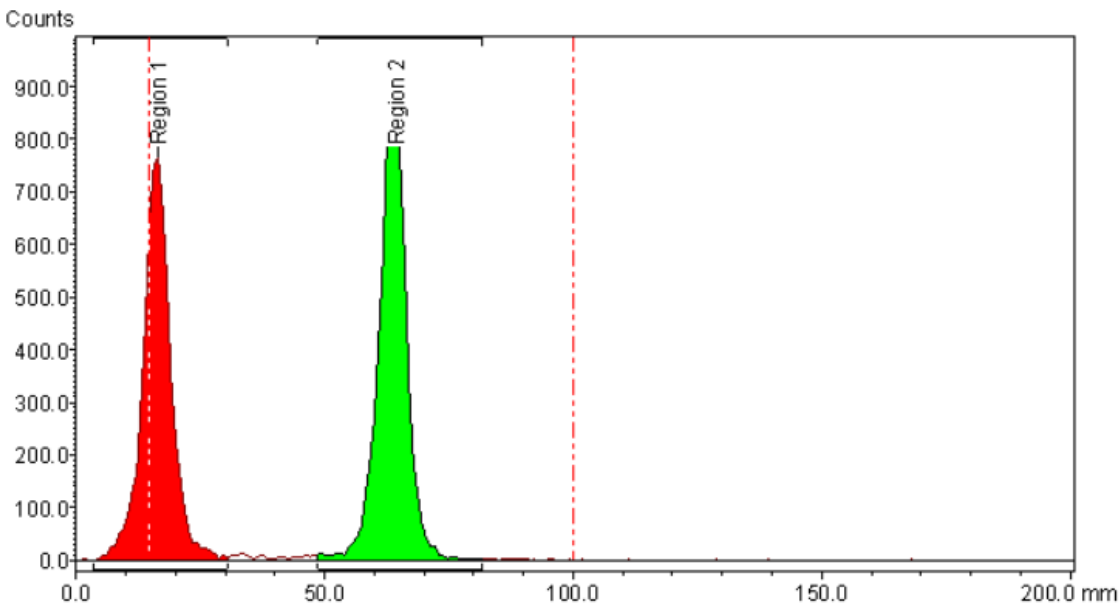

Figure S86. TLC radio-chromatogram of the crude product **[^{18}F]8e** (eluent: methanol).

Table S30. Determination of the radio-TLC purity of the crude product **[^{18}F]8e**

Retention factor (R_f, mm)	Ratio (%)
0.02	46 (impurity/by-product)
0.77	54 (desired crude product)

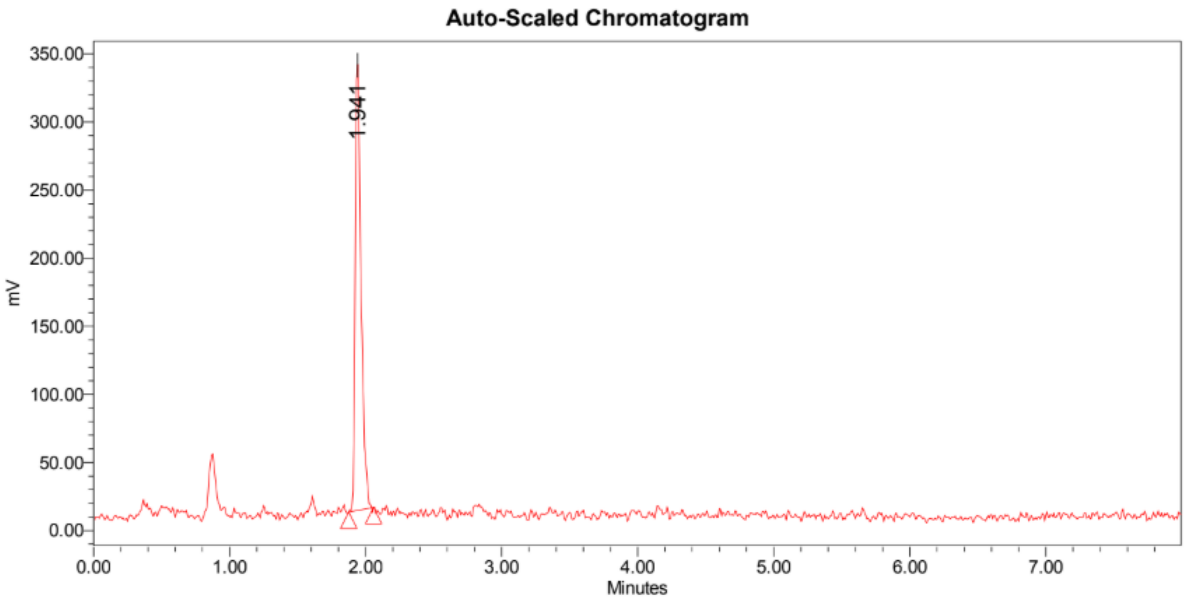

Figure S87. UPLC radio-chromatogram of the crude product **[^{18}F]8e** (gradient B).

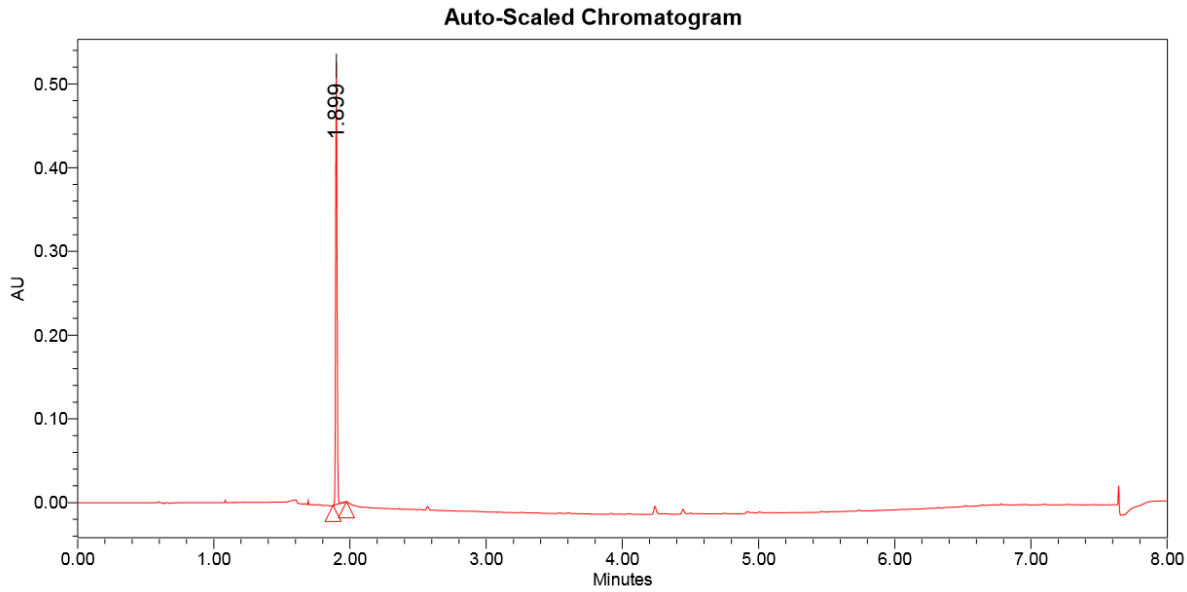

Figure S88. UPLC UV-chromatogram of the authentic reference **8e** (gradient B).

$$RCY\ (\%) = \frac{radioTLC\ purity\ (\%) \times radioUPLC\ purity\ (\%)}{100}$$

$$RCY\ (\%) = \frac{54 \times 100}{100}$$

$$RCY\ (\%) = 54\ \%$$

Note: In some cases, some peaks at 0.6 and 0.9 min were observed on the radio-UPLC chromatograms. Those two peaks were collected and their radio-TLC purity was analyzed. Since the retention factor corresponding to these peaks is approximately 0, their contribution for the radio-UPLC purity was not taken into consideration. The contribution of these peaks was accounted for the determination of the radio-TLC purity.

On the basis of the reported conditions for the C-H ^{18}F-difluoromethylation of the substrate **7e** with the reagent **[^{18}F]1**, the following table summarizes the results of the different optimization tests performed in the presence of the reagents **[^{18}F]5a**, **[^{18}F]5c**, and **[^{18}F]5f**.

Standard reaction conditions for the photoredox C-H ^{18}F-difluoromethylation: substrate **7e** (0.02 mmol), [^{18}F]difluoromethyl heteroaryl-sulfones **[^{18}F]5a**, **[^{18}F]5c**, or **[^{18}F]5f** (30-40 MBq), *fac*-Ir^{III}(ppy)$_3$ (mol%), residence time (min), flow rate (μL·min^{-1}), DMSO (250 μL), 35 °C, blue LED (470 nm, 2 W).

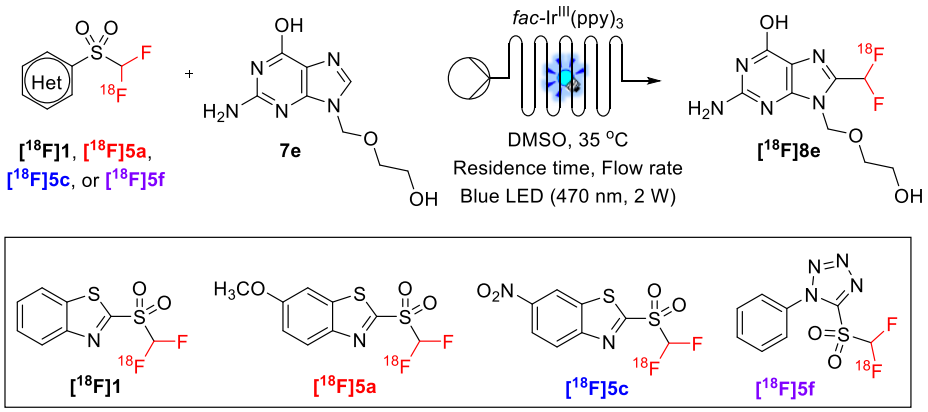

Entry	Reagents	*fac*-Ir^{III}(ppy)$_3$ (mol%)	Residence time (min)	Flow rate (μL·min^{-1})	Conversion (%)$^{(a)}$	RCY (%)$^{(b)}$
1	**[^{18}F]1**	**0.05**	**2**	**50**	**100**	**70 ± 7 (n=4)**
2	**[^{18}F]5a**	**0.05**	**2**	**50**	**100**	**57 ± 7 (n=3)**
3	[^{18}F]5c	0.05	2	50	17	14 ± 1 (n=3)
4	[^{18}F]5c	0.5	2	50	36	26 ± 3 (n=3)
5	**[^{18}F]5c**	**0.5**	**4**	**25**	**100**	**51 ± 7 (n=4)**
6	[^{18}F]5f	0.05	2	50	73	48 ± 8 (n=3)
7	[^{18}F]5f	0.1	2	50	98	55 ± 1 (n=3)
8	**[^{18}F]5f**	**0.1**	**2.5**	**40**	**100**	**56 ± 1 (n=3)**

(a) UPLC conversion of the reagents. (b) All RCYs were determined based on the radio-TLC and radio-UPLC purities of the crude product **[^{18}F]8e**.

The best conditions for the C-H ^{18}F-difluoromethylation of the substrate **7e** were:

- Conditions A: [^{18}F]difluoromethyl heteroaryl-sulfone **[^{18}F]5a** (30-40 MBq), *fac*-Ir^{III}(ppy)$_3$ (0.05 mol%), residence time (2 min), flow rate (50 μL·min^{-1}), DMSO (250 μL), 35 °C, blue LED (470 nm, 2 W).
- Conditions B: [^{18}F]difluoromethyl heteroaryl-sulfone **[^{18}F]5c** (30-40 MBq), *fac*-Ir^{III}(ppy)$_3$ (0.5 mol%), residence time (4 min), flow rate (25 μL·min^{-1}), DMSO (250 μL), 35 °C, blue LED (470 nm, 2 W).
- Conditions C: [^{18}F]difluoromethyl heteroaryl-sulfone **[^{18}F]5f** (30-40 MBq), *fac*-Ir^{III}(ppy)$_3$ (0.1 mol%), residence time (2.5 min), flow rate (40 μL·min^{-1}), DMSO (250 μL), 35 °C, blue LED (470 nm, 2 W).

Table S31. Determination of the radiochemical yield (%) of the synthesis of **[^{18}F]8e** using the reagent **[^{18}F]5a**

Reaction	Radio-TLC purity (%)	Radio-UPLC purity (%)	Radiochemical Yield (%)
1	54	100	54
2	67	100	67
3	51	100	51
Radiochemical Yield (%) ± Deviation			57 ± 7

Table S32. Determination of the radiochemical yield (%) of the synthesis of **[^{18}F]8e** using the reagent **[^{18}F]5c**

Reaction	Radio-TLC purity (%)	Radio-UPLC purity (%)	Radiochemical Yield (%)
1	74	79	58
2	68	57	39
3	63	84	53
4	67	80	54
Radiochemical Yield (%) ± Deviation			51 ± 7

Table S33. Determination of the radiochemical yield (%) of the synthesis of **[^{18}F]8e** using the reagent **[^{18}F]5f**

Reaction	Radio-TLC purity (%)	Radio-UPLC purity (%)	Radiochemical Yield (%)
1	63	85	54
2	69	83	57
3	71	80	57
Radiochemical Yield (%) ± Deviation			56 ± 1

2.7. General procedure for the C-H ^{18}F-difluoromethylation reaction with the [^{18}F]difluoromethyl heteroaryl-sulfones [^{18}F]5a, [^{18}F]5c, and [^{18}F]5f

A solution of the heteroarenes (0.02 mmol) and *fac*-Ir^{III}(ppy)$_3$ (0.05 mol% for **[^{18}F]5a**; 0.5 mol% for **[^{18}F]5c**; 0.1 mol% for **[^{18}F]5f**) in DMSO (200 μL) was prepared. Next, a solution of **[^{18}F]5a**, **[^{18}F]5c**, or **[^{18}F]5f** in DMSO (30-40 MBq, 50 μL) was added. The solution was injected in a 100 μL-microchip pumped with DMSO at a flow rate of 50 μL·min^{-1} (residence time: 2 min for **[^{18}F]5a**), 25 μL·min^{-1} (residence time: 4 min for **[^{18}F]5c**) or 40 μL·min^{-1} (residence time: 2.5 min for **[^{18}F]5f**) and irradiated under blue LED (470 nm, 2 W), at a temperature of 35 °C. An aliquot of the reaction mixture was then analyzed by radio-TLC and radio-UPLC for the RCY determination.

2.7.1. Synthesis of [^{18}F]2-(difluoromethyl)-4-methyl-1*H*-pyrrolo[2,3-b]pyridine ([^{18}F]8aa) and [^{18}F]6-(difluoromethyl)-4-methyl-1*H*-pyrrolo[2,3-b]pyridine ([^{18}F]8ab)

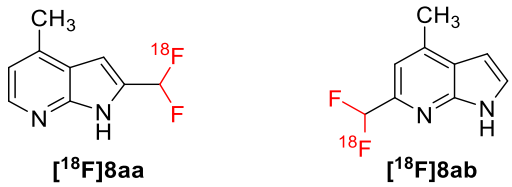

[^{18}F]8aa **[^{18}F]8ab**

The implementation of the general procedure for the C-H ^{18}F-difluoromethylation of 4-methyl-1*H*-pyrrolo[2,3-*b*]pyridine (2.6 mg, 0.02 mmol) provided the labeled compound **[^{18}F]8aa** in 32 ± 1%, 58 ± 3%, and 46 ± 3% RCY, using the reagents **[^{18}F]5a**, **[^{18}F]5c**, and **[^{18}F]5f**, respectively. The labeled compound **[^{18}F]8ab** was afforded in 5 ± 1%, 8%, and 7% RCY, using the reagents **[^{18}F]5a**, **[^{18}F]5c**, and **[^{18}F]5f**, respectively (see the Tables S34-S36 for more details of the RCY determination). The UPLC radio-chromatogram of the crude product **[^{18}F]8a** is depicted in Figure S89. Figures S90 and S91 represent the UPLC UV-chromatograms of the non-radioactive references **8aa** and **8ab**, respectively.

Table S34. Determination of the radiochemical yield (%) of the synthesis of **[^{18}F]8a** using the reagent **[^{18}F]5a**

Reaction	Radio-TLC purity (%)	Radio-UPLC purity (%)		Radiochemical Yield (%)	
	a + b	a	b	a	b
1	37	90	10	33	4
2	34	89	11	30	4
3	38	85	15	32	6
Radiochemical Yield (%) ± Deviation				32 ± 1	5 ± 1

Table S35. Determination of the radiochemical yield (%) of the synthesis of **[^{18}F]8a** using the reagent **[^{18}F]5c**

Reaction	Radio-TLC purity (%)	Radio-UPLC purity (%)		Radiochemical Yield (%)	
	a + b	a	b	a	b
1	67	80	12	54	8
2	76	82	12	62	9
3	76	75	11	57	8
Radiochemical Yield (%) ± Deviation				58 ± 3	8

Table S36. Determination of the radiochemical yield (%) of the synthesis of **[^{18}F]8a** using the reagent **[^{18}F]5f**

Reaction	Radio-TLC purity (%)	Radio-UPLC purity (%)		Radiochemical Yield (%)	
	a + b	a	b	a	b
1	64	74	11	47	7
2	58	73	10	42	6
3	67	72	10	48	7
Radiochemical Yield (%) ± Deviation				46 ± 3	7

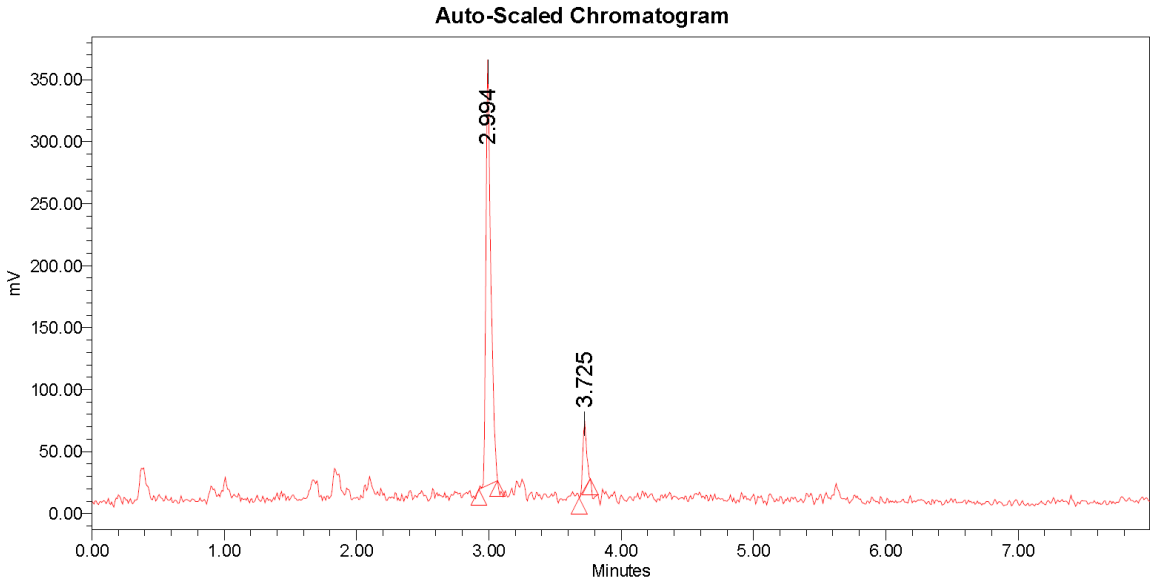

Figure S89. UPLC radio-chromatogram of the crude product **[^{18}F]8a** (gradient B).

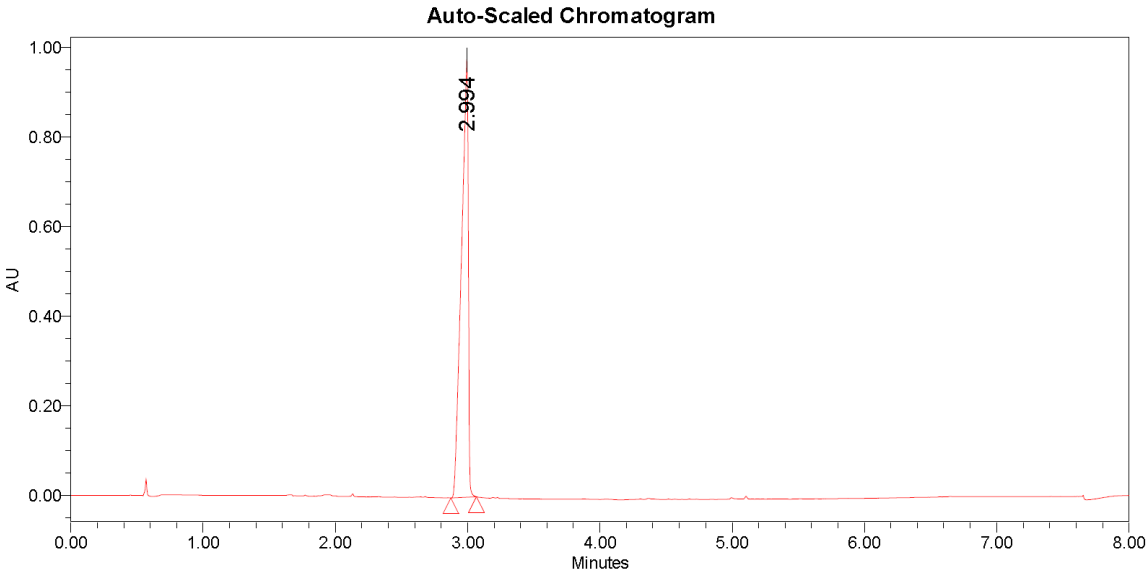

Figure S90. UPLC UV-chromatogram of the authentic reference **8aa** (gradient B).

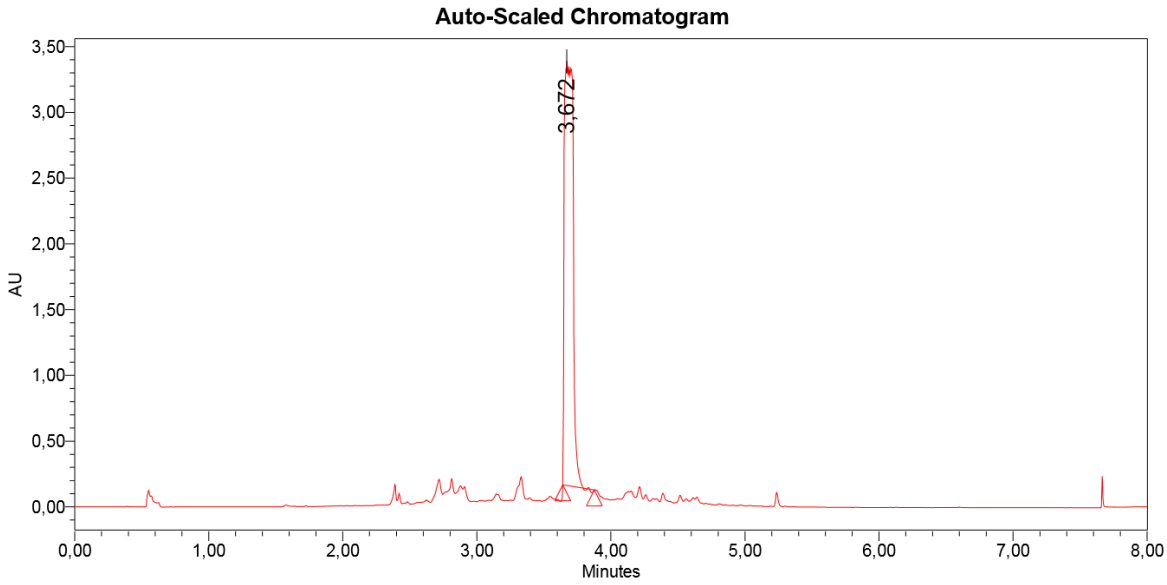

Figure S91. UPLC UV-chromatogram of the authentic reference **8ab** (gradient B).

2.7.2. Synthesis of [^{18}F]3-(difluoromethyl)-6-methyl-1*H*-pyrazolo[3,4-*b*]pyridine ([^{18}F]8ba) and [^{18}F]4-(difluoromethyl)-6-methyl-1*H*-pyrazolo[3,4-*b*]pyridine ([^{18}F]8bb)

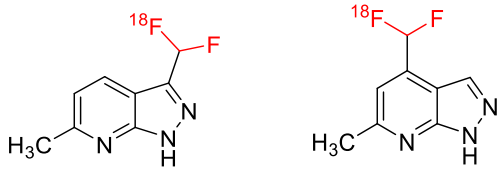

[^{18}F]8ba [^{18}F]8bb

The implementation of the general procedure for the C-H ^{18}F-difluoromethylation of 6-methyl-1*H*-pyrazolo[3,4-*b*]pyridine (2.7 mg, 0.02 mmol) provided the labeled compound **[^{18}F]8aa** in 41 ± 6%, 43 ± 3%, and 41 ± 5% RCY, using the reagents **[^{18}F]5a**, **[^{18}F]5c**, and **[^{18}F]5f**, respectively. The labeled compound

[^{18}F]8ab was afforded in 16 ± 1%, 17 ± 3%, and 17 ± 1% RCY, using the reagents **[^{18}F]5a**, **[^{18}F]5c**, and **[^{18}F]5f**, respectively (see the Tables S37-S39 for more details of the RCY determination). The UPLC radio-chromatogram of the crude product **[^{18}F]8b** is depicted in Figure S92. Figures S93 and S94 represent the UPLC UV-chromatograms of the non-radioactive references **8ba** and **8bb**, respectively.

Table S37. Determination of the radiochemical yield (%) of the synthesis of **[^{18}F]8b** using the reagent **[^{18}F]5a**

Reaction	Radio-TLC purity (%)	Radio-UPLC purity (%)		Radiochemical Yield (%)	
	a + b	a	b	a	b
1	53	67	33	36	17
2	67	75	25	50	17
3	55	68	27	37	15
Radiochemical Yield (%) ± Deviation				41 ± 6	16 ± 1

Table S38. Determination of the radiochemical yield (%) of the synthesis of **[^{18}F]8b** using the reagent **[^{18}F]5c**

Reaction	Radio-TLC purity (%)	Radio-UPLC purity (%)		Radiochemical Yield (%)	
	a + b	a	b	a	b
1	71	67	22	48	16
2	74	57	28	42	21
3	62	65	22	40	14
Radiochemical Yield (%) ± Deviation				43 ± 3	17 ± 3

Table S39. Determination of the radiochemical yield (%) of the synthesis of **[^{18}F]8b** using the reagent **[^{18}F]5f**

Reaction	Radio-TLC purity (%)	Radio-UPLC purity (%)		Radiochemical Yield (%)	
	a + b	a	b	a	b
1	70	50	25	35	18
2	65	61	24	40	16
3	74	63	21	47	16
Radiochemical Yield (%) ± Deviation				41 ± 5	17 ± 1

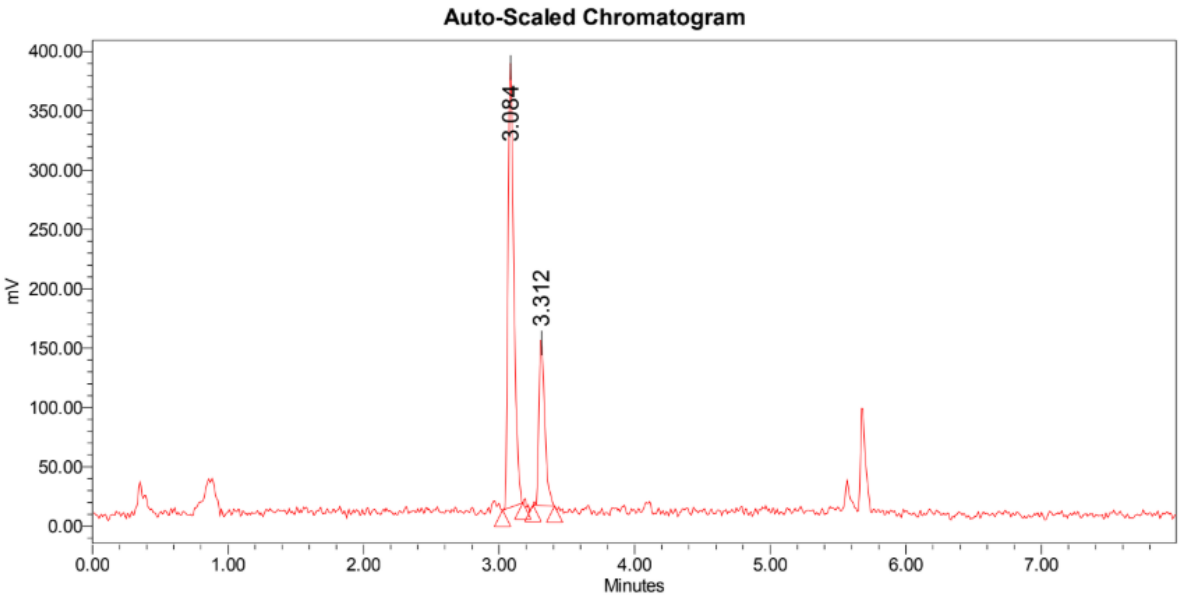

Figure S92. UPLC radio-chromatogram of the crude product **[^{18}F]8b** (gradient B).

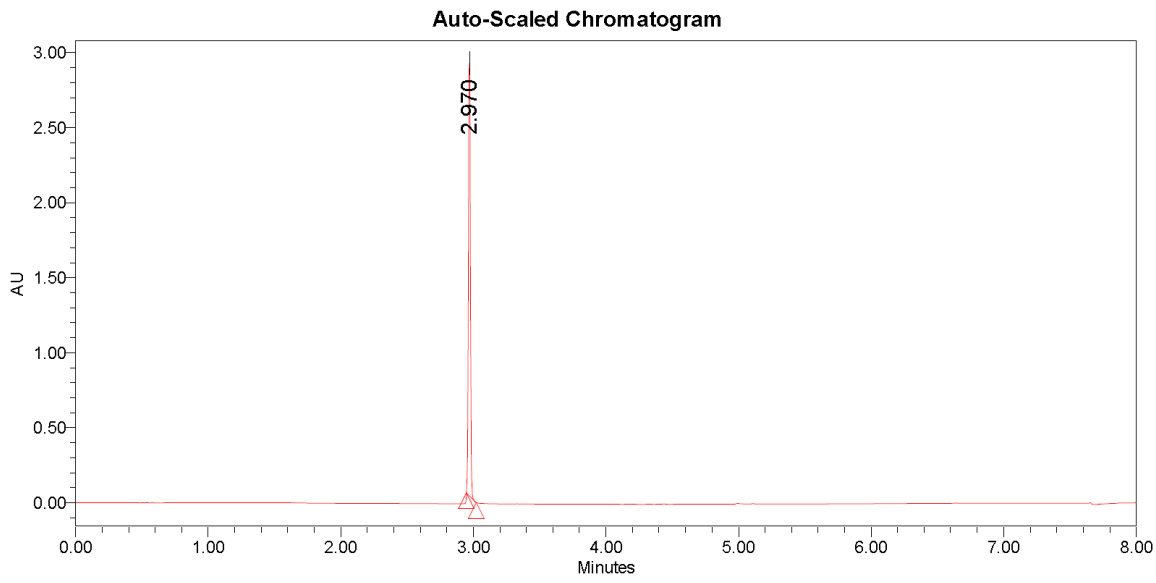

Figure S93. UPLC UV-chromatogram of the authentic reference **8ba** (gradient B).

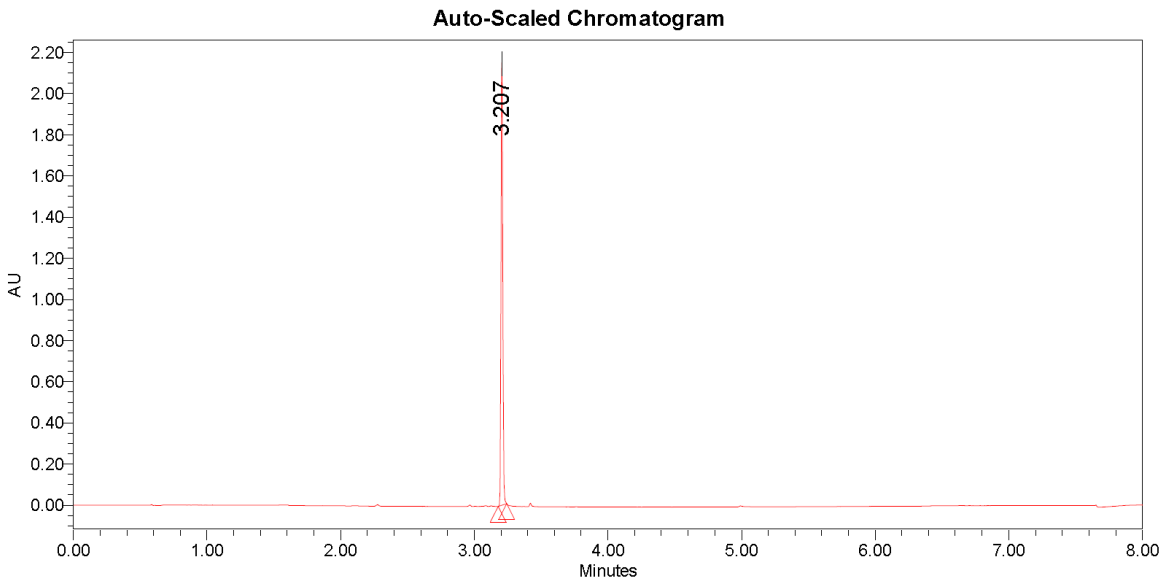

Figure S94. UPLC UV-chromatogram of the authentic reference **8bb** (gradient B).

2.7.3. Synthesis of [^{18}F]4-(difluoromethyl)-2-methyl-5,8-dihydropyrido[2,3-d]pyrimidin-7(6*H*)-one ([^{18}F]8c)

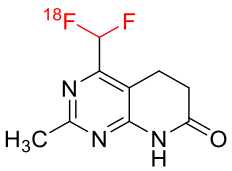

[^{18}F]8c

The implementation of the general procedure for the C-H ^{18}F-difluoromethylation of 2-methyl-5,8-dihydropyrido[2,3-*d*]pyrimidin-7(6*H*)-one (3.3 mg, 0.02 mmol) provided the labeled compound **[^{18}F]8c** in 17 ± 4%, 13 ± 3%, and 14% RCY, using the reagents **[^{18}F]5a**, **[^{18}F]5c**, and **[^{18}F]5f**, respectively (see the Tables S40-S42 for more details of the RCY determination). The UPLC radio-chromatogram of the crude

product **[^{18}F]8c** is depicted in Figure S95. Figure S96 represents the UPLC UV-chromatogram of the non-radioactive reference **8c**.

Table S40. Determination of the radiochemical yield (%) of the synthesis of **[^{18}F]8c** using the reagent **[^{18}F]5a**

Reaction	Radio-TLC purity (%)	Radio-UPLC purity (%)	Radiochemical Yield (%)
1	38	30	11
2	45	44	20
3	51	41	21
Radiochemical Yield (%) ± Deviation			17 ± 4

Table S41. Determination of the radiochemical yield (%) of the synthesis of **[^{18}F]8c** using the reagent **[^{18}F]5c**

Reaction	Radio-TLC purity (%)	Radio-UPLC purity (%)	Radiochemical Yield (%)
1	57	30	17
2	55	20	11
3	19	52	10
Radiochemical Yield (%) ± Deviation			13 ± 3

Table S42. Determination of the radiochemical yield (%) of the synthesis of **[^{18}F]8c** using the reagent **[^{18}F]5f**

Reaction	Radio-TLC purity (%)	Radio-UPLC purity (%)	Radiochemical Yield (%)
1	54	25	14
2	43	30	13
3	54	25	14
Radiochemical Yield (%) ± Deviation			14

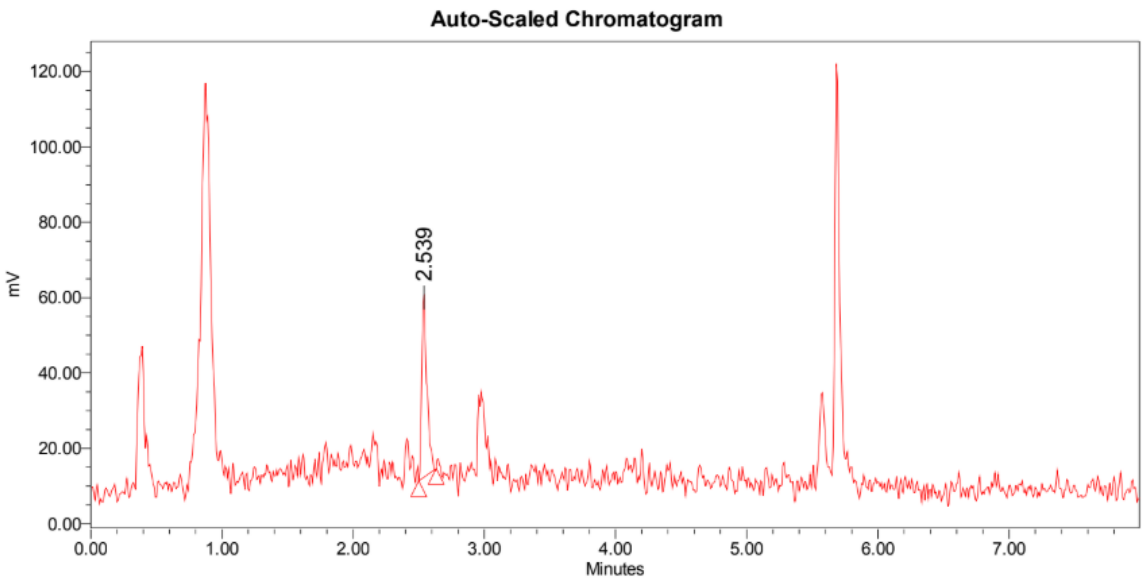

Figure S95. UPLC radio-chromatogram of the crude product **[^{18}F]8c** (gradient B).

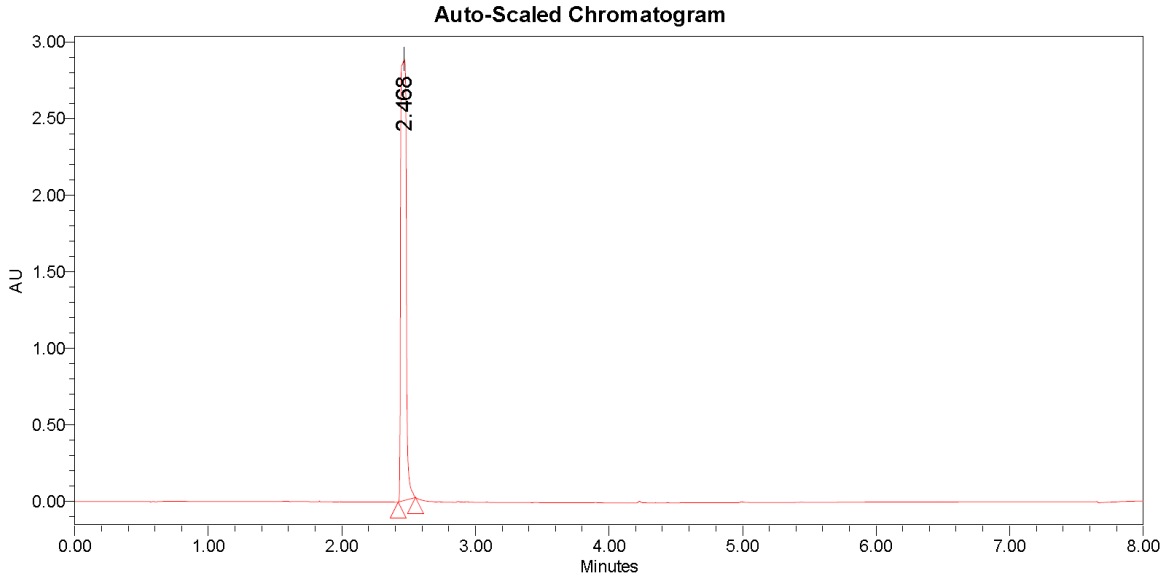

Figure S96. UPLC UV-chromatogram of the authentic reference **8c** (gradient B).

2.7.4. Synthesis of [^{18}F]ethyl 2-(difluoromethyl)isonicotinate ([^{18}F]8da) and [^{18}F]ethyl 3-(difluoromethyl)isonicotinate ([^{18}F]8db)

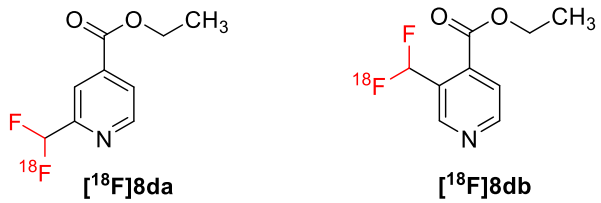

The implementation of the general procedure for the C-H ^{18}F-difluoromethylation of ethyl isonicotinate (3.0 mg, 0.02 mmol) provided the labeled compound **[^{18}F]8da** in 19 ± 7%, 24 ± 2%, and 36 ± 4% RCY, using the reagents **[^{18}F]5a**, **[^{18}F]5c**, and **[^{18}F]5f**, respectively. The labeled compound **[^{18}F]8db** was afforded in 10 ± 3%, 13 ± 1%, and 13 ± 2% RCY, using the reagents **[^{18}F]5a**, **[^{18}F]5c**, and **[^{18}F]5f**, respectively (see the Tables S43-S45 for more details of the RCY determination). The UPLC radio-chromatogram of the crude product **[^{18}F]8d** is depicted in Figure S97. Figures S98 and S99 represent the UPLC UV-chromatograms of the non-radioactive references **8da** and **8db**, respectively.

Table S43. Determination of the radiochemical yield (%) of the synthesis of **[^{18}F]8d** using the reagent **[^{18}F]5a**

Reaction	Radio-TLC purity (%)	Radio-UPLC purity (%)		Radiochemical Yield (%)	
	a + b	a	b	a	b
1	29	42	21	12	6
2	32	51	34	16	11
3	47	61	30	29	14
Radiochemical Yield (%) ± Deviation				19 ± 7	10 ± 3

Table S44. Determination of the radiochemical yield (%) of the synthesis of **[^{18}F]8d** using the reagent **[^{18}F]5c**

Reaction	Radio-TLC purity (%)	Radio-UPLC purity (%)		Radiochemical Yield (%)	
	a + b	a	b	a	b
1	50	51	25	26	12
2	50	49	24	24	12
3	49	45	30	22	15
Radiochemical Yield (%) ± Deviation				24 ± 2	13 ± 1

Table S45. Determination of the radiochemical yield (%) of the synthesis of **[^{18}F]8d** using the reagent **[^{18}F]5f**

Reaction	Radio-TLC purity (%)	Radio-UPLC purity (%)		Radiochemical Yield (%)	
	a + b	a	b	a	b
1	62	64	26	40	16
2	53	69	23	37	12
3	45	68	22	31	10
Radiochemical Yield (%) ± Deviation				36 ± 4	13 ± 2

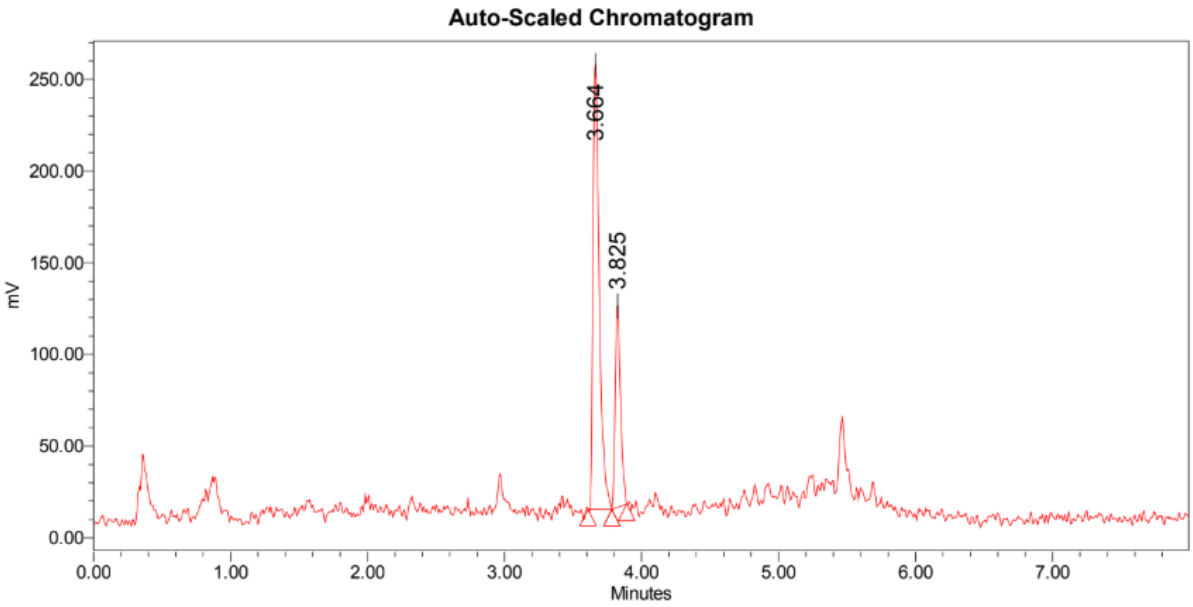

Figure S97. UPLC radio-chromatogram of the crude product **[^{18}F]8d** (gradient B).

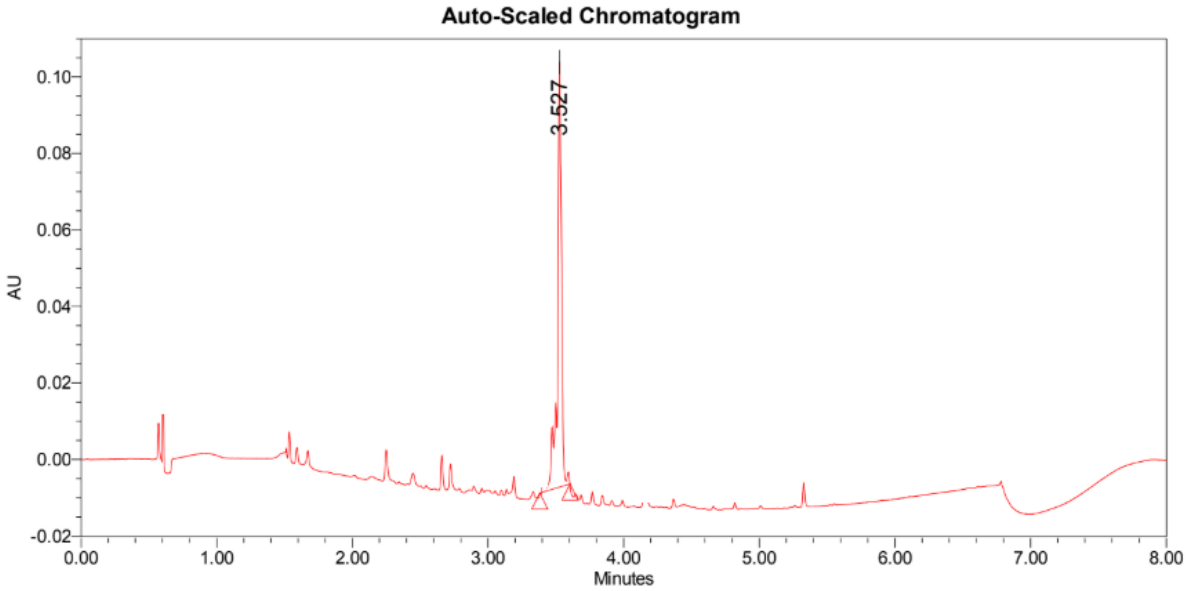

Figure S98. UPLC UV-chromatogram of the authentic reference **8da** (gradient B).

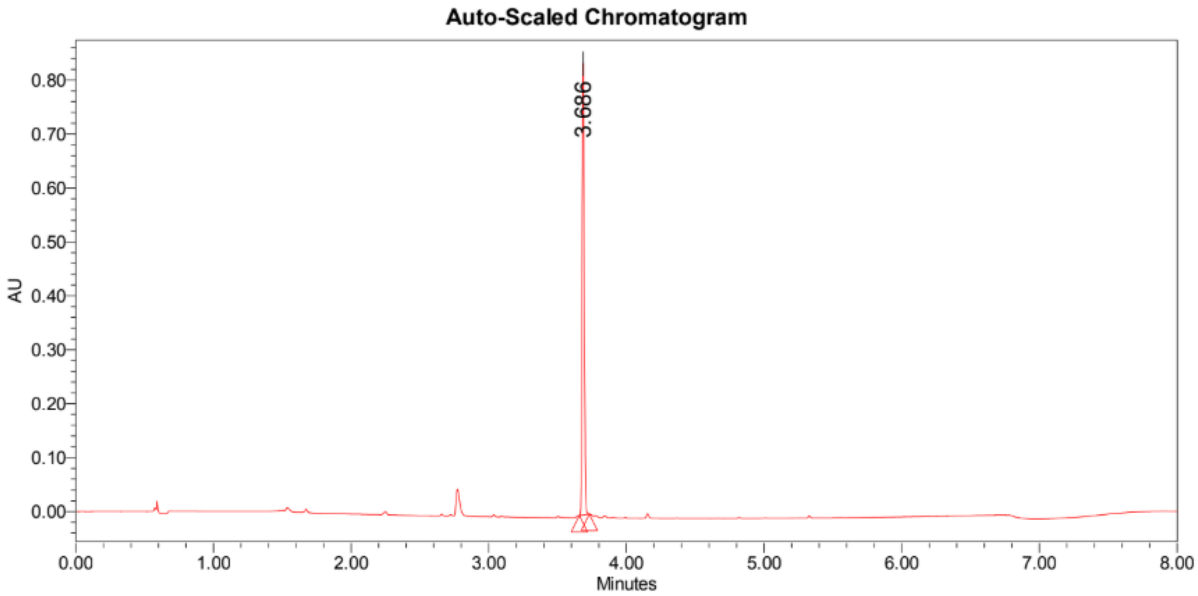

Figure S99. UPLC UV-chromatogram of the authentic reference **8db** (gradient B).

2.7.5. Synthesis of [^{18}F]4-chloro-2-(difluoromethyl)-*N*-(4,5-dihydro-1*H*-imidazol-2-yl)-6-methoxypyrimidin-5-amine ([^{18}F]8f)

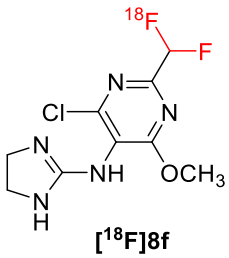

[^{18}F]8f

The implementation of the general procedure for the C-H ^{18}F-difluoromethylation of 4-chloro-*N*-(4,5-dihydro-1*H*-imidazol-2-yl)-6-methoxypyrimidin-5-amine (4.6 mg, 0.02 mmol) provided the labeled compound **[^{18}F]8f** in 52 ± 6%, 17 ± 3%, and 60 ± 3% RCY, using the reagents **[^{18}F]5a**, **[^{18}F]5c**, and **[^{18}F]5f**, respectively (see the Tables S46-S48 for more details of the RCY determination). The UPLC radio-chromatogram of the crude product **[^{18}F]8f** is depicted in Figure S100. Figure S101 represents the UPLC UV-chromatogram of the non-radioactive reference **8f**.

Table S46. Determination of the radiochemical yield (%) of the synthesis of **[^{18}F]8f** using the reagents **[^{18}F]5a**

Reaction	Radio-TLC purity (%)	Radio-UPLC purity (%)	Radiochemical Yield (%)
1	50	100	50
2	47	100	47
3	60	100	60
Radiochemical Yield (%) ± Deviation			52 ± 6

Table S47. Determination of the radiochemical yield (%) of the synthesis of **[^{18}F]8f** using the reagents **[^{18}F]5c**

Reaction	Radio-TLC purity (%)	Radio-UPLC purity (%)	Radiochemical Yield (%)
1	67	35	23
2	60	27	16
3	53	26	14
4	64	26	17
5	63	24	15
Radiochemical Yield (%) ± Deviation			17 ± 3

Table S48. Determination of the radiochemical yield (%) of the synthesis of **[^{18}F]8f** using the reagents **[^{18}F]5c**

Reaction	Radio-TLC purity (%)	Radio-UPLC purity (%)	Radiochemical Yield (%)
1	73	84	61
2	67	83	56
3	78	80	62
Radiochemical Yield (%) ± Deviation			60 ± 3

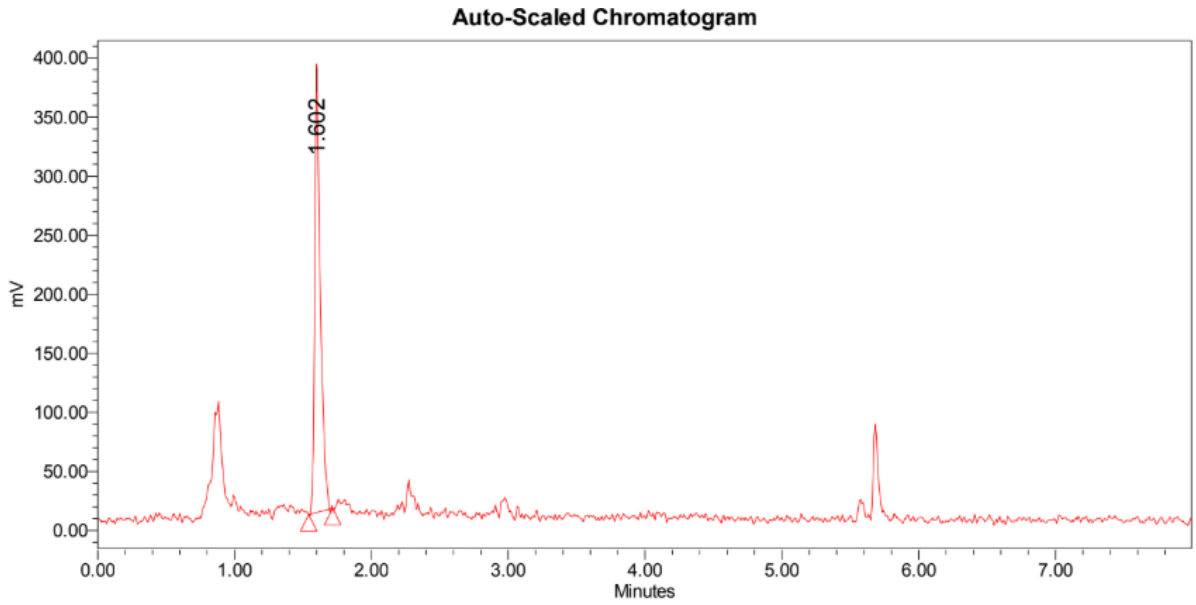

Figure S100. UPLC radio-chromatogram of the crude product **[^{18}F]8f** (gradient B).

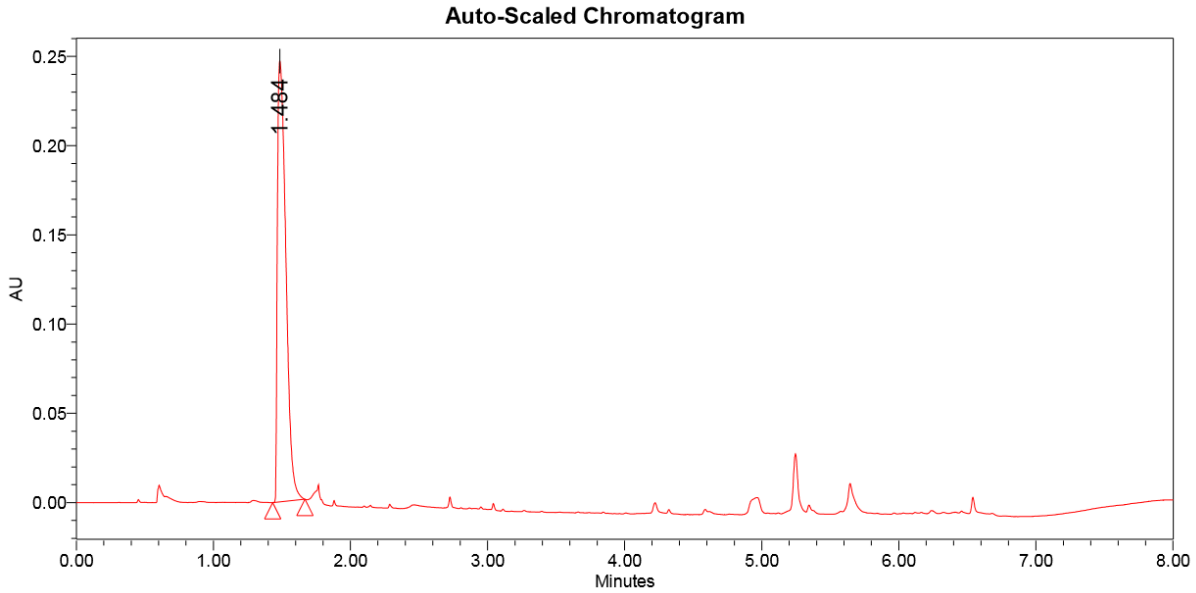

Figure S101. UPLC UV-chromatogram of the authentic reference **8f** (gradient B).

2.7.6. Synthesis of 8-(difluoromethyl)-3,7-dimethyl-1-(5-oxohexyl)-3,7-dihydro-1*H*-purine-2,6-dione ([^{18}F]8g)

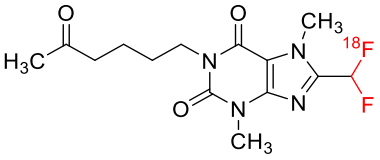

[^{18}F]8g

The implementation of the general procedure for the C-H ^{18}F-difluoromethylation of 3,7-dimethyl-1-(5-oxohexyl)-3,7-dihydro-1*H*-purine-2,6-dione (5.6 mg, 0.02 mmol) provided the labeled compound **[^{18}F]8g** in 52 ± 6%, 17 ± 3%, and 60 ± 3% RCY, using the reagents **[^{18}F]5a**, **[^{18}F]5c**, and **[^{18}F]5f**, respectively (see the Tables S49-S51 for more details of the RCY determination). The UPLC radio-chromatogram of the crude product **[^{18}F]8g** is depicted in Figure S102. Figure S103 represents the UPLC UV-chromatogram of the non-radioactive reference **8g**.

Table S49. Determination of the radiochemical yield (%) of the synthesis of **[^{18}F]8g** using the reagents **[^{18}F]5a**

Reaction	Radio-TLC purity (%)	Radio-UPLC purity (%)	Radiochemical Yield (%)
1	18	100	18
2	23	100	23
3	22	100	22
Radiochemical Yield (%) ± Deviation			21 ± 2

Table S50. Determination of the radiochemical yield (%) of the synthesis of **[^{18}F]8g** using the reagents **[^{18}F]5c**

Reaction	Radio-TLC purity (%)	Radio-UPLC purity (%)	Radiochemical Yield (%)
1	42	58	24
2	56	62	35
3	61	61	37
4	48	53	25
Radiochemical Yield (%) ± Deviation			30 ± 6

Table S51. Determination of the radiochemical yield (%) of the synthesis of **[^{18}F]8g** using the reagents **[^{18}F]5f**

Reaction	Radio-TLC purity (%)	Radio-UPLC purity (%)	Radiochemical Yield (%)
1	52	60	31
2	47	82	39
3	42	81	34
Radiochemical Yield (%) ± Deviation			35 ± 3

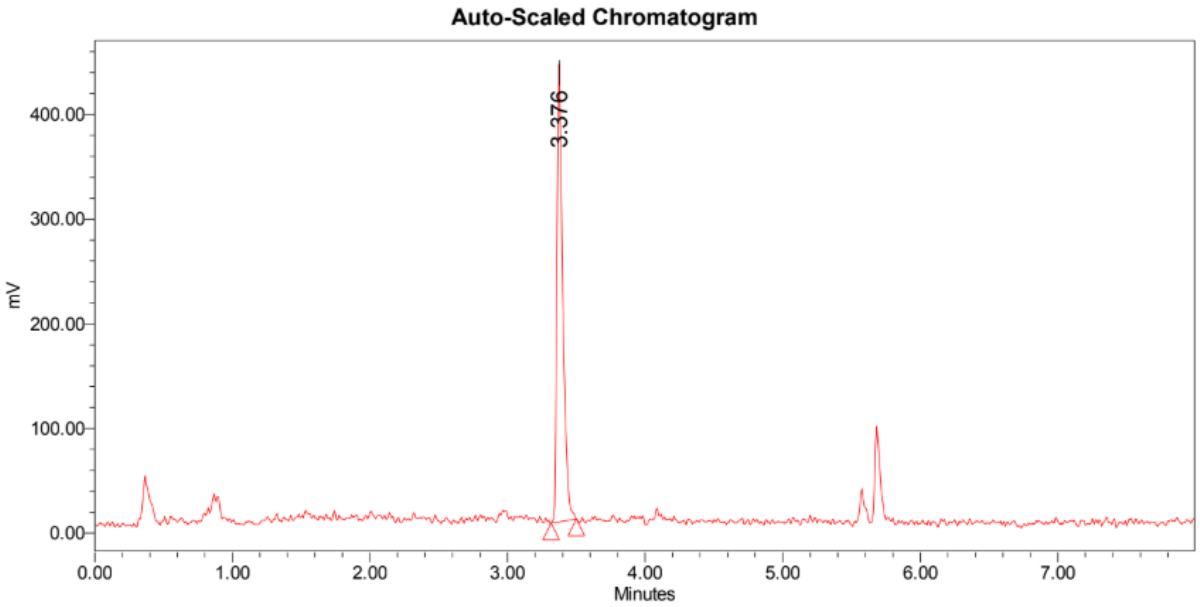

Figure S102. UPLC radio-chromatogram of the crude product **[^{18}F]8g** (gradient B).

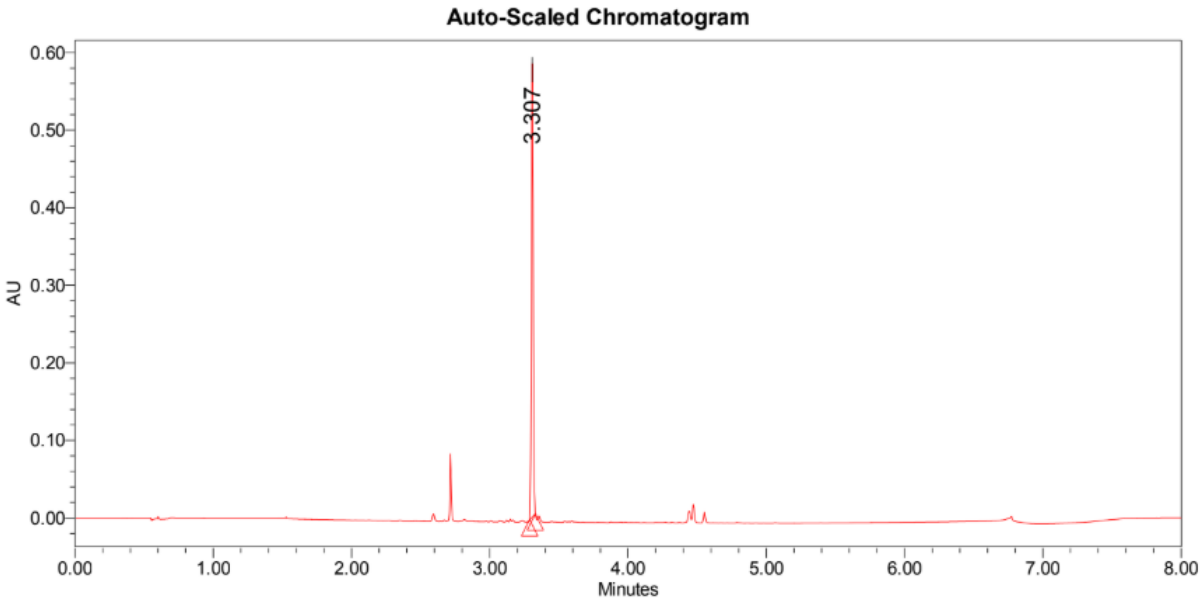

Figure S103. UPLC UV-chromatogram of the authentic reference **8g** (gradient B)**.**